THE NATURE OF MARKARIAN GALAXIES
AND
STUDIES OF STAR FORMATION IN BLUE GALAXIES

Thesis by

John Peter Huchra

In Partial Fulfilment of the Requirements

for the Degree of

Doctor of Philosophy

California Institute of Technology

Pasadena, California

1977

(Submitted July 14, 1976)

To my parents,

who always wanted their son to be a doctor

Noli te vexare nothis permittere

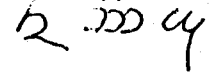

ACKNOWLEDGEMENTS

I would like to thank my thesis advisor, Wal Sargent, for suggesting this study of star formation in galaxies, and continuing guidance and patience during its execution. How he managed to survive my "Brooklynese" for this length of time will forever be a mystery to me.

I am very grateful to Dr. Leonard Searle and Dr. Allan Sandage for helpful discussions and data.

Several fellow graduate students (a few of whom have gone on to more exalted positions) provided much intellectual support. These include Jay Elias, Richard Green, John Hoessel, John Kormendy, Anneila Sargent, Ed Turner, Barry Turnrose, and Ted Williams.

Charlie Kowal gave me an introduction to observing and showed me that you don't have to walk on the promenade deck to do interesting science.

The night assistants and mountain crews at Palomar and Mount Wilson, especially Gene Hancock, Mike Marcario, Dennis Palm, and Chip Williams, have suffered with me through much good and bad weather.

Larry Blakee, Martin Olsiewski, Bob Cadman, and Bud Smith kept recalcitrant electronics in (on) line.

Richard Green, Jay Elias, Margaret Katz, and John Hoessel had the courage to read and comment on the rough

draft of this work.

Helen Knudsen (Fridenberg) provided invaluable assistance with the typing of this manuscript.

Dr. H. Babcock and the Hale observatories provided the immense quantity of telescope time needed for the observations.

The National Science Foundation and the State of California provided most of my financial support.

Finally, I would like to thank all my numerous friends, fellow graduate students, Hale staff members, Caltech faculty and postdocs, and the many mountaintop acquaintances who have made my stay at Caltech a pleasant one.

ABSTRACT

Integrated UBV photometry is given for 197 non-Seyfert Markarian galaxies and is compared with existing photometry of field galaxies. The distributions of galaxy colors overlap by almost seventy-five percent, and the color-color relations are the same. The color-aperture relations derived from multi-aperture observations show that the Markarian galaxies generally get bluer towards their centers, unlike all but the latest types of field galaxies.

Thirteen binary galaxies with good radial velocity data are used to derive the mean minimum mass-to-light ratio for Markarian galaxies. It is the same as the mean minimum mass-to-light ratio for field binary galaxies.

All Markarian galaxies with $m_{pg} \leq 14.0$ are morphologically classified in the modified Hubble sequence. The distibution of morphological types for Markarian galaxies is generally similar to that of field galaxies. The only significant difference is that the Markarian sample shows a factor of three excess of very late type galaxies. The Markarian galaxies are generally blue for their morphological type but fall within the distributions

of colors for their field counterparts. The bluest types - Magellanic spirals and irregulars - extend 0.3 magnitude bluer in U-B than the bluest field galaxies.

The Markarian galaxy luminosity function is derived from the available data for all seven lists of objects. Markarian galaxies represent approximately one tenth of all galaxies with absolute magnitudes fainter than $M_{pg} = -22$ ($H_o = 50$ km sec^{-1} Mpc^{-1}). A crude estimate is made of the space density as a function of color for both Markarian and field galaxies. Markarian appears to be finding all galaxies with U-B < -0.3 plus a decreasing fraction of the redder galaxies.

For the Markarian galaxies with available data, there are strong correlations of the emission line strength, measured by Hβ equivalent width, with color and absolute magnitude. There are also weaker correlations of the excitation parameter I([O III]λ5007)/I(Hβ) with color.

The optical and radio data indicate that the non-Seyfert Markarian galaxies (85% of all Markarian objects) are not a new class of object but rather a subset of normal galaxies. Markarian selects the bluest galaxies and those galaxies which are blue for their morphological type.

The Markarian galaxy photometry and photometry of galaxies in the lists of Haro and Zwicky extend the observed

galaxy two color distribution significantly bluewards. Existing evolutionary models of galaxy colors (Tinsley 1968, 1972; Searle, Sargent and Bagnuolo 1973) do not match the observed colors of these blue galaxies. Models of galaxies are constructed with a variety of star formation histories and initial mass functions. The models include the effects of emission by gas ionized by the hot stars in the galaxy.

Three general classes of models were studied. 'Old' galaxies are systems that are more than 10^{10} years old. 'Young' galaxies are systems that are less than one tenth that age. 'Composite' galaxies are 'old' galaxies, with properties similar to ordinary spirals and ellipticals, plus a burst of recent star formation. Powerlaw initial mass functions were used.

In order to fit the observed colors, 'old' galaxies must have high mass star enriched initial mass functions and nearly constant rates of star formation. 'Young' galaxies must have large amounts of internal reddening. If their initial mass function is the Salpeter function, they must be less than 10^{8} years old. 'Composite' galaxies must have bursts of star formation that contribute approximately twenty to fifty percent of the V band light.

Comparison of model predictions with the observed

metal abundance, color-magnitude distribution, and internal reddening lead us to conclude that 'composite' models best fit the observed properties. There is no compelling evidence for the existence of 'young' galaxies - objects only recently condensed out of the intergalactic medium.

In addition, comparison of model predictions with the observed Hβ emission as a function of color in blue galaxies leads to the conclusion that some of these galaxies are forming stars with an initial mass function flatter than the Salpeter function.

TABLE OF CONTENTS

CHAPTER 1

THE NATURE OF MARKARIAN GALAXIES

I. INTRODUCTION

Markarian and Lipovetsky (Markarian 1967, 1969a, 1969b; Markarian and Lipovetsky 1971, 1972, 1973, 1974) published seven lists of galaxies with ultraviolet continua found on a low dispersion (1800 Å/mm at Hγ) objective prism survey. Spectroscopic observations at intermediate dispersions by large numbers of observers have provided classifications for ∿ 500 of the 699 objects. Huchra and Sargent (1976) estimate that 11% of the objects are Seyfert galaxies, 2% are galactic stars, and 2% are quasars or non-stellar objects with featureless continua similar to BL Lacertae. The bulk of the objects are galaxies or parts of galaxies with spectroscopic properties ranging from absorption line spectra to high excitation, sharp emission line spectra similar to H II region spectra. This study will be devoted to this last class of non-Seyfert galaxies. Hereafter, the term 'Markarian galaxy' will refer to non-Seyfert, non-BL Lacertae type Markarian galaxies.

Various explanations have been proposed for the apparent UV excess in these galaxies. Markarian (1967, 1972) divided the galaxies into two classes - "stellar" and "diffuse" - based on their appearance on the prism survey plates. He concluded that the diffuse galaxies represent associations of stars and gas, but that the "stellar"

objects – galaxies with bright nuclei – are closely related to Seyfert galaxies, with excess ultraviolet radiation of non-thermal origin. However, a photometric study by Weedman (1973) showed that the continua of all the non-Seyfert galaxies could come from stars and gas. Weedman also showed that a definite separation exists between the Seyfert and non-Seyfert colors, but an overlap between the colors of diffuse and bright nucleus galaxies. Most of the galaxies he observed were much bluer than the field galaxies observed by de Vaucouleurs (1961, 1972).

More detailed studies of single objects, for example that of Sargent and Searle (1970), suggest that some are objects with much recent star formation. Radio surveys by Sramek and Tovmassion (1975) and other authors referenced therein discovered that very few of these galaxies have significant continuum radio emission. 21-cm neutral hydrogen studies by Bottinelli et al. (1973, 1975) showed that these galaxies contain neutral hydrogen.

Despite the work that has been done on the Markarian sample, there is no clear understanding of the Markarian galaxies and what their relationship is to the 'normal' or field galaxies. In this paper we will examine the properties of a large number of Markarian galaxies, including two well defined complete samples. We will compare these properties to those of field galaxies. We define what the non-

Seyfert Markarian galaxies are with respect to the field galaxies, and define what a Markarian galaxy is in terms of our observed parameters. We will find that the Markarian galaxies are basically an extension of the normal field galaxies.

In Section II of this paper we present new and summarize existing UBV photometry, morphological classifications, and spectroscopic data for Markarian galaxies. A Hubble constant of 50 km sec^{-1} Mpc^{-1} is used throughout. In Section III these and other available data are compared with data for field galaxies. Other properties of the Markarian galaxies are discussed. In Section IV the results of these comparisons are discussed and conclusions as to the nature of Markarian galaxies are presented.

II. THE DATA

We present here the available photometric spectroscopic and morphological data for a large sample of Markarian galaxies. The data have been obtained by the author or collected from sources in the literature. Complete UBV photometry is presented for the "photometric sample" — the 91 galaxies in lists I-IV with apparent photographic magnitude ≤ 16.0 and absolute photographic magnitude ≥ -20.35. Complete morphological data (classifications in the modified Hubble sequence of de Vaucouleurs (1961)) are presented for the 91 galaxies in all seven lists with apparent photographic magnitude ≤ 14.0. Photometry is available for 73 of these galaxies. In all, photometry is available for over 200 Markarian galaxies. Quantitative spectroscopic data in the form of the Hβ equivalent width in emission and the excitation parameter I([O III] λ 5007)/I(Hβ) are available for 103 of the Markarian galaxies with photometry.

a) Photometry and the Sky Survey Diameters

Photometric observations were made on 35 nights from 1972 to 1976 on the 2.5-m telescope at Mount Wilson and the 1.5-m telescope at Palomar Mountain. The observations were obtained with dry ice cooled ITT FW130, S20 photo-tubes in the S20-UBVR system of Sandage and Smith (1963) and Sandage (1973), designed to match the standard 1P21-UBV system.

Pulse counting electronics were employed. The Mount Wilson photometer was a single beam system so observations were made alternately on the object and sky until sufficient counts were recorded to bring the expected statistical error

$$\sigma \equiv \frac{[(\text{object} + \text{sky}) + (\text{sky})]^{\frac{1}{2}}}{(\text{object} + \text{sky}) - (\text{sky})} \qquad (1)$$

below 0.01 in B, V and R, and 0.01 to 0.03 in U - depending on the brightness of the object. At Palomar a two tube Oke coldbox was employed with a two-channel photometer. There objects were observed in each aperture once, integrating long enough to bring the statistical error below the limits for each channel. The channels were reduced independently, and the magnitudes and colors obtained were averaged after reduction. Stars from the list of Sandage (1973) were observed in order to derive extinction corrections and transformations to the standard system. The reductions were done by a computer least squares fit of the combined extinction and transformation coefficients to the instrumental magnitude and color, airmass and standard value data for all the standards observed during a night. Internal errors were calculated by comparing the reduced magnitudes and colors of the standard stars to the standard magnitudes and colors. At Palomar the mean standard deviation of a single measurement is 0.04 in V, 0.03 in U-B, and 0.02 in B-V and V-R. At Mount Wilson, because the sky brightness was higher and

larger fluctuations existed in transparency and sky brightness during the night, the accuracy of the photometry is reduced and the deviation in a single measurement is 0.05 in V and U-B, 0.03 in V-R, and 0.02 in B-V. External errors were checked by examining the differences in measurements made of the same object through similar apertures (or, in the case of colors, through apertures large enough that the color-aperture curve had flattened). For the Palomar data, we can also compare the magnitudes and colors observed in each channel. Both analyses yielded mean errors of a single measurement of approximately 0.05 in V, 0.04 in U-B, and 0.03 in B-V and V-R. Multiple observations of an object increased the accuracy of the final magnitudes and colors accordingly.

As galaxy colors and magnitudes are a function of the measuring aperture size, it is reasonable, for the purposes of comparison, to define some standard diameter system.

We chose to use diameters measured from enlargements of the Palomar Sky Survey prints. For galaxies brighter than $M_{pg} = 16.0$, resolution does not present a serious problem, and this diameter system has the advantage that the color-aperture curves are nearly flat. In addition, the magnitude-aperture (growth) curve is such that varying the diameter by ±25% will cause the integrated magnitudes to change by only 0.1.

The raw photometric data, consisting of 399 observations, including 120 from other sources, of 212 galaxies, are listed in Table 1. Column 1 gives the Markarian number, column 2 the aperture size rounded to the nearest arc second, and column 3 the sources for the data with references listed at the end of the table. The designation HP indicates that the photometry was obtained with the Palomar 1.5-m telescope.

Columns 4-7 give V, B-V, U-B, and V-R; columns 8 and 9 give the measured major (D_1) and minor (D_2) axis diameter in arc seconds, and column 10 gives the aperture to major axis diameter ratio. Where known, morphological types are given in column 11. The morphological data come from a variety of sources. The majority are derived from examination of large scale plate material by the author and from Kalloghlian (1971), and Borngen and Kalloghlian (1975). A few classifications in the Hubble sequence are derived from descriptions in the Morphological Catalogue of Galaxies (Voronstov-Velyaminov et al. 1962-63) and are given in parentheses. An asterisk (*) indicates the existence of a superposed star that might affect the colors of the galaxies. More detailed descriptions are given in the notes.

In general, there is reasonable agreement between the photometric measurements of different observers — especially when aperture effects are considered — which indicates that the photometric systems are consistent and well defined.

TABLE 1

PHOTOMETRIC OBSERVATIONS OF MARKARIAN GALAXIES

No.	A	Ob	V	B-V	U-B	V-R	D_1	D_2	A/D_1	Morph.
(1)	(2)	(3)	(4)	(5)	(6)	(7)	(8)	(9)	(10)	(11)
2	36	WK	13.54	0.60	-0.12	...	30	30	1.20	SBa
5	29	HP	15.51	0.51	-0.31	...	30	13	1.03	Im
	41	HP	15.25	0.54	-0.34	...			1.37	
7	24	BK	14.68	0.29	-0.35	...	31	17	0.77	Im
	32	BK	14.59	...	...	...			1.03	
	41	H	14.24	0.41	-0.36	...			1.32	
8	15	W	15.28	0.46	-0.52	...	30	27	0.50	Im
	24	BK	14.43	0.43	-0.37	...			0.80	
	32	BK	14.28	...	...	...			1.07	
	41	H	13.97	0.49	-0.37	...			1.37	
11	15	W	14.30	0.81	0.37	...	25	16	0.60	E5/S0
12	57	HP	12.86	0.47	-0.35	...	52	40	1.10	Sc
13	15	W	15.33	0.50	-0.27	...	43	40	0.35	SBbc
	57	HP	14.03	0.54	-0.07	0.73			1.33	
	114	DV	13.77	0.57	-0.04	...			2.65	
14	15	W	14.81	0.42	-0.31	...	22	21	0.68	S0?
	29	H	14.53	0.42	-0.35	0.60			1.32	
16	15	W	15.15	0.47	-0.08	...	25	16	0.60	
	29	HP	14.69	0.61	0.00	0.75			1.16	
18	41	HP	13.93	0.78	-0.06	0.93	27	16	1.52	
19	15	H	15.42	0.45	-0.69	0.56	16	12	0.94	
20/	15	W	15.17	0.46	-0.24	...	28	23	0.54	(E?)
107	29	H	14.50	0.42	-0.29	.54			1.04	
21	15	W	14.85	0.78	0.09	...	40	14	0.38	SBb?
22	11	H	16.11	0.60	-0.43	.35	16	11	0.69	
	24	H	15.76	0.62	-0.42	.41			1.50	

Table 1 (continued)

Photometric Observations of Markarian Galaxies

No.	A	Ob	V	B-V	U-B	V-R	D_1	D_2	A/D_1	Morph.
(1)	(2)	(3)	(4)	(5)	(6)	(7)	(8)	(9)	(10)	(11)
25	15	W	14.45	0.56	-0.20	...	19	19	0.79	(E)
	24	H	14.26	0.62	-0.20	0.79			1.26	
26	24	H	15.60	0.42	-0.33	0.54	19	13	1.26	Sc
27	11	H	16.46	0.46	-0.23	0.43	13	8	0.85	
31	15	W	15.55	0.82	0.04	...	40	28	0.38	SBb
32	15	H	16.23	0.24	-0.16	0.49	17	13	0.88	
	24	H	15.96	0.29	-0.19	0.47			1.41	
	37	H	15.79	0.37	-0.05	...			2.18	
33	15	W	13.58	0.35	-0.42	...	30	25	0.50	Im
	30	HI	13.30	0.33	-0.52	...			1.00	
35	21	HP	13.54	0.41	-0.42	0.65	46	28	0.46	Sm
	29	HP	13.24	0.45	-0.41	0.61			0.63	
	30	HI	...	0.32	-0.35	...			0.65	
	30	W	13.17	0.36	-0.33	...			0.65	
	41	HP	13.06	0.44	-0.39	0.62			0.89	
	105	DV	12.75	0.50	-0.31	...			2.28	
36	15	W	15.46	0.34	-0.76	...	15	13	1.00	
	24	H	15.24	0.34	-0.61	0.34			1.60	
41	15	D	15.01	0.66	-0.15	...	20	15	0.75	
43	38	H	15.22	0.60	-0.21	0.31	20	8	1.90	
44	15	W	15.27	0.62	0.01	...	18	13	0.83	
45	29	HP	15.28	0.66	-0.09	0.74	20	9	1.45	(S0)
46	15	H	16.47	0.49	0.02	0.61	10	10	1.50	
	24	H	16.05	0.42	-0.13	0.44			2.40	
47	38	H	14.86	0.71	0.33	0.70	18	11	2.11	
	38	H	14.91	0.71	0.14	0.68			2.11	
	15	H	15.48	0.76	0.25	0.71			*	
48	24	H	14.76	0.95	0.45	0.77	14	14	1.71	S0

Table 1 (continued)

Photometric Observations of Markarian Galaxies

No.	A	Ob	V	B-V	U-B	V-R	D_1	D_2	A/D_1	Morph.
(1)	(2)	(3)	(4)	(5)	(6)	(7)	(8)	(9)	(10)	(11)
49	15	WK	15.68	0.48	-0.45	...			0.56	
	15	W	15.32	0.32	-0.44	...	27	20	0.56	
	24	H	14.64	0.48	-0.39	0.62			0.89	
51	17	WK	15.54	0.21	-0.13	...	17	11	1.00	
	24	H	15.05	0.62	-0.21	0.67			1.41	
52	15	W	14.12	0.51	-0.30	...	13	13	*	SBab
	17	WK	14.08	0.53	-0.25	...				
	21	W	13.86	0.58	-0.26	...				
	35	W	13.50	0.63	-0.18	...				
	64	DV	12.88	0.67	-0.05	...				
53	24	H	15.28	0.40	-0.35	0.61	13	10	1.85	
	24	H	15.33	0.43	-0.29	0.67			1.85	
55	24	H	15.33	0.68	0.03	0.73	15	13	1.60	
58	15	W	15.34	0.49	-0.06	...	16	16	0.94	(S0?)
59	15	WK	14.09	(0.33)	-0.61	...	26	24	0.58	Sm, Im
	15	H	13.95	0.39	-0.66	0.19			0.58	
	24	H	13.65	0.38	-0.75	0.08			0.92	
60	15	H	15.91	0.48	-0.08	0.76	13	13	1.15	
66	15	W	14.98	0.42	-0.31	...	19	14	0.79	
67	15	H	16.01	0.52	-0.40	0.45	11	11	1.36	
71	10	D	14.11	0.48	-0.58	...	40	20	0.25	Im
	20	H	13.76	0.56	-0.34	...			0.50	
	21	W	13.79	0.24	-0.42	...			0.53	
	43	H	13.72	0.42	-0.25	...			1.08	
73	10	D	15.17	0.74	...	...	15	15	0.67	
	20	H	14.71	0.73	-0.11	0.91			1.33	
81	15	W	14.28	1.02	0.62	...	50	28	0.30	S0
82	15	H	14.88	0.91	0.25	0.78	12	12	1.25	

Table 1 (continued)

Photometric Observations of Markarian Galaxies

No.	A	Ob	V	B-V	U-B	V-R	D_1	D_2	A/D_1	Morph.
(1)	(2)	(3)	(4)	(5)	(6)	(7)	(8)	(9)	(10)	(11)
84	41	HP	13.91	0.45	-0.19	...	38	23	1.08	Sm
85	15	W	14.29	0.91	0.34	...	30	30	0.50	S0/a
	41	HP	13.55	0.85	0.32	...			1.37	
86	38	H	12.86	0.57	-0.11	0.70	80	70	0.48	Sm
	83	H	11.90	0.57	0.02	0.75			1.04	
	83	H	12.09	0.63	-0.25	0.57			1.04	
	106	DV	11.96	0.62	-0.05	...			1.33	
	138	DV	11.72	0.67	-0.17	...			1.73	
87	15	W	14.53	0.86	0.10	...	52	40	0.29	SB0/a
	29	HP	14.00	0.93	0.28	...			0.56	
	57	HP	13.35	0.90	0.23	...			1.10	
88	15	W	14.66	0.62	-0.06	...	15	15	1.00	
89	10	D	15.35	0.56	-0.40	...	16	12	0.63	Im
	25	D	14.83	0.55	-0.33	...			1.56	
90	41	HP	13.95	0.73	0.03	...	37	34	1.11	SBb
92	10	D	15.02	0.53	-0.41	...	26	10	0.38	
	25	D	14.30	0.50	-0.20	...			0.96	
93	10	D	15.63	0.63	-0.29	...	15	9	0.67	
	25	D	15.23	0.70	-0.27	...			1.67	
94	11	H	16.34	0.75	-0.50	-0.26	7	6	1.57	
95	10	D	16.21	0.46	-0.34	...	19	11	0.53	
	25	D	15.40	0.46	-0.11	...			1.32	
96	10	D	15.30	0.63	-0.59	...	22	12	0.45	
	25	D	14.95	0.39	-0.30	...			1.14	
98	25	D	14.78	0.51	-0.16	...	24	15	1.04	
99	25	D	15.86	0.49	-0.38	...	16	11	1.56	
100	15	W	14.27	0.82	0.21	...	32	32	0.47	
	25	AA	13.87	0.64	0.40	...			0.78	

Table 1 (continued)

Photometric Observations of Markarian Galaxies

No.	A	Ob	V	B-V	U-B	V-R	D_1	D_2	A/D_1	Morph.
(1)	(2)	(3)	(4)	(5)	(6)	(7)	(8)	(9)	(10)	(11)
101	10	D	14.29	0.64	0.05	...	32	27	0.31	S0*
	25	D	13.58	0.59	0.03	...			0.78	
102	15	W	14.58	0.53	-0.07	...	22	19	0.68	
104	10	D	15.39	0.45	-0.38	...	25	15	0.40	
	25	D	14.43	0.45	-0.28	...			1.00	
105	15	W	15.72	0.69	-0.07	...	13	10	1.15	Sc
	25	D	15.81	0.68	-0.10	...			1.92	
108	19	H	15.34	0.44	-0.71	0.56	22	15	0.86	Im?
	41	HP	15.05	0.42	-0.58	0.51			1.86	
111	25	D	14.20	0.51	-0.26	...	35	23	0.71	Im
	35	W	13.96	0.43	-0.27	...			1.00	
116	15	H	16.11	0.17	-0.76	0.39	14	9	1.07	
	15	H	16.31	0.18	-0.65	0.47			1.07	
118	41	HP	14.77	0.50	-0.13	0.72	40	15	1.03	
119	29	HP	13.87	0.51	-0.18	0.69	21	16	1.38	
129	24	H	14.92	0.72	0.05	0.74	20	15	1.20	
131	15	H	14.42	0.59	0.10	0.69	27	25	0.56	E1
	38	H	13.75	0.63	0.06	0.69			1.41	
133	25	AA	13.50	0.70	0.03	...	42	42	0.60	Sc
	30	DV	13.37	0.66	-0.09	...			0.71	
	35	W	13.33	0.67	0.05	...			0.83	
138	29	H	15.52	0.65	-0.28	0.69	15	8	1.93	
140	15	W	15.19	0.45	-0.38	...	15	13	1.00	
	15	H	15.08	0.47	-0.36	0.61			1.00	
146	29	HP	14.06	0.59	-0.05	0.75	20	20	1.45	
149	15	W	14.48	0.73	0.18	...	18	15	0.83	S0
	28	H	14.43	0.61	0.26	0.68			1.56	

Table 1 (continued)

Photometric Observations of Markarian Galaxies

No.	A	Ob	V	B-V	U-B	V-R	D_1	D_2	A/D_1	Morph.
(1)	(2)	(3)	(4)	(5)	(6)	(7)	(8)	(9)	(10)	(11)
150	24	H	14.84	0.42	-0.27	0.63	16	9	1.50	
151	24	H	15.32	0.62	-0.20	0.58	21	12	1.14	(S0)
	24	H	15.31	0.56	-0.22	0.61			1.14	
153	15	H	15.05	0.22	-0.66	0.28	28	15	0.54	(Scp)
	38	H	14.81	0.19	-0.65	0.31			1.36	
155	15	W	13.22	0.71	0.29	...	26	15	0.58	S0/a
	24	H	13.09	0.70	0.32	0.74			0.92	
156	38	H	14.69	0.36	-0.34	0.50	45	14	0.84	
157	41	H	14.17	0.26	-0.57	0.56	27	16	1.52	Im
158	35	W	13.28	0.72	0.09	...	75	38	0.47	Sab
	41	HP	13.11	0.72	0.17	0.82			0.55	
	81	HP	12.73	0.72	0.20	0.81			1.08	
159	10	AA	13.23	0.46	-0.06	...	16	13	0.63	
161	15	W	14.54	0.56	-0.12	...	35	24	0.43	SBc
	41	HP	13.66	0.53	-0.15	0.75			1.17	
165	15	W	14.73	0.51	-0.21	...	20	20	0.75	
	15	H	14.79	0.45	-0.15	0.67			0.75	
	24	H	14.52	0.53	-0.19	0.63			1.20	
166	10	AA	15.78	0.34	0.23	...	12	12	0.83	
	29	HP	15.19	0.40	-0.23	0.69			2.42	
169	15	W	14.40	0.51	-0.19	...	27	22	0.56	
	41	HP	13.96	0.58	-0.31	0.79			1.52	
170	41	HP	14.61	0.47	-0.30	0.60	40	16	1.03	
	57	HP	14.26	0.55	-0.24	0.65			1.43	
171	30	W	12.86	0.33	-0.41	...	70	70	0.43	Scp +
	31	DV	12.65	0.44	-0.42	...			0.44	Imp
	64	DV	11.85	0.56	-0.34	...			0.91	
175	35	W	13.76	0.93	0.32	...	39	23	0.90	SBab

Table 1 (continued)

Photometric Observations of Markarian Galaxies

No.	A	Ob	V	B-V	U-B	V-R	D_1	D_2	A/D_1	Morph.
(1)	(2)	(3)	(4)	(5)	(6)	(7)	(8)	(9)	(10)	(11)
177	24	H	15.54	0.44	-0.14	0.57	18	14	1.33	
178	24	H	15.19	0.27	-0.53	0.34	47	27	0.51	Im
	30	W	14.94	0.14	-0.38	...			0.64	
	38	H	14.61	0.34	-0.41	0.44			0.81	
	56	H	14.23	0.37	-0.28	0.44			1.19	
179	35	W	13.79	0.67	0.11	...	58	46	0.60	SBbc
181	29	HP	14.09	0.50	-0.15	0.72	24	16	1.21	SBc
185	81	HP	12.70	0.65	0.02	0.77	82	65	0.99	SBcdp
186	15	W	13.98	0.38	-0.33	...	40	26	0.38	SB0/a?
	15	H	13.75	0.41	-0.23	0.65			0.38	
	24	H	13.44	0.44	-0.22	0.65			0.60	
	38	H	13.26	0.47	-0.22	0.66			0.95	
188	81	HP	12.32	0.63	-0.04	0.77	88	54	0.92	SBbc
190	41	HP	12.88	0.66	-0.10	0.84	40	40	1.03	S0?
	57	HP	12.71	0.68	-0.07	0.86			1.43	
195	15	W	14.57	0.50	-0.20	...	25	19	0.60	(Sa)
	41	HP	14.05	0.63	-0.13	0.78			1.64	
197	15	W	14.54	0.82	0.18	...	27	27	0.56	E0/S0
	29	HP	14.11	0.84	0.22	0.78			1.07	
199	43	H	15.12	0.42	-0.35	0.47	27	9	1.59	
201	15	W	13.30	0.49	-0.25	...	(43)	32	0.35	Smp
	41	HP	12.86	0.53	-0.18	0.79			0.95	
202	21	HP	15.32	0.69	-0.16	0.79	11	11	1.91	
206	15	W	15.19	0.64	-0.22	...	13	13	1.15	
	29	HP	14.85	0.68	-0.21	0.84			2.23	
207	41	HP	13.49	0.48	-0.22	0.72	40	28	1.03	Sbc
209	29	HP	14.62	0.49	-0.53	0.16	29	16	1.00	Sm?

Table 1 (continued)

Photometric Observations of Markarian Galaxies

No.	A	Ob	V	B-V	U-B	V-R	D_1	D_2	A/D_1	Morph.
(1)	(2)	(3)	(4)	(5)	(6)	(7)	(8)	(9)	(10)	(11)
215	15	W	14.45	0.58	-0.16	...	15	15	1.00	
219	38	H	14.98	0.64	-0.22	0.26	20	8	1.90	
220	15	W	14.49	0.33	-0.25	...	24	13	0.63	
223	21	HP	14.82	0.60	-0.21	0.85	15	15	1.40	
224	38	H	15.43	0.65	-0.50	0.38	18	9	2.11	Im
	38	H	15.51	0.27	-0.39	0.50			2.11	
235	15	H	15.05	0.46	-0.16	0.69	28	20	0.54	
	38	H	14.37	0.46	-0.22	0.56			1.36	
241	24	H	15.27	0.61	-0.13	0.65	15	10	1.60	
	24	H	15.35	0.56	-0.03	0.72			1.60	
242	24	H	15.64	0.52	-0.05	0.66			1.85	
245	20	H	15.42	0.67	0.04	0.60	12	12	1.67	
	29	HP	15.18	0.62	-0.21	0.75			2.42	
247	15	W	15.00	0.53	-0.20	...	14	11	1.07	
249	38	H	13.55	0.82	0.24	0.91	35	25	1.09	S0
	38	H	13.54	0.86	0.37	0.35			1.09	
251	24	H	15.64	0.41	-0.27	0.58	12	9	2.00	
	24	H	15.57	0.49	-0.25	0.54			2.00	
253	24	H	15.36	0.81	0.01	0.83	20	8	1.20	
256	57	HP	13.30	0.36	-0.42	0.59	61	43	0.93	Sd
258	15	H	15.68	0.67	0.08	0.65	9	9	1.67	
	15	H	15.50	0.81	-0.07	0.74			1.67	
	24	h	15.54	0.79	-0.04	0.75			2.67	
266	15	H	13.42	0.77	0.06	0.81	24	24	0.63	
	24	H	13.25	0.83	0.20	0.78			1.00	

Table 1 (continued)

Photometric Observations of Markarian Galaxies

No.	A	Ob	V	B-V	U-B	V-R	D_1	D_2	A/D_1	Morph.
(1)	(2)	(3)	(4)	(5)	(6)	(7)	(8)	(9)	(10)	(11)
267	15	W	14.95	0.50	-0.15	...	24	13	0.63	(S)
	15	H	14.96	0.63	-0.15	0.74			0.63	
	24	H	14.75	0.60	-0.13	0.74			1.00	
277	41	H	15.27	0.46	-0.49	0.35	20	12	2.05	Im
281	15	W	13.82	0.66	-0.13	...	112	112	0.13	SBb
	106	DV	11.89	0.71	0.13	...			0.95	
286	41	HP	13.54	0.50	-0.12	0.70	35	28	1.17	Scd?
288	29	HP	14.46	0.29	-0.56	0.42	38	14	0.76	Sdm?
291	29	H	15.14	0.51	-0.37	0.62	17	11	1.71	
294	41	HP	14.65	0.59	-0.19	0.64	25	15	1.64	Im?*
296	15	W	16.02	0.33	-0.52	...	28	11	0.54	Im
	41	H	15.53	0.35	-0.51	0.34			1.46	
297	12	H	14.56	0.34	-0.31	0.68	40	35	0.30	Smp
	19	H	13.94	0.42	-0.31	0.66			0.48	
	29	H	13.67	0.37	-0.36	0.63			0.73	
	43	H	13.18	0.45	-0.37	0.57			1.08	
	106	DV	12.99	0.44	-0.30	...			2.65	
298	24	H	14.80	0.99	0.15	0.90	22	20	1.09	
303	17	W	14.81	0.80	0.31	...	30	16	0.57	
	38	H	14.10	0.61	-0.16	0.82			1.27	
	41	HP	14.21	0.60	0.02	0.79			1.37	
307	17	W	14.47	0.51	-0.10	...	43	43	0.40	SBc
	38	H	13.47	0.53	-0.20	0.79			0.88	
	56	H	13.20	0.58	-0.15	0.74			1.30	
308	15	W	14.65	0.63	-0.06	...	24	16	0.63	
	25	AA	14.38	0.68	0.14	...			1.04	
	41	HP	14.37	0.61	-0.07	0.78			1.71	
309	15	H	15.22	0.47	-0.46	0.68	27	13	0.56	
	38	H	14.91	0.57	-0.34	0.65			1.36	

Table 1 (continued)

Photometric Observations of Markarian Galaxies

No.	A	Ob	V	B-V	U-B	V-R	D_1	D_2	A/D_1	Morph.
(1)	(2)	(3)	(4)	(5)	(6)	(7)	(8)	(9)	(10)	(11)
311	24	H	14.42	0.68	-0.05	0.91	20	20	1.20	SBb?
	29	HP	14.46	0.69	0.04	0.86			1.45	
312	24	H	14.72	0.57	-0.22	0.80	23	14	1.04	S
313	11	H	13.41	0.76	0.01	0.97	45	26	0.24	Ep
	24	H	12.97	0.77	0.04	0.95			0.53	
	56	H	12.72	0.76	0.05	0.95			1.24	
314	15	W	14.37	0.43	-0.13	...	28	19	0.54	Im
	15	H	14.37	0.43	-0.38	0.63			0.54	
	24	H	13.92	0.48	-0.34	0.60			0.86	
	38	H	13.77	0.47	-0.32	0.60			1.36	
	41	HP	13.76	0.47	-0.30	0.61			1.46	
	41	HP	13.76	0.48	-0.25	0.57			1.46	
316	15	W	15.09	0.66	-0.28	...	28	16	0.54	
317	24	H	15.19	0.68	-0.03	1.07	20	14	1.20	
	29	HP	15.13	0.73	-0.08	.87			1.45	
318	38	H	13.76	0.56	-0.14	0.82	35	24	1.09	Sdm
319	15	W	14.44	0.72	0.08	...	27	22	0.56	SBb
	29	HP	13.98	0.66	0.03	...			1.07	
321	15	H	14.23	0.72	0.12	0.90	41	40	0.37	Sbc
	21	W	14.24	0.52	-0.12	...			0.51	
	24	H	13.81	0.67	0.04	0.86			0.59	
	38	H	13.50	0.65	0.07	0.85			0.93	
323	32	W	13.88	0.71	0.10	...	45	30	0.71	Scd
	57	HP	13.28	0.77	0.09	...			1.27	
324	15	H	15.18	0.42	-0.31	0.63	14	14	1.07	
	24	H	15.10	0.42	-0.23	0.68			1.71	
	29	HP	14.99	0.47	-0.24	0.59			2.07	
325	20	S	13.47	0.38	-0.31	...	39	39	0.51	Sd-dm
	21	W	13.56	0.38	-0.24	...			0.54	
	41	HP	13.11	0.37	-0.41	...			1.05	

Table 1 (continued)

Photometric Observations of Markarian Galaxies

No.	A	Ob	V	B-V	U-B	V-R	D_1	D_2	A/D_1	Morph.
(1)	(2)	(3)	(4)	(5)	(6)	(7)	(8)	(9)	(10)	(11)
326	15	W	14.81	0.47	-0.18	...	36	30	0.42	SBb
	41	HP	13.66	0.73	0.08	...			1.14	
328	29	HP	14.92	0.63	-0.08	0.77	18	16	1.61	E3
	29	H	14.89	0.61	-0.10	0.82			1.61	
330	29	HP	14.53	0.36	-0.21	...	41	26	0.71	Sa?
	41	HP	14.40	0.39	-0.24	...			1.00	
331	15	H	14.20	0.88	0.18	1.15	30	21	0.50	Sa
	24	H	13.86	0.85	0.21	1.14			0.80	
	38	H	13.82	0.81	0.37	1.19			1.27	
332	15	H	13.95	0.76	0.08	0.97	60	60	0.25	SBc
	56	H	12.45	0.67	-0.07	0.84			0.93	
333	15	HP	14.09	1.00	0.57	0.90	23	18	0.65	E0/S0
	29	HP	13.65	1.01	0.59	0.89			1.26	
334	25	AA	14.42	0.13	0.31	...	43	22	1.72	(Sc)
336	41	H	13.64	0.78	0.19	...	28	18	1.46	E5
339	38	H	14.27	0.56	-0.07	.79	26	26	1.46	SBbc
341	15	W	14.78	0.69	-0.05	...	24	16	0.63	E2?
	29	HP	14.24	0.75	0.14	...			1.21	
343	41	HP	14.36	0.84	0.22	0.87	54	40	0.76	S0/a
345	41	HP	14.69	0.82	0.08	0.77	20	20	2.05	
	41	HP	14.56	0.67	0.12	0.77			2.05	
347	24	H	14.63	0.44	-0.30	0.75	19	19	1.26	
350	29	HP	15.05	0.51	-0.21	0.53	21	14	1.38	(Sp)
	41	HP	14.88	0.53	-0.06	0.62			1.95	
357	15	H	15.40	0.36	-0.68	0.39	14	14	1.07	
359	41	H	13.68	0.67	-0.08	...	27	24	1.52	SB0/a

Table 1 (continued)

Photometric Observations of Markarian Galaxies

No.	A	Ob	V	B-V	U-B	V-R	D_1	D_2	A/D_1	Morph.
(1)	(2)	(3)	(4)	(5)	(6)	(7)	(8)	(9)	(10)	(11)
360	15	H	15.10	0.44	-0.17	0.67	28	28	0.54	(Scd)
	38	H	14.56	0.42	-0.20	0.62			1.36	
363	24	H	14.03	0.57	-0.17	0.87	33	20	0.73	Sc
	38	H	13.87	0.57	-0.17	0.90			1.15	
367	24	H	15.21	0.66	-0.02	0.85	19	12	1.26	
368	21	W	14.84	0.62	0.09	...	24	20	0.88	
	38	H	14.50	0.56	-0.18	0.67			1.58	
369	15	H	15.31	0.44	-0.46	0.65	12	12	1.25	
	29	HP	15.30	0.39	-0.40	0.61			2.42	
370	15	H	14.40	0.47	-0.34	0.72	50	30	0.30	Sm
	15	HP	14.58	0.47	-0.33	...			0.30	
	24	H	13.90	0.48	-0.25	0.82			0.48	
	29	HP	13.92	0.51	-0.23	0.65			0.58	
	38	H	13.56	0.55	-0.29	0.79			0.76	
	41	HP	13.69	0.53	-0.27	...			0.82	
	57	HP	13.39	0.55	-0.16	0.70			1.14	
	81	HP	13.28	0.61	-0.19	...			1.62	
375	29	H	15.63	0.74	-0.27	0.43	11	11	2.64	
384	15	W	14.42	0.81	0.11	...	72	40	0.21	SBbc
386	57	HP	12.45	0.92	0.43	0.87	81	41	0.70	SBbp*
	21	HP	13.33	1.06	0.70	0.90			...	
389	21	HP	13.30	0.85	0.38	...	37	35	0.57	S0/a
	41	HP	12.93	0.86	0.34	...			1.11	
391	21	HP	13.99	0.72	0.08	...	30	18	0.70	S0/a
	29	HP	13.91	0.75	0.13	...			0.97	
398	29	HP	14.95	0.58	-0.17	0.77	27	13	1.07	
400	24	H	14.30	0.39	-0.25	0.64	24	20	1.00	
	24	H	14.33	0.49	-0.25	0.67			1.00	

Table 1 (continued)

Photometric Observations of Markarian Galaxies

No.	A	Ob	V	B-V	U-B	V-R	D_1	D_2	A/D_1	Morph.
(1)	(2)	(3)	(4)	(5)	(6)	(7)	(8)	(9)	(10)	(11)
401	15	H	13.87	0.58	-0.10	0.78	40	40	0.38	SBb
	24	H	13.53	0.68	-0.05	0.78			0.60	
	38	H	13.33	0.69	-0.06	0.74			0.95	
407	24	H	14.90	0.43	-0.27	0.59	15	14	1.60	
408	24	H	14.53	0.45	-0.34	0.55	19	16	1.26	
416	41	HP	14.13	0.70	-0.07	0.67	26	13	1.58	
418	41	HP	13.46	0.42	-0.26	0.65	32	30	1.28	Sab
426	38	H	14.51	0.45	-0.40	0.54	35	16	1.09	(Sc)
429	24	H	14.45	0.68	0.01	0.83	18	16	1.33	
430	29	HP	13.35	0.79	0.39	0.80	41	41	0.71	P
	57	HP	12.95	0.76	0.32	0.74			1.40	
432	29	HP	13.85	0.41	-0.29	0.62	54	27	0.51	SBdmp
	57	HP	13.66	0.46	-0.27	0.67			1.06	
439	21	HP	12.93	0.46	-0.19	0.71	88	84	0.24	Sa
	41	HP	12.45	0.54	-0.13	0.74			0.47	
	81	HP	11.99	0.64	-0.03	0.76			0.92	
442	38	H	13.54	1.01	0.37	0.87	30	28	1.27	
444		DP	14.90	0.55	-0.22	...	15	14	1^+	(*)
	29	HP	14.88	0.47	-0.36	0.71			1.94	
449	81	HP	12.99	0.66	0.02	0.72	84	22	0.97	Sap
450	56	H	14.06	0.52	-0.44	0.50	43	32	1.30	(Im)
452	41	HP	13.48	0.95	0.45	0.87	31	16	1.32	E5
479	41	HP	13.96	0.56	-0.12	0.73	41	25	1.00	SBc
487	11	H	15.27	0.50	-0.52	0.30	13	13	0.85	
	15	H	15.20	0.41	-0.33	...			1.15	
	24	H	14.95	0.54	-0.46	0.37			1.92	

Table 1 (continued)

Photometric Observations of Markarian Galaxies

No.	A	Ob	V	B-V	U-B	V-R	D_1	D_2	A/D_1	Morph.
(1)	(2)	(3)	(4)	(5)	(6)	(7)	(8)	(9)	(10)	(11)
489	24	H	14.24	0.47	-0.12	0.65	38	20	0.63	SBb
	38	H	13.94	0.50	-0.13	0.64			1.00	
491	24	H	14.04	0.92	0.52	0.77	16	14	1.50	
	29	HP	14.04	0.93	0.40	0.82			1.81	
496	29	HP	14.07	0.53	-0.35	0.84	22	17	1.32	Sdp+Sdp
499	29	HP	14.55	0.41	-0.26	0.58	15	15	1.93	
534	21	HP	13.21	0.46	-0.23	...	41	35	0.51	Sap
	41	HP	12.94	0.51	-0.18	...			1.00	
	64	DV	12.96	0.58	-0.01	...			1.56	
538	21	HP	13.30	0.44	-0.49	...	54	40	0.39	SBdm?
	57	HP	12.67	0.49	-0.44	...			1.06	
617	31	DV	13.37	0.68	-0.08	...	43	30	0.72	SBbp
	31	DV	13.38	0.65	-0.01	...			0.72	
	43	DV	13.06	0.68	-0.05	...			1.00	
	43	DV	13.04	0.74	-0.01	....			1.00	
620	56	H	12.29	0.98	0.44	0.92	57	45	0.98	SBab
626	41	HP	13.75	0.68	0.01	0.81	28	27	1.46	E0
656	57	H	12.83	0.39	-0.47	0.55	55	41	1.04	Imp?
669	41	HP	13.42	0.94	0.46	0.85	32	22	1.28	E3
685		DP	14.50	0.44	-0.41	...	34	19	1^+	(Sc*)
686	29	HP	13.39	0.88	0.27	0.84	58	36	0.50	
	57	HP	12.93	0.82	0.24	0.83			0.98	SBb*
	57	HP	12.94	0.85	0.23	0.80			0.98	
691	57	HP	13.03	0.43	-0.28	0.68	96	44	0.59	SBd
	81	HP	12.90	0.43	-0.26	0.67			0.84	

Table 1 (continued) (additional observations)

Photometric Observations of Markarian Galaxies

No.	A	Ob	V	B-V	U-B	V-R	D_1	D_2	A/D_1	Morph.
(1)	(2)	(3)	(4)	(5)	(6)	(7)	(8)	(9)	(10)	(11)
48	29	HP	14.70	0.95	0.42	0.78			2.05	
94	14	HP	16.35	0.71	-0.62	0.43			2.00	
178	41	HP	14.58	0.39	-0.48	0.44			0.88	
	81	HP	14.27	0.34	-0.34	0.59			1.72	
188	21	HP	13.55	0.74	0.08	0.84			0.24	
	41	HP	12.78	0.66	-0.01	0.77			0.47	
	81	HP	12.30	0.62	-0.02	0.76			0.92	
190	10	HP	14.10	0.66	-0.21	0.86			0.25	
	21	HP	13.41	0.62	-0.15	0.83			0.50	
	29	HP	13.14	0.65	-0.11	0.81			0.73	
	41	HP	12.95	0.65	-0.07	0.78			1.03	
	81	HP	12.62	0.69	-0.03	...			2.03	
194	29	HP	14.97	0.53	-0.13	0.57	18	13	1.61	
199	41	HP	15.23	0.33	-0.35	0.47	27	9	1.53	
213	57	HP	12.80	0.62	-0.05	0.73	68	26	1.20	SBa
230	29	HP	15.27	0.88	0.11	0.75	13	12	2.23	
234	29	HP	15.37	0.59	-0.24	0.64	25	14	1.16	
271	81	HP	13.05	0.59	0.04	0.70	60	34	1.35	Scp+ SBabp

Table 1 (continued)

Photometric Observations of Markarian Galaxies

SOURCES

AA Arakelian, et al. (1972)

BK Borngen & Kalloghlian (1974)

D Dibay (1970)

DP DuPuy (1968, 1970)

DV Vaucouleurs, G. de (1961) & A. de (1972)

H,HP This paper

HI Hiltner & Iriarte (1958)

S Sargent (1970)

W Weedman (1973)

WK Weedman & Khachikian (1968, 1969)

Table 1 (continued)

Photometric Observations of Markarian Galaxies

NOTES TO TABLE 1

2. MCG 6-5-44

7. MCG 12-7-38, u shaped core of knots

8. IC 2184, ring of H II regions

11. MCG 12-8-11 pair with 12

12. MCG 12-8-13 pair with 11

13. IC 2209, MCG 10-12-17 bright nucleus

14. Bright nucleus

18. MCG 10-13-54

19. MCG 10-13-71. Faint companion to SE

20. MCG 12-9-41

21. MCG 10-14-41, two armed, possibly barred spiral

22. Double knots

25. MCG 10-15-4

26. MCG 10-15-26, bright nucleus

27. Bright star to SE

31. MCG 10-15-65, pair with 30, bright nucleus

33. Haro 2, MCG 9-17-70, patchy with wisps, high surface brightness

35. NGC 3353, Haro 3, MCG 9-18-22, double condensations, high surface brightness

36. Haro 4, MCG 5-26-46, compact

44. IC 2987

45. MCG 10-17-133

Table 1 (continued) (Notes to Table 1)

Photometric Observations of Markarian Galaxies

47. Double object, d = 12", wisp opposite fainter object, the 15" observation refers to just the brighter object

48. Bright nucleus

49. Haro 8, double condensations in patchy halo

52. NGC 4385, Markarian object is the bright blue nucleu

55. Double object

58. MCG 5-31-57, coma cluster member

59. NGC 4861 + IC 3961, I Zw 49, MCG 6-29-3, Arp 266, condensation (H II region or OB association) in a dwarf irregular

60. Coma cluster member with several nearby companions

66. MCG 10-19-72, faint companion

71. NGC 2366, DDO 42. Markarian object is H II region in dwarf irregular

81. MCG 10-11-130

84. MCG 9-13-90, nucleus

85. NGC 2534, elliptical in halo with dust lane

86. NGC 2537, Arp 6, VV 138, circular halo plus 3 bands of H II regions

87. NGC 2544, ringed, barred system with bright nucleus

88. Star to W

89. Patchy lenticular object

90. Bright nucleus, ringed

92. Double, central separation $\sim$ 15".

94. H II region or OB association in SBd spiral

Table 1 (continued) (Notes to Table 1)
Photometric Observations of Markarian Galaxies

96. Companion or star to N. Colors uncertain

100. Colors uncertain

101. Lenticular galaxy with superposed star

108. IC 2458, companion to NGC 2820

111. MCG 12-9-49, bright companion to NW, very knotty

116. I Zw 18, pair of compacts plus outlying fuzz

118. Two knots in an elongated halo

131. NGC 3073, possible structure in outer halo

133. NGC 3066, bright nucleus

138. Irregular plus wisp or companion to N

149. Bright nucleus

151. MCG 8-20-16

153. MCG 9-18-32, nucleus plus fuzz and condensations

158. NGC 3471, possible bar, ring, some structure in disk

161. MCG 8-20-69, very bright arms and nucleus

169. IC 691, lenticular plus condensation

171. NGC 3690 + IC 694, Holm 256, Arp 299, interacting pair, both patchy and bright in Hα

175. MCG 11-14-28, bright central bulge in bar

178. MCG 8-21-53

179. NGC 3725, irregular arms plus ring

185. NGC 3811, disrupted spiral with rings and arms extending south; bright nucleus

186. NGC 3870, patchy with high surface brightness

188. NGC 3888, many H II regions, distorted arm to NW

Table 1 (continued) (Notes to Table 1)

Photometric Observations of Markarian Galaxies

190. NGC 3928

195. MCG 11-15-12, knots to N and S

201. NGC 4194, Arp 160, patchy with fanning wisp to N

207. NGC 4384, bright, irregular nucleus, star to E

213. NGC 4500, strong central bar, bright nucleus, two faint arms

215. MCG 8-23-52

220. MCG 9-21-33, I Zw 41, pair with 221

224. MCG 8-33-92

235. MCG 6-29-10

249. IC 875

251. MCG 9-22-49

256. NGC 5144, perturbed spiral with 3 arms

266. NGC 5256, interacting double object

267. MCG 7-28-45

271. NGC 5278-9, Arp 239, spiral with spiral companion — similar to M51

277. MCG 11-17-9, two condensations plus tail

281. NGC 5383, barred spiral with peculiar arms, bar inside bar. In the Hubble Atlas.

286. NGC 5607

288. MCG 12-14-43

294. Patchy irregular system with superposed star to WSW

297. NGC 6052, Arp 209, VV 86 interacting double system with many H II regions

Table 1 (continued) (Notes to Table 1)

Photometric Observations of Markarian Galaxies

298. IC 1182, in Hercules cluster, jet plus condensations (H II regions) to E, possibly a Seyfert

303. NGC 7244

307. NGC 7316, bright nucleus

308. MCG 3-57-31, knot to N of nucleus

309. IV Zw 121, curved system of condensations with a wisp to S

311. Bright bar

313. NGC 7465, patchy with central bar-like structure perpendicular to the disk

314. NGC 7468. Three condensations with jets N and S

316. NGC 7525, elliptical with companion to N

318. NGC 7580

319. MCG 4-55-1, bright nucleus

321. NGC 7620, bright nucleus

323. NGC 7624, bright nucleus, faint arms

325. NGC 7673, IV Zw 149, disrupted spiral with multiple arms, pair with 326

326. NGC 7677, bright nucleus, two arms almost form outer ring, pair with 325

328. Zwicky compact 2335.2+2952

330. MCG 3-60-20, extension of disk to SE

331. MCG 3-60-36

332. NGC 7798

333. NGC 7805, companion to NGC 7806

334. IV Zw 1, MCG 4-1-13, disrupted spiral? with arm to ESE and wisp to W

Table 1 (continued) (Notes to Table 1)

Photometric Observations of Markarian Galaxies

339. Bright nucleus

341. IC 1559, MCG 4-2-34, companion to NGC 169

343. MCG 2-2-25, bright nucleus with disk and partial ring-like structure

347. IC 1586, III Zw 12

350. MCG 4-3-23

357. Double object

359. MCG 3-4-41, ringed

360. III Zw 33, MCG 3-5-13, distorted spiral, bright nucleus

363. NGC 694, V Zw 122, bright nucleus

368. IC 235

369. II Zw 4, III Zw 50, compact elliptical

370. NGC 1036

384. NGC 2512

386. NGC 2565, barred nucleus plus outside ring, bright blue superposed star to SSE of nucleus. 21" measure is nucleus excluding star

389. NGC 2599, large patchy halo

391. NGC 2691, possible arms

398. MCG 3-24-55

400. MCG 3-24-58, star to NNE

401. NGC 2893, bright bar, faint spiral arms

416. MCG 4-25-44

418. NGC 3442, bright nucleus

426. MCG 6-26-16

Table 1 (continued) (Notes to Table 1)

Photometric Observations of Markarian Galaxies

430. NGC 3921, I Zw 28, Arp 224, peculiar wispy system, bright nucleus

432. NGC 4004, peculiar patchy spiral with long arm to S

439. NGC 4369

442. NGC 4687

444. Haro 37, MCG 6-28-32, superposed star?

449. NGC 5014, edge on spiral with perpendicular dust lane, faint companion to N

450. MCG 6-29-65, low surface brightness, knotty

452. NGC 5142

479. IC 1076, possibly barred

487. I Zw 123

489. NGC 5992, bright bar, faint arms, companion to NGC 5993

491. IC 1144

496. NGC 6090, I Zw 135, interacting pair with bright nucleii, dust lanes, and faint tails like the "mice"

499. I Zw 165

534. NGC 7679. Long extension with knots, possibly spiral arm, to E

538. NGC 7714, Arp 284, tidally disrupted spiral by companion NGC 7715

617. NGC 1614, disrupted system with tail to S and wisp to SE

620. NGC 2273, very near the galactic plane

626. MCG 6-19-21

656. NGC 4673, D.V. calls this E1 but object has distorted, possibly barred structure in halo

Table 1 (continued) (Notes to Table 1)

Photometric Observations of Markarian Galaxies

669. MCG 7-29-51

685. Haro 42, MCG 5-34-61, superposed star?

686. NGC 5695, superposed star

691. NGC 5996, Arp 72. Disrupted spiral, long faint arm from N, broad arm to companion from S

b) Spectroscopic Data

The flux in the Balmer lines is a useful parameter for measuring the contribution of hot stars to the ionization of gas in the galaxy (Zanstra 1931, 1961). We made eye estimates of the relative strength of Hβ with respect to the continuum, and the ratio of the [OIII] λ 5007Å emission intensity to Hβ emission for these galaxies with photometry and available blue spectroscopic data (Sargent 1970a, 1972; Huchra and Sargent 1973, 1976). Equivalent widths in Hβ were available for more than half of these galaxies and some additional galaxies from the work of Weedman (1972) and Arakelian et al. (1970a,b, 1971). These values were used to calibrate our eye estimates in terms of the logarithm of the equivalent width. Equivalent width in emission is defined as a positive quantity. The comparison between our estimated equivalent widths and the measured values gave a standard deviation of 0.11 in the logarithm or about 30% in the actual intensity.

c) Integrated Magnitudes and Colors

Corrections for aperture effects, galactic absorption and redshift are applied to the magnitudes and colors of galaxies. Photometry corrected in these ways to the sky survey diameter system, to zero redshift and to outside the galaxy will be called "integrated" photometry.

Magnitudes are corrected to the Sky Survey (Dss)

diameter system using the standard growth curve of Sandage (1975) adapted from Humason, Mayall and Sandage (1956). For large aperture/diameter (A/D) ratios, this curve is nearly independent of morphological type (de Vaucouleurs and de Vaucouleurs 1964). Figure 1 shows a plot of the multi-aperture data and the growth curve. The multi-aperture data are derived by fitting smooth curves to the magnitudes at different A/D's to find the magnitude at A/D = 1. A comparison of the sky survey diameters and Holmberg's (1958) diameters for galaxies in his catalogue shows that the sky survey diameters are approximately 2.6 times smaller than the Holmberg diameters. Thus the correction to the Holmberg magnitude system, which is based on a limiting blue surface brightness of 26.0 magnitudes per square arc second, is $\Delta B = 0.41$, and our limiting surface brightness is about 23 mag. per square arc sec.

The effect of aperture size on colors is handled by using measurements through apertures with $A/D \geq 0.75$. The color-aperture curves (de Vaucouleurs 1961) are flat or nearly flat there, so corrections are negligible. We try to measure galaxies with apertures as near to their sky survey diameters as possible in order to minimize aperture corrections.

Corrections for galactic absorption are made using the cosecant formula given by Sandage (1973), and using

FIGURE 1

The growth curve. Points are from multi-aperture observations of Markarian galaxies. The curve is adapted from Sandage (1975). This relation is used to correct magnitudes to the standard Dss diameter system.

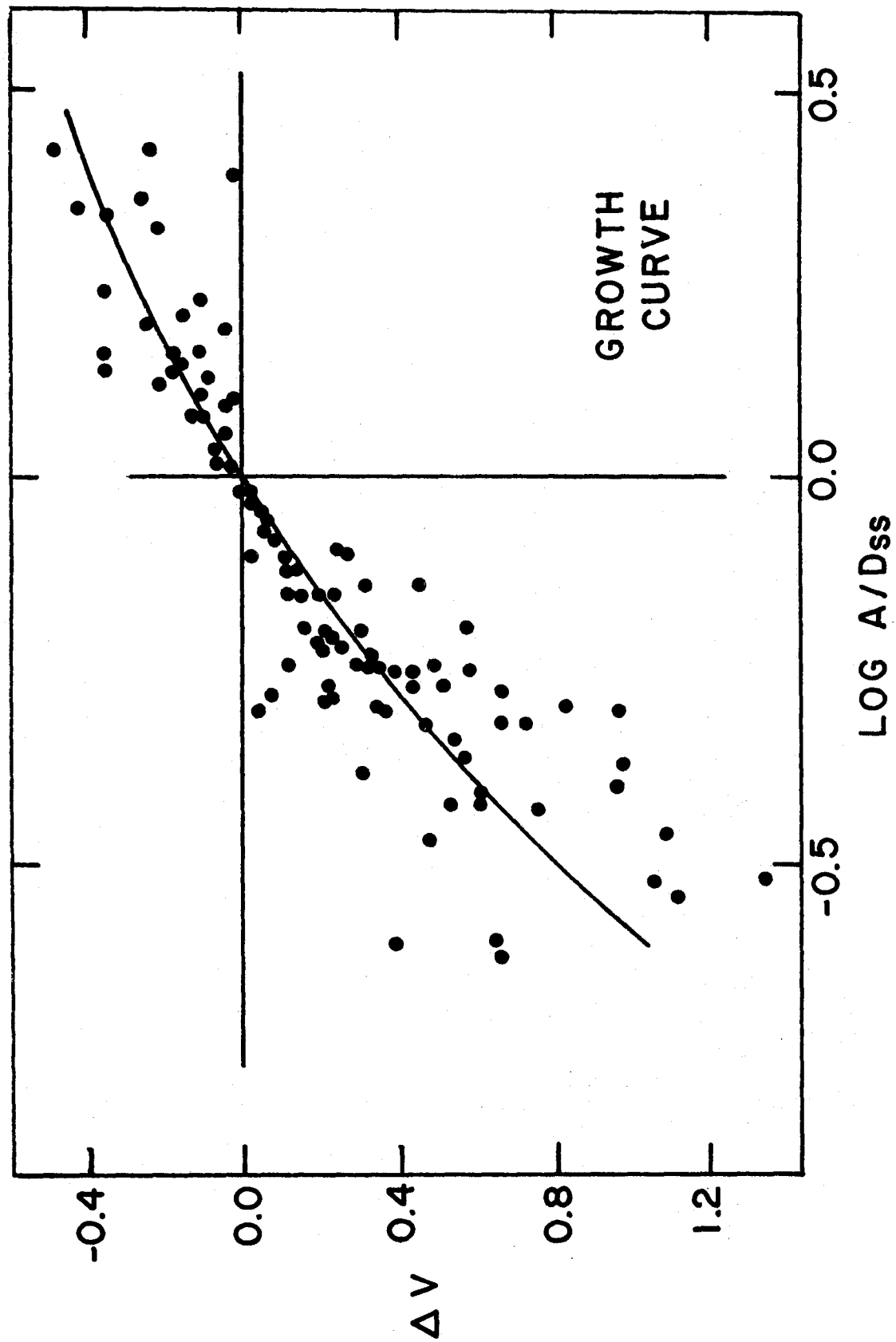
GROWTH
CURVE
0.5
0.0
-0.5
LOG A/Dss
-0.4
0.0
0.4
0.8
1.2
Δ V

the Whitford (1958) law to derive the color corrections:

$$\Delta B = \begin{cases} 0.132\ (\csc(b_{II}) - 1), & |b_{II}| < 50°, \\ 0, & |b_{II}| \geq 50°, \end{cases} \quad (2)$$

$$\Delta(B-V) = 0.25 \times \Delta B, \quad (3)$$

$$\Delta(U-B) = 0.75 \times \Delta(B-V), \quad (4)$$

$$\Delta(V-R) = 0.80 \times \Delta(B-V). \quad (5)$$

No color corrections for radial velocity are applied. It is difficult to apply any simple correction because there is a wide range of spectral energy distributions. In addition, the redshifts of the galaxies studied are generally small, so that the corrections should not be important.

No corrections are applied for inclination effects or internal absorption. These corrections require knowledge of the morphological type, the geometry, and the spatial orientation of the galaxy, information not available for all of the Markarian galaxy sample.

The corrected photometry, several derived parameters, and the available spectroscopic data are presented in Table 2 for the 197 galaxies with reliable large aperture data. The first 91 galaxies are the galaxies in the complete photometric sample. Column (1) lists the Markarian number, column (2) lists the radial velocity in km sec^{-1} corrected

TABLE 2

INTEGRATED PROPERTIES

# (1)	AMB (2)	Vr (3)	V (4)	B-V (5)	U-B (6)	V-R (7)	Hβ† (8)	O/H† (9)	BSB (10)	Log D (11)	Sp type (12)
13	-18.33	1644	14.15	0.52	-0.08	0.71	1.21	1.2	22.47	0.82	sd1(e)
14	-19.57	3281	14.53	0.39	-0.37	0.57	0.79	0.3	21.33	0.85	s12
16	-18.59	2475	14.71	0.59	-0.02	0.73	1.21	2.5	21.51	0.69	ds1
18	-19.73	3401	14.08	0.76	-0.07	0.91	0.79	2.0	21.21	0.87	ds2
19	-19.33	4308	15.33	0.43	-0.68	0.55	1.21	3.0	21.16	0.77	ds1e
20	-19.78	3614	14.52	0.40	-0.31	0.52	1.00	0.6	21.61	0.94	d2
22	-16.41	1561	15.89	0.58	-0.43	0.40	1.42	6.0	21.80	0.31	d1e
25	-19.28	2808	14.27	0.61	-0.21	0.78	0.79	1.0	20.98	0.71	s12(e)
32	-15.31	917	16.13	0.29	-0.16	0.47	0.58	1.0	22.01	0.13	d2
33	-19.52	1681	13.19	0.33	-0.52	...	1.30	2.5	20.43	0.65	sd1e
35	-18.65	1089	13.00	0.45	-0.37	0.62	1.48	3.5	20.95	0.59	ds1e
36	-15.09	623	15.46	0.34	-0.68	0.34	1.86	3.0	21.26	-0.07	d1e
43	-19.74	6128	15.60	0.51	-0.21	0.44	0.58	2.0	21.30	0.92	d12
45	-18.91	4280	15.50	0.66	-0.19	0.74	0.79	2.0	21.48	0.78	ds2
47	-19.74	5930	15.33	0.71	0.23	0.69	0.37	**	21.46	0.92	sd2
48	-19.27	4760	15.08	0.95	0.45	0.77	**	**	21.44	0.81	s2
49	-17.47	1323	14.57	0.48	-0.39	0.62	1.54	4.0	21.60	0.48	ds1e
51	-16.10	1025	15.25	0.62	-0.21	0.67	0.58	2.0	21.28	0.14	ds12
52	-19.22	1938	13.50	0.63	-0.18	...	1.28	0.8	21.56	0.82	s12(e)
53	-19.23	4806	15.67	0.42	-0.31	0.64	1.21	1.0	21.05	0.73	ds12
55	-19.06	4863	15.61	0.68	0.05	0.73	1.00	0.5	21.69	0.82	sd2
59	-17.52	825	13.60	0.38	-0.70	0.08	1.84	2.5	20.70	0.30	d1e
60	-19.01	5156	15.99	0.48	-0.08	0.76	0.58	**	21.72	0.81	ds2(e)
71	-15.64	350	13.61	0.38	-0.30	0.54	1.63	4.0	20.99	0.01	d1e
73	-19.68	4519	14.81	0.69	-0.13	0.88	1.18	0.7	21.07	0.82	sd3e
82	-19.92	5727	14.91	0.88	0.23	0.75	**	**	20.86	0.82	s2(e)
86	-17.48	420	11.99	0.56	-0.15	0.65	0.79	3.0	21.35	0.42	d1e+d3(e)
89	-17.59	1748	15.01	0.53	-0.35	...	0.60	3.0	20.96	0.38	sd2(e)

TABLE 2 (continued) INTEGRATED PROPERTIES

# (1)	AMB (2)	Vr (3)	V (4)	B-V (5)	U-B (6)	V-R (7)	Hβ† (8)	O/H† (9)	BSB (10)	Log D (11)	Sp type (12)
92	-20.40	4330	14.21	0.48	-0.22	...	1.00	1.5	20.42	0.88	sle
93	-19.49	5330	15.39	0.68	-0.29	...	1.48	3.5	21.07	0.79	sdle
95	-18.74	3718	15.59	0.44	-0.13	...	1.00	4.0	21.52	0.73	d2
98	-19.47	3582	14.73	0.49	-0.18	...	0.78	1.3	21.30	0.83	dle
104	-18.86	2251	14.38	0.43	-0.29	...	1.18	3.6	20.96	0.64	sl(e)
105	-18.31	3628	15.73	0.67	-0.12	...	1.40	1.0	21.38	0.61	s2
108	-17.11	1518	15.29	0.41	-0.59	0.49	1.63	4.0	21.77	0.45	dle
116	-15.16	823	16.15	0.19	-0.73	0.41	1.83	2.0	21.31	-0.04	sdle+sdl(e)
118	-18.68	2453	14.71	0.48	-0.14	0.70	0.37	**	21.84	0.82	d3
119	-19.90	3104	13.98	0.49	-0.19	0.68	...	...	20.49	0.75	d2(e)
129	-19.49	4617	15.03	0.72	0.08	0.74	**	**	21.63	0.89	sd3
138	-19.02	4610	15.58	0.63	-0.29	0.68	...	...	21.61	0.85	d2
140	-17.40	1648	15.14	0.46	-0.37	0.61	1.30	3.0	21.04	0.35	sdle
146	-19.65	3326	14.28	0.59	-0.05	0.75	0.58	**	21.07	0.81	sl
149	-18.23	1821	14.33	0.66	0.21	0.67	...	...	20.79	0.46	s3(e)
150	-19.24	3676	15.08	0.42	-0.27	0.63	0.90	2.5	20.59	0.65	sdle
151	-16.86	1538	15.40	0.59	-0.21	0.60	1.18	3.0	21.71	0.39	s2
153	-18.73	2455	14.95	0.19	-0.61	0.31	...	...	21.41	0.71	dl(e)
155	-19.41	1824	13.11	0.70	0.32	0.74	...	...	19.96	0.55	ds3(e)
156	-17.56	1318	14.59	0.36	-0.31	0.50	0.70	3.0	21.67	0.58	d2e
157	-18.29	1456	14.18	0.26	-0.57	0.56	1.60	1.2	20.75	0.48	d2e
165	-19.45	3443	14.62	0.53	-0.19	0.63	0.84	1.7	21.35	0.82	s2(e)
166	-18.48	3238	15.59	0.40	-0.23	0.69	0.78	1.1	21.08	0.58	sl(e)
169	-18.20	1639	14.21	0.58	-0.30	0.79	1.34	3.3	21.44	0.59	sd2(e)
170	-16.96	1058	14.61	0.47	-0.30	0.60	1.21	3.0	21.82	0.46	ds2(e)
177	-17.14	1875	15.71	0.43	-0.19	0.71	...	...	21.86	0.46	ds2
178	-14.31	269	14.36	0.39	-0.34	0.44	1.54	5.0	22.24	-0.02	sd2e
186	-17.39	690	13.25	0.47	-0.22	0.66	0.60	2.0	20.99	0.34	dsle
190	-18.41	1023	12.89	0.66	-0.10	0.84	0.58	0.3	21.29	0.60	sd2

TABLE 2 (continued) INTEGRATED PROPERTIES

# (1)	AMB (2)	Vr (3)	V (4)	B-V (5)	U-B (6)	V-R (7)	Hβ† (8)	O/H† (9)	BSB (10)	Log D (11)	Sp type (12)
195	-17.86	1500	14.31	0.63	-0.13	0.78	1.11	1.8	21.35	0.51	s1e
197	-18.80	2322	14.12	0.83	0.21	0.78	0.48	**	21.81	0.78	s2(e)
199	-17.99	2296	15.36	0.37	-0.36	0.47	**	**	21.40	0.60	d2
202	-19.68	6400	15.58	0.69	-0.16	0.79	...	...	21.15	0.83	d2(e)
206	-16.07	1030	15.24	0.67	-0.21	0.83	1.30	2.3	21.20	0.11	s1(e)
207	-19.91	2488	13.50	0.48	-0.22	0.72	0.48	1.0	21.31	0.91	ds2(e)
209	-15.93	667	14.62	0.49	-0.53	0.16	1.78	3.2	21.51	0.16	d1e
219	-18.37	3097	15.36	0.64	-0.22	0.26	...	...	21.21	0.62	si(e)
223	-16.99	1345	14.98	0.59	-0.21	0.84	1.18	0.5	21.10	0.28	s1(e)
224	-16.23	1274	15.75	0.46	-0.45	0.44	...	...	21.46	0.22	d3
241	-20.20	7829	15.59	0.59	-0.06	0.69	...	...	21.30	0.98	d3(e)
242	-19.75	7233	15.94	0.52	-0.05	0.66	0.79	2.5	21.18	0.87	d3(e)
245	-19.55	6141	15.67	0.64	-0.07	0.81	0.84	0.9	21.38	0.85	s1
249	-19.70	2786	13.60	0.84	0.30	0.88	**	**	21.50	0.91	sd3(e)
251	-19.07	4600	15.71	0.45	-0.24	0.56	...	...	21.48	0.81	d3(e)
253	-19.77	6713	15.47	0.81	0.03	0.83	...	...	21.47	0.96	d3
258	-19.72	7607	15.80	0.80	-0.06	0.74	...	...	21.05	0.82	d3(e)
267	-19.39	3680	14.75	0.60	-0.11	0.74	...	...	21.28	0.82	s1(e)
277	-17.35	1944	15.55	0.46	-0.49	0.35	...	...	21.67	0.48	d1(e)
294	-18.72	2616	14.70	0.58	-0.20	0.63	1.11	2.5	21.42	0.71	d3
296	-19.34	4896	15.61	0.42	-0.42	0.50	...	...	21.93	0.97	s1(e)
314	-19.40	2224	13.80	0.45	-0.34	0.57	1.00	3.0	20.78	0.70	d2(e)
317	-20.04	6507	15.24	0.70	-0.10	0.85	...	...	21.74	1.03	s3(e)
324	-17.49	1700	15.14	0.43	-0.25	0.62	0.58	3.0	21.02	0.36	d2
328	-17.05	1409	15.02	0.59	-0.11	0.77	1.21	0.6	21.48	0.37	ds1e
343	-20.50	5627	14.34	0.83	0.21	0.86	...	...	22.85	1.34	d3e
345	-19.63	4672	14.91	0.73	0.08	0.75	...	...	21.82	0.96	sd3(e)
350	-19.86	5266	15.16	0.50	-0.14	0.56	...	...	21.51	0.95	d2
369	-19.11	3841	15.37	0.37	-0.42	0.59	...	...	20.82	0.65	sd1e

TABLE 2 (continued) INTEGRATED PROPERTIES

# (1)	AMB (2)	Vr (3)	V (4)	B-V (5)	U-B (6)	V-R (7)	Hβ† (8)	O/H† (9)	BSB (10)	Log D (11)	Sp type (12)
370	-17.69	860	13.36	0.53	-0.21	0.68	1.00	1.5	21.56	0.52	ds2
375	-18.25	3719	15.82	0.70	-0.30	0.39	...	...	21.42	0.60	d2
398	-19.47	4099	14.94	0.56	-0.18	0.76	...	...	21.56	0.90	d3
400	-19.04	2306	14.26	0.42	-0.26	0.65	...	...	21.10	0.69	d2
401	-19.16	1748	13.29	0.68	-0.07	0.73	...	...	21.33	0.76	sd3
2	-21.63	5682	13.51	0.55	-0.16	...	0.79	**	21.12	1.22	s12
5	-16.17	1018	15.30	0.48	-0.35	...	1.63	5.0	21.98	0.33	d1e
7	-19.68	3174	14.48	0.25	-0.38	...	0.58	3.0	21.24	0.87	d12
8	-19.98	3420	14.21	0.39	-0.40	...	1.32	3.0	21.58	0.98	d1
12	-21.73	4119	12.82	0.44	-0.37	...	0.79	**	21.39	1.29	d2
26	-20.60	9132	15.71	0.41	-0.34	0.53	...	...	21.77	1.15	d12(e)
27	-16.85	2215	16.34	0.46	-0.24	0.42	1.21	3.5	21.55	0.35	d1
41	-20.26	5870	14.84	0.66	-0.15	...	**	**	21.37	1.00	sd12(e)
44	-20.34	6924	15.16	0.62	0.01	...	0.37	**	21.38	1.02	s12
46	-18.04	3753	16.34	0.41	-0.13	0.44	0.58	3.5	21.44	0.56	d2
58	-19.77	5362	15.30	0.49	-0.06	...	...	...	21.49	0.92	s2
66	-20.82	6807	14.84	0.42	-0.31	...	0.79	2.5	21.00	1.04	d2(e)
67	-15.45	1120	16.19	0.52	-0.40	0.45	1.63	3.5	21.64	0.08	sd1e
84	-21.57	6120	13.86	0.42	-0.21	...	1.00	**	21.31	1.26	s2
85	-20.21	3582	13.65	0.82	0.30	...	**	**	21.56	1.02	s3(e)
87	-20.01	2870	13.32	0.87	0.21	...	1.00	**	22.19	1.11	ds3e
88	-21.55	9197	14.59	0.60	-0.08	...	0.79	0.4	20.75	1.13	d2(e)
90	-20.43	4284	13.94	0.71	0.01	...	0.37	**	22.08	1.17	s3
94	-14.12	754	16.48	0.70	-0.58	0.41	1.63	4.5	20.97	-0.32	d1e
99	-18.28	3683	16.00	0.47	-0.40	...	0.84	3.0	21.77	0.68	d3(e)
101	-21.37	4793	13.38	0.57	0.02	...	0.79	0.3	20.97	1.14	s1
111	-20.47	3745	13.90	0.41	-0.28	...	0.88	2.5	21.27	1.02	s2(e)

TABLE 2 (continued) INTEGRATED PROPERTIES

# (1)	AMB (2)	Vr (3)	V (4)	B-V (5)	U-B (6)	V-R (7)	Hβ† (8)	O/H† (9)	BSB (10)	Log D (11)	Sp type (12)
131	-17.57	1094	13.92	0.62	0.05	0.68	0.26	**	21.33	0.44	sd2
133	-19.87	2260	13.16	0.65	-0.03	...	0.18	2.0	21.64	0.96	s1(e)
158	-20.08	2144	12.77	0.72	0.20	0.81	0.30	0.2	21.84	1.07	s2(e)
161	-21.51	5937	13.74	0.53	-0.15	0.75	0.48	1.4	21.26	1.23	s2(e)
171	-21.90	3062	11.89	0.56	-0.34	...	1.45	1.1	21.38	1.32	sd1e+d1
175	-20.16	3750	13.70	0.93	0.32	...	**	**	21.70	1.05	ds3(e)
181	-21.19	6170	14.18	0.50	-0.15	0.72	0.58	0.6	20.82	1.08	ds3
185	-21.01	3090	12.70	0.65	0.02	0.77	**	**	22.37	1.34	sd3
188	-21.01	2502	12.27	0.63	-0.04	0.77	**	**	21.80	1.24	sd3
194	-22.20	15622	15.15	0.53	-0.13	0.57	...	...	21.28	1.37	s1(e)
201	-20.68	2670	12.84	0.53	-0.18	0.79	1.00	1.7	20.92	0.99	ds2e
213	-20.99	3101	12.76	0.62	-0.05	0.73	...	...	21.20	1.15	sd2(e)
215	-20.69	5760	14.45	0.58	-0.16	...	0.48	2.7	20.59	0.92	s1(e)
230	-22.02	21427	15.67	0.88	0.11	0.75	...	...	21.71	1.41	d3
234	-17.63	2229	15.44	0.59	-0.24	0.64	...	...	22.10	0.62	d3(e)
235	-21.29	7527	14.55	0.46	-0.22	0.56	...	...	21.56	1.24	ds3(e)
247	-21.28	9706	15.04	0.53	-0.20	...	0.84	0.9	20.72	1.07	s1e
256	-20.83	3151	13.23	0.35	-0.43	0.58	...	...	21.83	1.20	d1e
266	-22.36	8495	13.40	0.80	0.13	0.80	1.30	2.0	20.82	1.30	d3+d3
271	-22.59	7768	13.19	0.59	0.04	0.70	0.47	1.7	21.60	1.53	d3e+d3e
281	-21.20	2349	11.86	0.71	0.13	...	**	**	22.53	1.41	sd2e
286	-22.36	7965	13.58	0.49	-0.13	0.69	0.89	1.0	21.22	1.39	sd2
288	-21.82	7675	14.25	0.27	-0.57	0.41	...	...	21.01	1.29	d2
297	-21.71	4801	13.18	0.44	-0.37	0.56	1.34	2.5	21.16	1.24	s1(e
303	-21.62	7706	14.15	0.58	-0.09	0.78	...	...	21.11	1.24	d2
307	-21.86	5721	13.29	0.55	-0.17	0.71	0.58	**	21.40	1.32	d2e
308	-21.09	7207	14.53	0.58	-0.09	0.76	1.42	2.5	21.25	1.15	sd2e
309	-21.95	12844	14.97	0.54	-0.36	0.62	0.79	**	21.55	1.40	sdie

TABLE 2 (continued) INTEGRATED PROPERTIES

# (1)	AMB (2)	Vr (3)	V (4)	B-V (5)	U-B (6)	V-R (7)	Hβ† (8)	O/H† (9)	BSB (10)	Log D (11)	Sp type (12)
311	-21.62	9322	14.47	0.67	-0.01	0.87	0.58	**	21.33	1.26	ds2e
312	-21.69	10095	14.69	0.55	-0.23	0.78	...	...	21.19	1.26	d3
313	-19.99	2008	12.70	0.74	0.04	0.93	0.58	2.0	20.83	0.84	sd2
318	-21.08	4951	13.76	0.54	-0.15	0.81	0.37	**	21.30	1.15	d2
319	-21.91	8140	13.93	0.63	0.01	...	...	...	21.17	1.29	sd2e
321	-22.85	9805	13.40	0.62	0.05	0.83	...	...	21.74	1.59	sd2e
323	-21.19	4711	13.36	0.73	0.07	...	...	...	21.59	1.23	sd2
325	-21.23	3501	13.06	0.35	-0.43	...	...	...	21.05	1.12	d2e
326	-20.60	4100	13.67	0.71	0.06	...	...	...	21.65	1.12	ds3(e)
330	-20.34	4260	14.35	0.37	-0.22	....	0.37	6.0	21.98	1.14	ds1(e)
331	-21.06	5548	13.78	0.79	0.24	1.17	...	...	21.25	1.14	sd3e
332	-21.21	2882	12.35	0.65	-0.08	0.82	...	...	21.60	1.22	s2e
333	-20.77	4944	13.64	0.98	0.57	0.86	**	**	20.93	1.01	d3e
336	-21.06	5302	13.73	0.74	0.16	...	...	...	20.91	1.07	d3e
339	-20.67	5555	14.42	0.55	-0.08	0.78	...	...	21.72	1.15	d3
341	-20.25	4671	14.28	0.73	0.13	...	...	...	21.15	0.96	sd2(e)
347	-20.73	6161	14.71	0.42	-0.31	0.73	...	...	21.09	1.03	d2e
357	-22.26	16343	15.38	0.34	-0.69	0.37	...	...	21.13	1.35	s2e
359	-21.01	5230	13.84	0.65	-0.09	...	...	...	21.21	1.11	sd2e
360	-21.39	8214	14.70	0.41	-0.21	0.61	...	...	22.02	1.35	sd2e
363	-19.83	2947	13.88	0.55	-0.18	0.88	0.58	**	21.22	0.89	d2
367	-21.22	11195	15.30	0.64	-0.03	0.84	...	...	21.52	1.23	d3
368	-21.59	9092	14.58	0.54	-0.20	0.65	...	...	21.50	1.29	d3e
386	-21.67	3604	12.14	0.88	0.40	0.84	...	...	21.53	1.33	sd3e
389	-21.39	4406	12.91	0.83	0.32	...	**	**	21.21	1.19	sd3(e)
391	-20.29	3891	13.84	0.73	0.12	...	...	...	21.10	0.96	d2(e)
407	-17.45	1640	15.11	0.43	-0.27	0.59	...	...	21.06	0.36	sd3(e)
408	-17.58	1434	14.67	0.45	-0.34	0.55	...	...	21.05	0.39	ds2

TABLE 2 (continued) INTEGRATED PROPERTIES

# (1)	AMB (2)	Vr (3)	V (4)	B-V (5)	U-B (6)	V-R (7)	Hβ† (8)	O/H† (9)	BSB (10)	Log D (11)	Sp type (12)
411	-17.59	1466	14.68	0.48	-0.20	0.58	...	...	21.09	0.40	d3
416	-17.36	1262	14.36	0.70	-0.07	0.67	...	...	21.10	0.38	sd2(e)
418	-19.05	1689	13.58	0.42	-0.26	0.65	...	...	21.17	0.71	d2(e)
426	-17.78	1499	14.56	0.45	-0.40	0.54	...	...	21.60	0.57	d3
429	-17.17	1290	14.62	0.68	0.01	0.83	...	...	21.17	0.33	ds2(e)
430	-20.94	6023	14.11	0.76	0.32	0.74	...	...	22.61	1.38	sd2e
432	-20.44	3417	13.68	0.46	-0.27	0.67	...	...	21.75	1.13	ds2(e)
439	-19.45	1053	11.94	0.64	-0.03	0.76	...	...	21.98	0.94	sd2(e)
444	-19.43	4526	15.25	0.51	-0.29	0.71	...	...	21.25	0.80	d2(e)
449	-18.66	1183	12.96	0.66	0.02	0.72	...	...	21.51	0.78	d2e
450	-16.90	880	14.22	0.52	-0.44	0.50	...	...	22.31	0.51	dle
452	-20.99	5350	13.62	0.95	0.45	0.87	**	**	20.99	1.09	sd3
479	-21.43	6417	13.96	0.56	-0.12	0.73	...	...	21.72	1.31	d3
487	-15.68	783	15.21	0.50	-0.52	0.31	1.63	3.5	21.01	-0.01	d2e
489	-22.35	9440	13.94	0.50	-0.13	0.64	...	...	21.32	1.42	d2+d2e
491	-23.10	19049	14.28	0.93	0.46	0.80	...	...	20.76	1.44	d3e
496	-21.95	8874	14.19	0.52	-0.36	0.83	...	...	20.82	1.22	s2e+sd2
499	-21.20	7685	14.75	0.39	-0.26	0.56	...	...	20.77	1.06	s3(e)
534	-22.09	5301	12.94	0.51	-0.18	...	...	...	21.02	1.29	ds3e
538	-21.10	2974	12.69	0.49	-0.44	...	...	...	21.22	1.13	s2e
617	-21.74	4959	12.97	0.68	-0.05	...	...	...	21.11	1.24	sd2e+sd3
620	-21.56	2100	11.31	0.66	0.20	0.64	...	...	20.20	1.02	sd3
626	-20.34	3914	13.88	0.66	-0.01	0.79	...	...	21.42	1.02	ds3
656	-22.91	6988	12.84	0.39	-0.47	0.55	...	...	21.29	1.51	ds2(e)
669	-21.09	5386	13.54	0.94	0.46	0.85	**	**	21.28	1.15	sd3(e)
685	-20.18	4571	14.60	0.44	-0.41	...	...	...	21.75	1.07	d3e
686	-21.38	4367	12.92	0.82	0.24	0.83	0.26	**	21.72	1.30	ds2
691	-21.31	3310	12.79	0.42	-0.27	0.66	1.00	1.2	21.97	1.35	s2e

TABLE 2 (continued) INTEGRATED PROPERTIES

† asterisks indicate that Hβ and/or [O III]λ5007 were not found on spectra taken in the blue.

assuming a galactic rotation of 250 km sec^{-1} at the sun, and column (3) lists the absolute B magnitude corrected to the Holmberg system as outlined above. Column (4) lists the corrected V magnitude inside a circular aperture of Dss, and columns (5) to (7) list the corrected B-V, U-B, and V-R colors. Column (8) lists the logarithm of the Hβ equivalent width in emission. Column (9) lists the λ 5007 to Hβ ratio. Column (10) lists the mean blue surface brightness defined as

$$\text{BSB (magnitudes per square arc second)} = B + 2.5 \log (\pi D_1 D_2), \quad (6)$$

and column (11) lists the logarithm of the average of the major and minor axes in kiloparsecs.

Finally, column (12) gives the two-dimensional spectral characterization of Markarian - s, sd, ds, d describing "stellar" to "diffuse" appearance of the spectrum (the apparent concentration on the objective prism plate); 1, 2, 3 describing the extent of the spectrum into the ultraviolet and e, e: indicating the presence or possible presence of emission. Markarian's color characterization is correlated with the integrated colors. From our photometry, class 1 has a mean U-B of -0.33, class 2 has a mean of -0.17, and class 3 has a mean of -0.03.

d) Morphological Classifications

Classifications of all the galaxies in the morphological sample defined above were made from a photographic survey plus available material from other sources. Seventy percent of the classifications have been made on the basis of large scale (15".5 per mm) photographs taken with a 40-mm ITT-F4539-S20 image tube (10%)or a 90-mm ITT-F4092-S25 image tube (60%) in the bandpass between 6000 Å and 7000 Å with the 1.5-m Palomar telescope. Twenty percent have been classified on the basis of 1.2-m Palomar Schmidt plates (67".5 per mm) taken mostly in the blue, and the remaining ten percent have been classified using material in the Arp Atlas (Arp 1966), the Palomar Sky Survey, and classifications given in de Vaucouleurs and de Vaucouleurs (1964), Kalloghlian (1971), and Borngen and Kalloghlian (1975). Table 3 lists the classifications, sources, apparent photographic magnitude from the Zwicky catalogue (Zwicky et al. 1961-1968), integrated colors when available, and classifications by other observers. Our classifications agree well with those of Borngen and Kalloghlian, and with the Reference Catalogue classifications of brighter galaxies, but tend to be later in type for the fainter and more peculiar systems than the Reference Catalogue. For most galaxies the classification is relatively straightforward. For the more disturbed, interacting, or otherwise structurally peculiar

TABLE 3

THE MORPHOLOGICAL SAMPLE

No.	Morph.	Source	Mp	B-V	U-B	Remarks
3	E	P	13.8	1.15	0.14	Seyfert
7	Im	P,S	13.9	0.25	-0.38	(K) Im
8	Im	P,S	13.8	0.39	-0.40	(K) Im
10	SBbc	S,BK	14.0	0.63	-0.39	(K) SBb; (BK) SBbc; Seyfert
12	SBc	P	12.7	0.44	-0.37	(K) Sc
33	Im?	P	13.5	0.33	-0.52	(BK) S0; Haro 2
35	Im	P	14.0	0.45	-0.37	(V)(S*); Haro 3
52	SBab	P	13.4	0.63	-0.18	(R) LBT + *; (V) (SB2 4)
59	Im	A,SS	(13.2)	0.38	-0.70	H II region in NGC 4861, (R) SBS9*, (V) (I 8), Arp 266
71	Im	S	(12.6)	0.38	-0.30	H II region in DDO 42
79	SBc	SS	13.3	0.47	-0.64	Seyfert
84	Im	P	13.6	0.42	-0.21	
85	E1p	P	13.8	0.82	0.30	(R) E1
86	Sm	P,S	12.0	0.56	-0.15	(R) IBS9P; (V)(S *); Arp 6
87	SB0/a	P	13.4	0.87	0.21	(R) L..*
90	SBb	K	13.9	0.71	-0.01	(K) SBb
101	S0*	P	13.6	0.57	-0.02	Superposed star
111	Im	SS	13.9	0.41	-0.28	
131	E1	S	13.8	0.62	0.05	(R) E...P$
133	Sc	P	12.8	0.65	-0.03	(R) SAB (s) bc p
155	S0/a	P	13.2	0.70	0.32	
157	Im	P	14.0	0.26	-0.57	
158	Sab	P	13.0	0.72	0.20	
161	SBc	P	13.4	0.53	-0.15	
171	Sc+Im	S	11.8	0.56	-0.34	(R) S...P; (V) (S T), Arp 299
178	Sm	S	13.9	0.39	-0.34	
179	SBbc	P	13.6	0.67	0.11	(BK) SB(r)bc
181	SBc	P	13.9	0.50	-0.15	
185	SBcdp	P	13.0	0.65	-0.02	
186	SB0/a?	P,S	13.2	0.47	-0.22	(BK) SB0/a
188	Sc	P	12.6	0.63	-0.04	(R) SXT5; (V) (S 3 4*)
190	S0/E	P,S	13.1	0.66	-0.10	(BK) S0
201	Smp	P,A	13.0	0.53	-0.18	(R) LB .. P; Arp 160
207	Sbc	P	13.5	0.48	-0.22	
213	SBa	S	13.2	0.62	-0.05	(R) SBS1

Table 3 (continued)

The Morphological Sample

No.	Morph.	Source	Mp	B-V	U-B	Remarks
249	S0	S	13.9	0.84	0.30	
256	Sd	P,S	13.2	0.35	-0.43	(R) S..7P$
271	Sc+SBab	S,A	13.6	0.59	-0.04	(R) SAS.P+SBS1P, Arp 239
281	SBb	P,H	12.5	0.71	0.13	(R) SBT.P; (V) (SB3 3)
286	Scd?	P,S	13.9	0.49	-0.13	
307	SBc	P,S	13.7	0.55	-0.17	
313	Ep	P,S,R	13.3	0.74	0.04	(R) E....*
314	Im?	P,S	14.0	0.45	-0.34	
319	SBb	P	14.0	0.63	-0.01	(BK) Sb
321	Sc	P,S	13.5	0.62	-0.05	(BK) Sc
323	Scd	P	13.7	0.73	0.07	
325	Sdm	P,S	12.7	0.35	-0.43	
326	SBb	P,S	13.9	0.71	0.06	(BK) Sb(r)bc
332	SBc	S	12.7	0.65	-0.08	(BK) SBb
336	E5	P	13.8	0.74	0.16	
341	E3	P	13.3	0.73	0.13	(R) E
359	SB0r	P	13.8	0.65	-0.09	
363	Scp	P,S	13.7	0.55	-0.18	(R) S...5
370	Sm	P,S	13.5	0.53	-0.21	
386	SBb*p	SS	13.8	0.88	0.40	Superposed star; (R) SB.3
389	S0/a	S	13.4	0.83	0.32	
391	Sa	P	13.9	0.73	0.12	
401	SBb	SS	13.6	0.68	-0.07	
418	Sab	P	13.2	0.42	-0.26	
421	E1	S	13.1	0.45	-0.54	BL Lac type spectrum
430	P	A	13.4	0.76	0.32	(R) L...P, Arp 224
432	SBdmp	P	14.0	0.46	-0.27	
439	Sa	R	12.3	0.64	-0.03	(R) RSAT1; (V)(S 0)
449	Sap	P	13.5	0.66	0.02	
452	E5	P	14.0	0.95	0.45	
479	SBc	P	13.9	0.56	-0.12	
496	Sdp+Sdp	P	14.0	0.52	-0.36	
501	E2/S0	P,S	13.7	0.83	-0.01	BL Lac type spectrum
531	S0/E3	P	13.1	...	...	
533	SBbc	P	13.6	...	...	
534	Sap	P	13.2	0.51	-0.18	(R) LB..P*; (V) (S N+)
538	Sdmp	A	13.1	0.49	-0.44	(R) SBS3P*; Arp 284
545	SBab	SS,R	12.3	...	...	(R) SBS1; (V) (S T *)
555	Sd	P	12.9	...	...	(R) SAT3P*; (V) (I *)

Table 3 (continued)

The Morphological Sample

No.	Morph.	Source	Mp	B-V	U-B	Remarks
558	S0	P	14.0			
565	S0p	P,SS	13.8			
573	S0	P	14.0			Seyfert
575	SBbc	SS	14.0			(BK) SBb
582	Im	P,SS	14.0			
590	Sa?	S	14.0			(BK) S0/a; Seyfert
602	SBbc	P	13.8			
607	S0/a	P	14.0			
608	E3*	P	13.7			Superposed star
616	E2p	P,SS	13.3			
617	SBbp	S	14.0	0.68	-0.05	(R) SBS.P
620	SBab	SS	12.5	0.66	0.20	
626	E0	P,S	13.8	0.66	-0.01	
656	Imp?	S	13.7	0.39	-0.47	(R) E.1+
669	S0/E3	P	13.9	0.94	0.46	
686	SBb	P	13.9	0.82	0.24	
691	SBd	A	13.2	0.42	-0.27	Arp 72

Sources

P - Palomar 1.5 m plates
S - Palomar 1.2 m Schmidt plates
SS - Palomar Sky Survey
A - Arp (1966)
K - Kalloghlian (1971)
BK - Borngen and Kalloghlian (1975)
R - de Vaucouleurs and de Vaucouleurs (1964)
V - van den Bergh in de Vaucouleurs and de Vaucouleurs (1964)
H - Sandage (1961)

Table 3 (continued)

NOTES TO TABLE 3

3. MCG 12-6-19

10. MCG 10-11-138, bright nucleus

79. MCG 8-14-33

421. Double object, elliptical with bright nucleus plus much fainter lenticular companion

501. MCG 7-35-2, very bright nucleus

531. NGC 7648, large halo, possible structure in halo

533. NGC 7674

545. NGC 23

555. NGC 245, knot to S

558. NGC 279

565. IC 89, outer ring

573. MCG 0-5-33

590. NGC 863

602. IC 277, bright nucleus

607. NGC 1320, edge on, companion to MK 608

608. NGC 1321, superposed star to ENE, companion to MK 607

616. NGC 1588, II Zw 12, wisps to S, interacting with NGC 1587

systems, however, classification in the modified Hubble sequence is difficult. Our classifications of such galaxies is meant only for the purpose of general comparison. More detailed descriptions are available for the Markarian galaxies with photometry in the notes to Table 1, and for the galaxies without photometry and Markarian Seyferts in the notes to Table 3.

III. COMPARISONS WITH FIELD GALAXIES

(a) Integrated Colors

A large amount of raw UBV photometric data for field galaxies is available from the work of de Vaucouleurs (1959, 1961) and de Vaucouleurs and de Vaucouleurs (1972). A comparison of our measured diameters and the de Vaucouleurs and de Vaucouleurs (1964) Reference Catalogue (DRC) diameters for 75 galaxies shows that $D_{SS}/\Delta RC \cong 1.50$, with small dependence on morphological type. Using this calibration we correct the field galaxy photometry for 336 galaxies that have been observed through apertures with $A/D_{SS} \geq 0.70$, in exactly the same manner as we corrected the Markarian galaxy photometry. We stress again that magnitudes and colors in this system are well defined because the growth curve and the color-aperture curves are fairly flat for large apertures. Unfortunately observational effects exist which affect the measurement of galaxy diameters.

Two examples are the change in limiting isophote as a function of morphological type (de Vaucouleurs and de Vaucouleurs 1964) and as a function of apparent magnitude (Paturel 1975a, 1975b). These will limit our ability to compare diameters and surface brightnesses.

Figure 2 shows the corrected U-B versus B-V plot for field galaxies. The color-color relation is well

FIGURE 2

The color-color distribution of field galaxies. The rectangular envelope is described in the text.

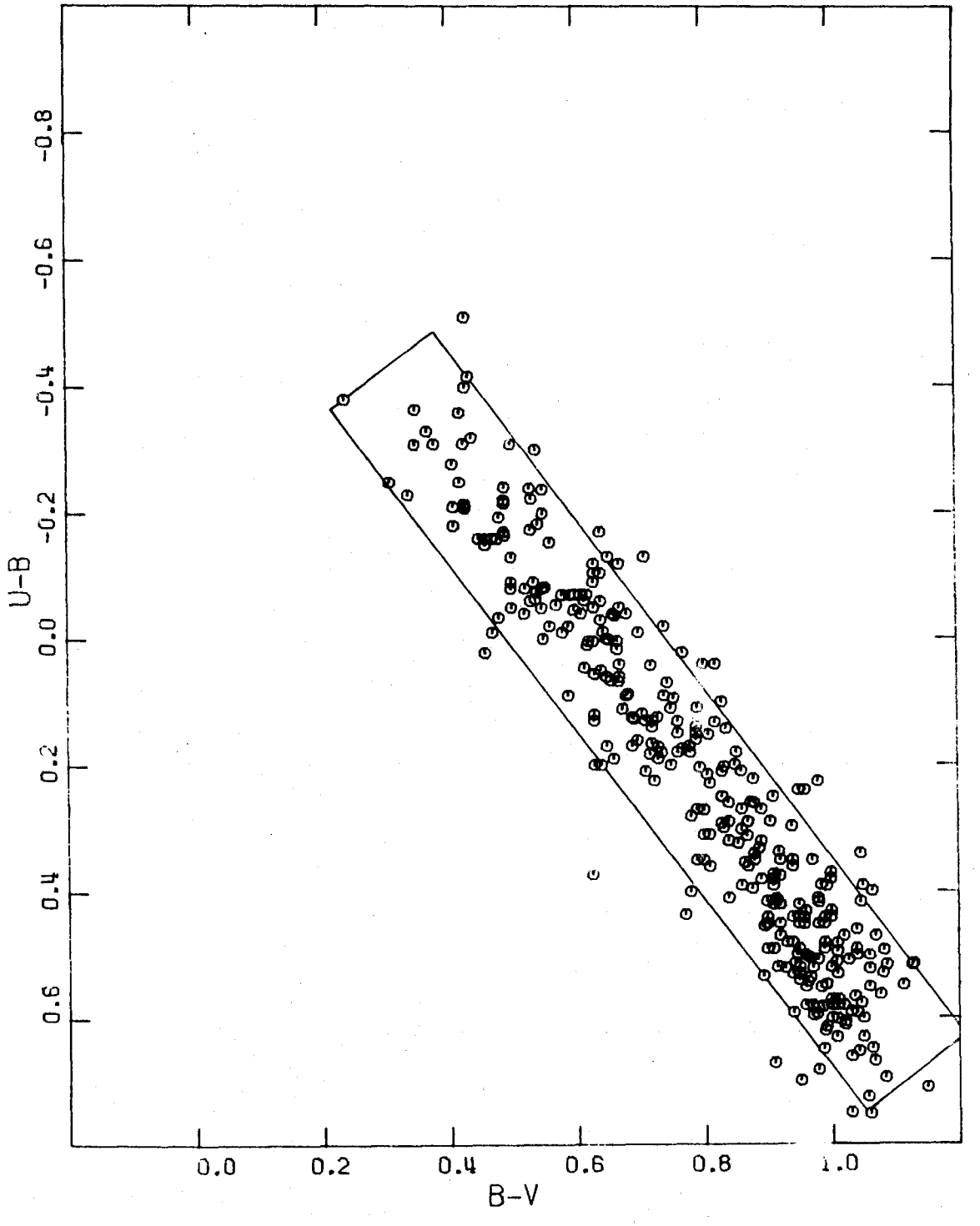
U-B
-0.8
-0.6
-0.4
-0.2
0.0
0.2
0.4
0.6
0.0
0.2
0.4
0.6
0.8
1.0
B-V

represented by the linear fit

$$(U-B) = [1.33\pm0.03] \times (B-V) - [-0.82\pm0.02] \quad (7)$$

The rectangle drawn has sides parallel to this relation 0.2 magnitude wide, and ends defined by the bluest and reddest galaxies in the sample. This rectangle contains 92% of the field galaxies.

Figure 3 shows the U-B versus B-V plot for the Markarian galaxies superposed on the field galaxy rectangle. The linear fit to these data is given by:

$$(U-B) = [1.32\pm0.06] \times (B-V) - [-0.90\pm0.04] \quad (8)$$

The color-color relations are essentially the same except for a U-B excess of the Markarian galaxies at the blue end. There are little data there for field galaxies. Seventy-four percent of the Markarian galaxies fall inside the field galaxy rectangle. The distribution of galaxy colors is continuous.

Few observations of field galaxies exist in the V-R color, so comparisons cannot be made with the available data for Markarian galaxies.

Table 5 contains the mean colors, mean blue surface brightness and the reddening independent parameter, $Q \equiv (U-B) - 0.72\ (B-V)$, for the field galaxies and the galaxies with photometry in the morphological sample as a function of morphological type. Also presented are the parameters for all field galaxies, all Markarian galaxies, and all Markarian galaxies in the photometric sample. The variation in

FIGURE 3

The color-color distribution of Markarian galaxies superposed on the field galaxy envelope (Figure 2).

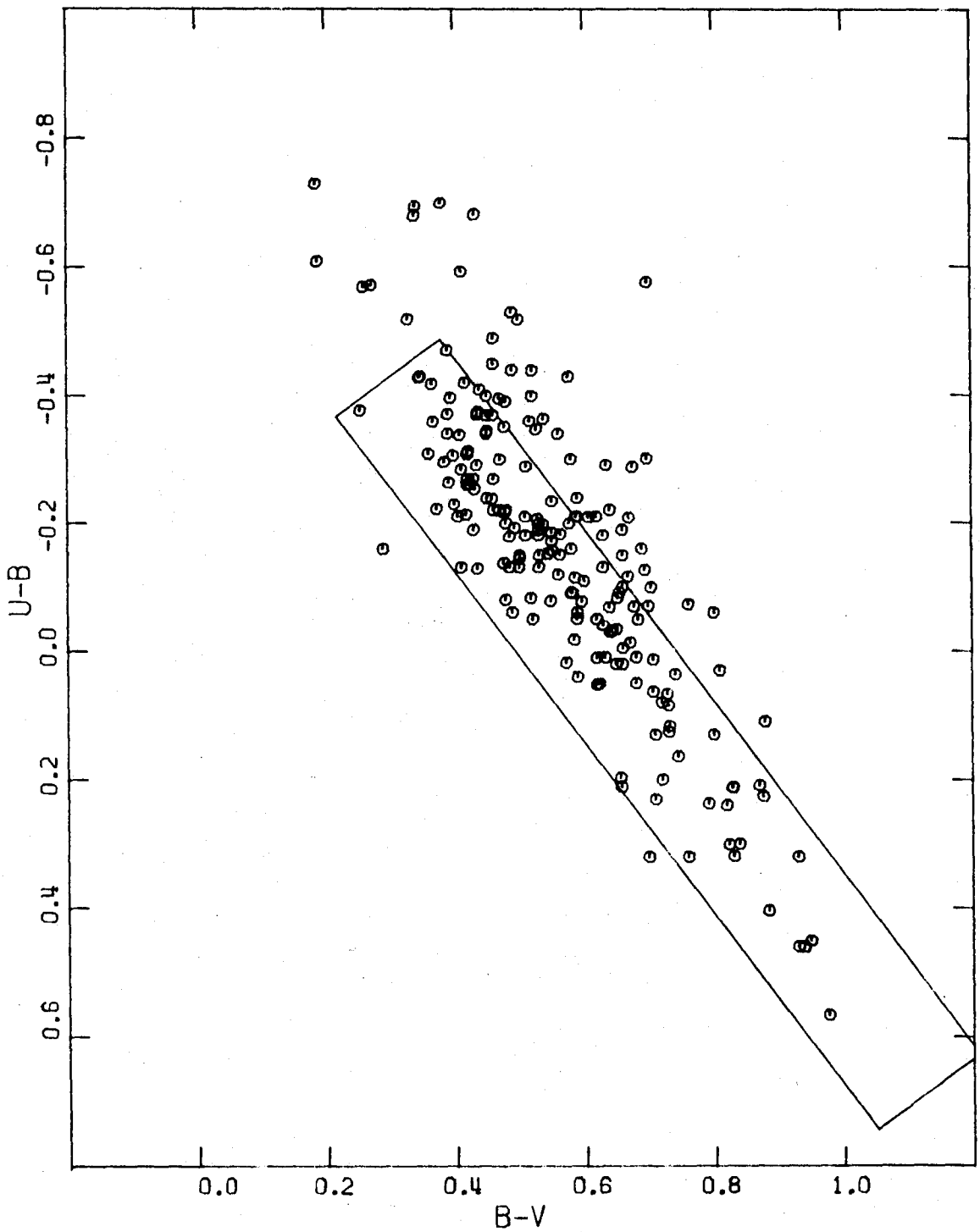
U-B
-0.8
-0.6
-0.4
-0.2
0.0
0.2
0.4
0.6
0.0
0.2
0.4
0.6
0.8
1.0
B-V

TABLE 5

MEAN COLORS OF GALAXIES

Type	#	B-V	U-B	Q	BSB
FIELD GALAXIES					
E	64	0.96	0.49	-0.20	21.0
E^+	11	0.95	0.46	-0.23	21.0
L^-	17	0.97	0.46	-0.24	21.0
L	20	0.92	0.44	-0.22	21.1
L^+	16	0.91	0.42	-0.23	21.5
S0/a	8	0.90	0.40	-0.25	21.6
Sa	11	0.87	0.31	-0.32	21.6
Sab	14	0.83	0.26	-0.34	21.6
Sb	36	0.77	0.18	-0.38	21.8
Sbc	32	0.71	0.08	-0.43	21.9
Sc	28	0.62	0.00	-0.44	21.9
Scd	8	0.54	-0.14	-0.52	21.9
Sd	8	0.58	-0.09	-0.51	22.3
Sdm	5	0.54	-0.14	-0.53	21.8
Sm	5	0.42	-0.28	-0.58	21.7
Im	4	0.46	-0.23	-0.55	21.4
Irr II	9	0.83	0.25	-0.35	21.2
E,L,S0 P	17	0.74	0.18	-0.35	21.2
Sa-Im P	19	0.57	-0.05	-0.46	21.8
P	9	0.73	0.07	-0.46	21.3
All Types	341	0.79	0.23	-0.34	21.5
MARKARIAN GALAXIES					
All Types	197	0.57	-0.15	-0.57	21.4
Photometric Sample	91	0.54	-0.21	-0.61	21.4
E-L †	7	0.75	0.16	-0.39	21.2
S0-S0/a †	9	0.73	0.14	-0.40	21.2

TABLE 5 (continued)

MEAN COLORS OF GALAXIES

Type	#	B-V	U-B	Q	BSB
Sa-Sab †	9	0.62	-0.02	-0.39	21.5
Sb-Sbc †	10	0.70	0.06	-0.46	21.6
Sc-Scd †	15	0.58	-0.11	-0.54	21.5
Sd-Sdm †	6	0.43	-0.37	-0.69	21.4
Sm-Im †	15	0.41	-0.36	-0.66	21.2

† Photometry from the non-Seyfert galaxies in the Morphological Sample.

mean surface brightness as a function of morphological type can be ascribed to the diameter versus morphological effect mentioned earlier.

On the average, the mean surface brightness of Markarian galaxies is similar to that of field galaxies of the same morphological type. On the other hand, the average colors of the Markarian galaxies are significantly bluer for each morphological type than the field galaxy colors. The average colors of all the Markarian galaxies are similar to the average colors of the late type field galaxies.

(b) Color-Aperture Relations

For many of the Markarian galaxies, observations have been made through several apertures of different size. Figures 4, 5, and 6 are plots of the color versus aperture data in U-B, B-V, and V-R. The points are derived from fitting a smooth curve to colors measured through three or more aperture sizes or from two aperture measurements with one aperture within 10% of the galaxy's diameter, defined as having $\Delta C = 0$. The scatter is large because the data are inhomogeneous in morphological type, because observations from different sources are used and because the error in color differences are expected to be larger than the errors in the colors themselves. A general trend of decreasing color (bluer) with smaller aperture size is visible in U-B and B-V. This effect is weak if not reversed in V-R and is weaker in B-V than in U-B. The bluer colors get bluer

FIGURE 4

The color-aperture relation for U-B. Log A/Dss is the logarithm of the measuring aperture size over the standard sky survey diameter for any galaxy. The points are from the Markarian galaxy multi-aperture photometry. The curves are for normal field galaxies (de Vaucouleurs 1961).

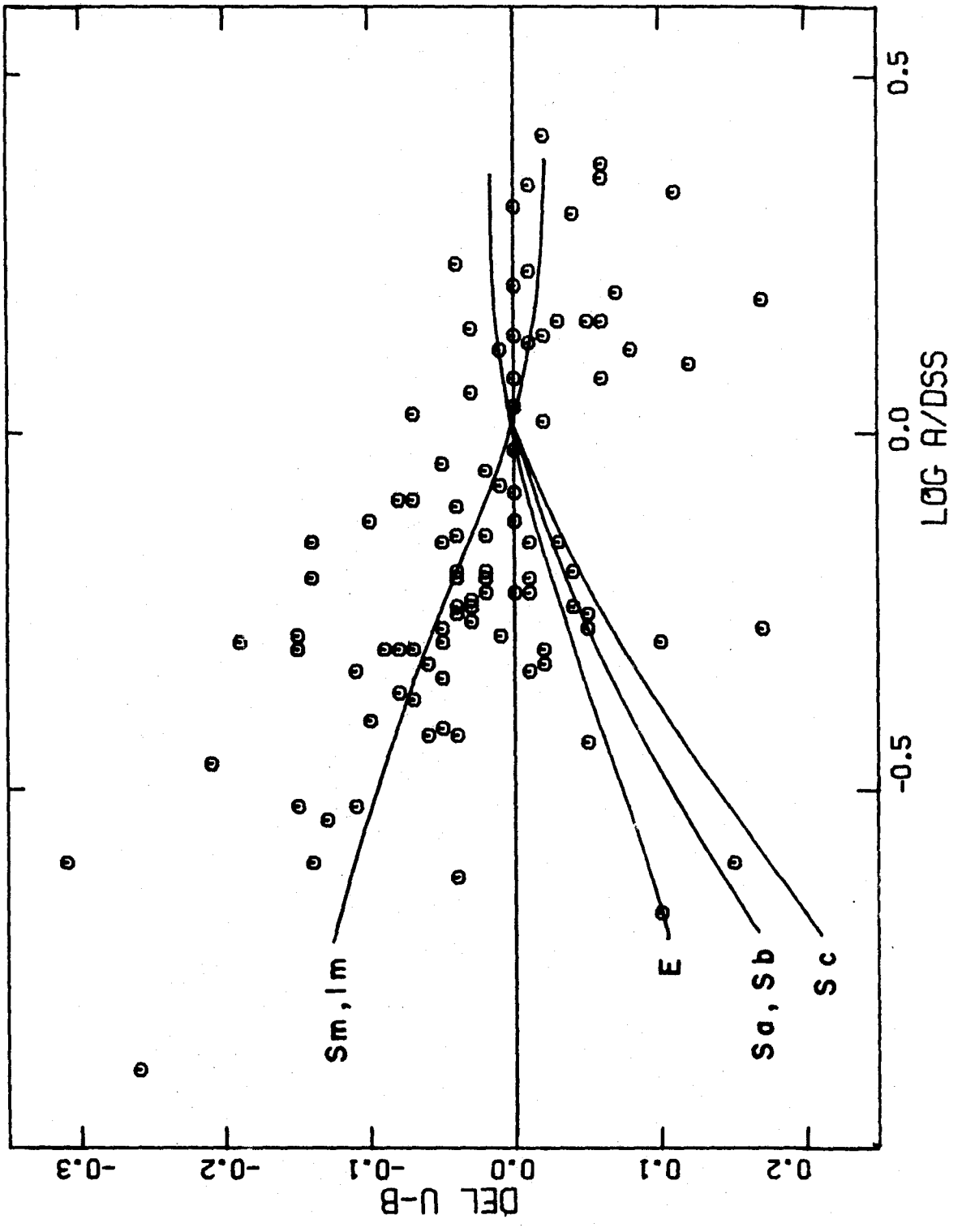
DEL U-B
0.2
0.1
0.0
-0.1
-0.2
-0.3
LOG A/DSS
0.5
0.0
-0.5
Sm,Im
E
Sa,Sb
Sc

FIGURE 5

The same as Figure 4 for B-V.

0.5
0.0
-0.5
LOG A/DSS
0.2
0.1
0.0
-0.1
-0.2
-0.3
DEL B-V
Sm,Im
E
Sa,Sb
Sc

FIGURE 6

The same as Figure 4 for V-R. No curves are available for field galaxies.

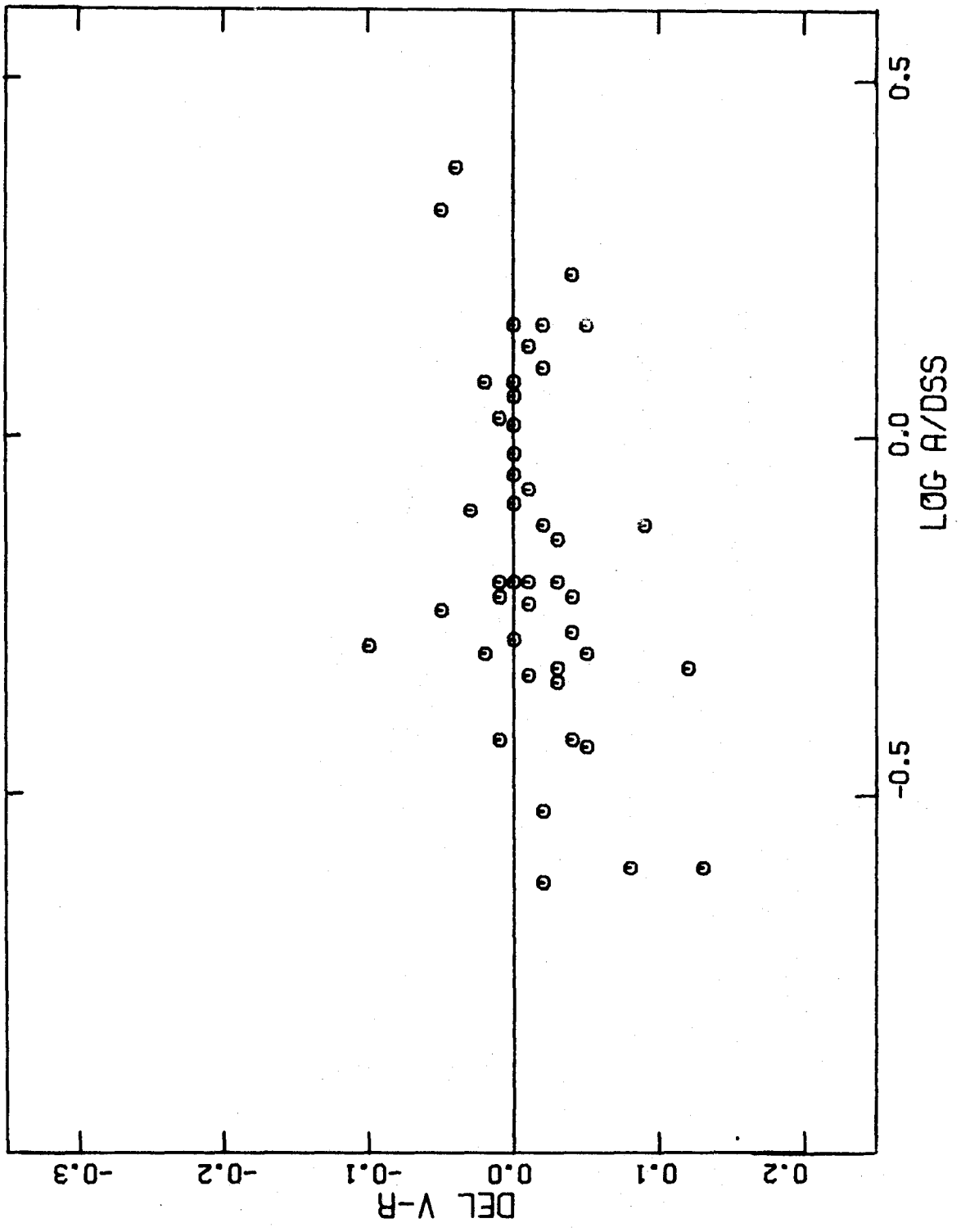
LOG A/DSS
0.5
0.0
-0.5
DEL V-R
0.2
0.1
0.0
-0.1
-0.2
-0.3

towards the center. In Figures 4 and 5 we have also plotted the mean color-aperture curves for several morphological types, adapted from de Vaucouleurs (1961). Only the Sm and Im field galaxies generally become bluer with decreasing aperture sizes.

(c) The Mass-to-Light Ratio

The masses, and in particular, mass-to-light ratios of galaxies can be studied using velocity and separation data for binary galaxies if the systems are bound (Page 1961, 1966). Heidmann and Kalloghlian (1973) suggested that Markarian galaxies have abnormally high M/Ls or are unbound, based on the rather poor velocity data available at that time. We have collected and obtained velocity and separation data for 20 Markarian pairs and Markarian double galaxies with separations less than 8 arc min. An estimate of the mimimum system mass is made using Page's (1966) formula and assuming H_o = 50 km sec^{-1} mpc^{-1}:

$$M / M_{\odot} \geq 1350\ D\ V_r\ (\Delta V)^2 \qquad (9)$$

The system luminosity is given by:

$$L / L_{\odot} = \text{dex}\ [\ -0.4\ *\ (\ M_{pg} - 5.26)] \qquad (10)$$

D is the separation in arc min, Vr the mean radial velocity, ΔV is the velocity difference, and M_{pg} is the absolute photographic magnitude. Table 4 presents the parameters of the Markarian pairs and doubles. Column (1) gives the Markarian number, column (2) the absolute photographic magnitude, and columns (3) and (4) the measured radial velocity and quoted

TABLE 4

MARKARIAN PAIRS WITH COMPLETE RADIAL VELOCITY DATA

#	M_{pg}	V_r †	σ †	S*	ΔV †	D'	d_{kpc}	$M/M_\odot$	$L/L_\odot$	M/L	Remarks
11	-20.3	3866	84	HS	115	5.9	133	4.1E+11	9.7E+10	4.1	Faint companion
12	-22.0	3981	60	S							
30	-19.1	8000	92	D,S	255	0.7	32	4.8E+11	4.8E+10	10	
31	-21.3	7745	60	S							
38	-21.5	10773	110	D,S	130	0.6	38	1.5E+11	5.8E+10	2.6	
39	-19.7	10903	60	S							
56	-20.4	7287	60	S	311	5.3	228	5.2E+12	3.9E+10	133	Diffuse cluster of galaxies
57	-20.5	7598	60	S							
121	-20.4	6604	120	D,S	118	2.8	108	3.5E+11	6.7E+10	5.1	121 is part of a pair itself
122	-21.5	6722	15	D,HS							
181	-21.6	6189	45	S	41	2.7	97	4.2E+10	5.6E+10	0.8	181 is part of a galaxy chain
182	-18.4	6230	60	DS							
211	-20.0	12300	300	ADE	5400	3.0	--	-	-	-	Probably not a pair
212	-20.9	6900	300	ADE							
220	-20.9	4950	60	S	15	0.6	17	9.0E+08	5.9E+10	0.015	
221	-20.9	4935	15	DS,S							
261	-21.2	9300	300	ADE	300	1.1	59	1.2E+12	5.4E+10	23	In a diffuse cluster
262	-20.4	9000	300	ADE							
325	-21.6	3402	70	AKN	218	6.7	137	1.5E+12	8.2E+10	18	
326	-20.8	3620	30	AKN							
355	-20.0	9174	45	HS	119	0.5	27	8.7E+10	2.4E+10	3.7	
356	-19.9	9055	45	HS							

TABLE 4 (continued)

MARKARIAN PAIRS WITH COMPLETE RADIAL VELOCITY DATA

#	M_{pg}	V_r †	σ	S*	ΔV†	D'	d_{kpc}	$M/M_\odot$	$L/L_\odot$	M/L	Remarks
481	-18.6	3290	10	HS	283	7.0	141	2.6E+12	1.2E+10	202	
482	-19.6	3573	60	D							
499	-21.5	7962	60	D	21	1.9	88	9.0E+09	6.1E+10	0.15	Foreground companion ?
500	-19.6	7941	60	D							
607	-19.8	2679	60	HS	51	1.7	27	1.6E+10	2.2E+10	0.7	Companion
608	-19.8	2730	100	HS							
Markarians that are double galaxies											
116	-15.5	764	10	SS	40	0.12	0.53	2.0E+08	2.1E+08	0.9	
		804	10	SS							
171	-22.2	3212	100	T	115	0.62	11.4	3.5E+10	9.0E+10	0.4	Holmberg binary #256
		3097	100	T							
271	-22.1	7523	142	R	43	0.7	31	1.3E+10	1.1E+11	0.1	
		7566	142	R							
280	-21.6	11200	60	DS	220	0.54	35	3.8E+11	5.3E+10	7.1	
		10980	60	DS							
297	-20.9	4736	45	HS	64	0.2	5.5	5.2E+09	2.8E+10	0.2	
		4672	45	HS							
496	-22.4	8898	25	T	78	0.22	11.3	1.6E+10	1.1E+11	0.1	
		8820	37	T							

† in km sec^{-1}

TABLE 4 (continued)

MARKARIAN PAIRS WITH COMPLETE RADIAL VELOCITY DATA

* Sources

HS	-	Huchra and Sargent (1973,1976)
D	-	Denisyuk (1971a,1971b,1974)
DS	-	Denisyuk et al. (1974)
S	-	Sargent (1970,1972)
SS	-	Searle and Sargent (1972)
T	-	Turner (1975)
AKN	-	Afanasjev et al. (1975)
ADE	-	Arakelian et al. (1971,1972)
R	-	de Vaucouleurs and de Vaucouleurs (1964)

error in km sec^{-1}. If more than one source is listed in column (5), the error given is the standard deviation of the mean of the observations. Columns (6) through (8) give the measured separation in arc minutes, the projected separation in kpc, and the velocity difference in km sec^{-1}. Columns (9) through (11) give the derived system minimum masses, luminosities, and mass-to-light ratios in solar units. Markarians 211 and 212 are probably a chance superposition. Column (12) contains a description of the surrounding field with respect to the nearest neighbor parameter $x = 5$, (Turner, 1975). Twenty pairs or doubles are listed. Only one pair has a ΔV greater than 300 km sec^{-1}, while seven pairs have additional galaxies associated with them or appear to be members of clusters.

By using Markarian-Markarian binaries, we can make an estimate of the mean mass-to-light ratio for Markarian galaxies as a class and compare it to estimates for field galaxy mass-to-light ratios. Turner (1975) has obtained data for a well defined sample of binary galaxies. Thirteen of our pairs or doubles (assuming that the resolved companion to 499/500 is in the foreground) conform to Turner's "binary" separation and nearest neighbor cutoffs, but almost all of the systems have one component fainter than Turner's $m_{pg} = 15.0$ cutoff. Does the limiting magnitude difference introduce selection effects? There are two competing processes--fainter galaxies are, on the average, further away,

so that a given projected separation will become a larger spatial separation, but it is easier to find pairs with smaller projected separations as the magnitude limit decreases. We checked the hypothesis that the Markarian and Turner binary galaxies represent a similar sample of spatial galaxy separations by using the Wilcoxon rank-sum test (Bury 1975, Noether 1967). This is a nonparametric test that compares two samplings of data distributions by ordering the combined sample and comparing the summed ranks of the smaller sample with the expected sum of a random sampling of that size. The test shows that there is no significant difference between the two samples--they are drawn from the same parent population and can be used to compare mass-to-light ratios.

For the comparison of mass-to-light ratios, we use the ratio defined by equations (9) and (10). Table 6 gives the arithmetic mean of this parameter and its one sigma mean error intervals for Turner's spiral and irregular (OS, S, I) sample, Turner's complete sample and for both the selected sample of Markarian binaries and the sample of 19 pairs or doubles (excluding 211-212).

Contrary to the claim of Heidmann and Kalloghlian (1973), the Markarian binaries are not unbound and violently flying apart, and, in fact, appear to have the same $\langle M/L \rangle$ as the field spiral and irregular binaries. A comparison of the distribution of individual M/L values for the Markarian and

TABLE 6

MEAN MASS TO LIGHT RATIOS

Sample	# of galaxies	mean M/L
FIELD GALAXIES		
OS,S,I pairs	40	21 (14 - 28)
All pairs	73	23 (16 - 30)
MARKARIAN GALAXIES		
Selected pairs	13	19 (3 - 34)
All pairs	19	22 (10 - 34)

Turner binary galaxies show that both samples are very probably drawn from the same parent population of separations and velocity differences. The actual value of the mean M/L for Markarian binaries, after correction for selection and orbital effects (Turner 1975), is then about 50 in solar units.

Heidmann and collaborators (Heidmann and Kalloghlian 1973, 1975; Casini and Heidmann 1975) find that Markarian galaxies tend to be associated with themselves and other galaxies. There is an excess of pairs with small separations over the number predicted by a random distribution of galaxies. Peebles and others (Peebles and Hauser 1974, Davis and Geller 1975) find the same effect in all catalogs of galaxies. We think that this can be interpreted simply as the tendency for galaxies to cluster. Coupled with the above evidence that pairs of Markarian galaxies are bound, the clustering interpretation negates Heidmann's hypothesis of the "pair production" of Markarian galaxies. In fact, this suggests that Markarian galaxies are distributed in space in the same way as other galaxies. A further study of selection effects--such as the limiting magnitudes of the catalogues--is necessary before a definitive comparison can be made.

(d) The Luminosity Function

Redshift data or identification as galactic stars now exists for 327 of the 428 Markarian objects with $m_{pg} \leq 15.5$

in seven of Markarian's and Markarian and Lipovetsky's lists. Using the V/V_m method and correcting for the completeness of the sample as outlined in Huchra and Sargent (1973), we have calculated the space density of Markarian galaxies including Seyfert galaxies. No absorption correction to the volume has been applied. The Markarian survey is generally at high galactic latitutdes where the Sandage (1973) absorption is zero. This luminosity function is then compared in Figure 7 and Table 7 to that derived by Christensen (1975) for field galaxies. The general conclusions drawn in the earlier work of Huchra and Sargent (1973) still hold. Markarians represent approximately 10% of the field galaxies between $m_{pg} = -22$ and -15, with the proportion of all galaxies that are Markarians and Seyferts rising to the higher luminosities. We can also make a rough estimate of the space density of galaxies as a function of color. We make the assumption, admittedly crude, that the distributions of measured Markarian galaxy and field galaxy colors represent the actual distributions. We then use the total space densities (galaxies per Mpc^3) given by the two luminosity functions integrated between $m_{pg} = -23.0$ and -15.0. Table 8 gives the log space density (log Φ) versus color results for both Markarian and field galaxies. Figure 8 shows the plot of log Φ versus U-B. Several features are readily apparent. The field galaxy distribution drops off sharply at the red end and drops more gradually at the blue end. The Markarian

FIGURE 7

Log space density (galaxies per cubic mega-parsec per absolute magnitude interval) versus absolute photographic magnitude for field galaxies (filled circles), Markarian galaxies (filled triangles), and Markarian Seyfert galaxies (open circles).

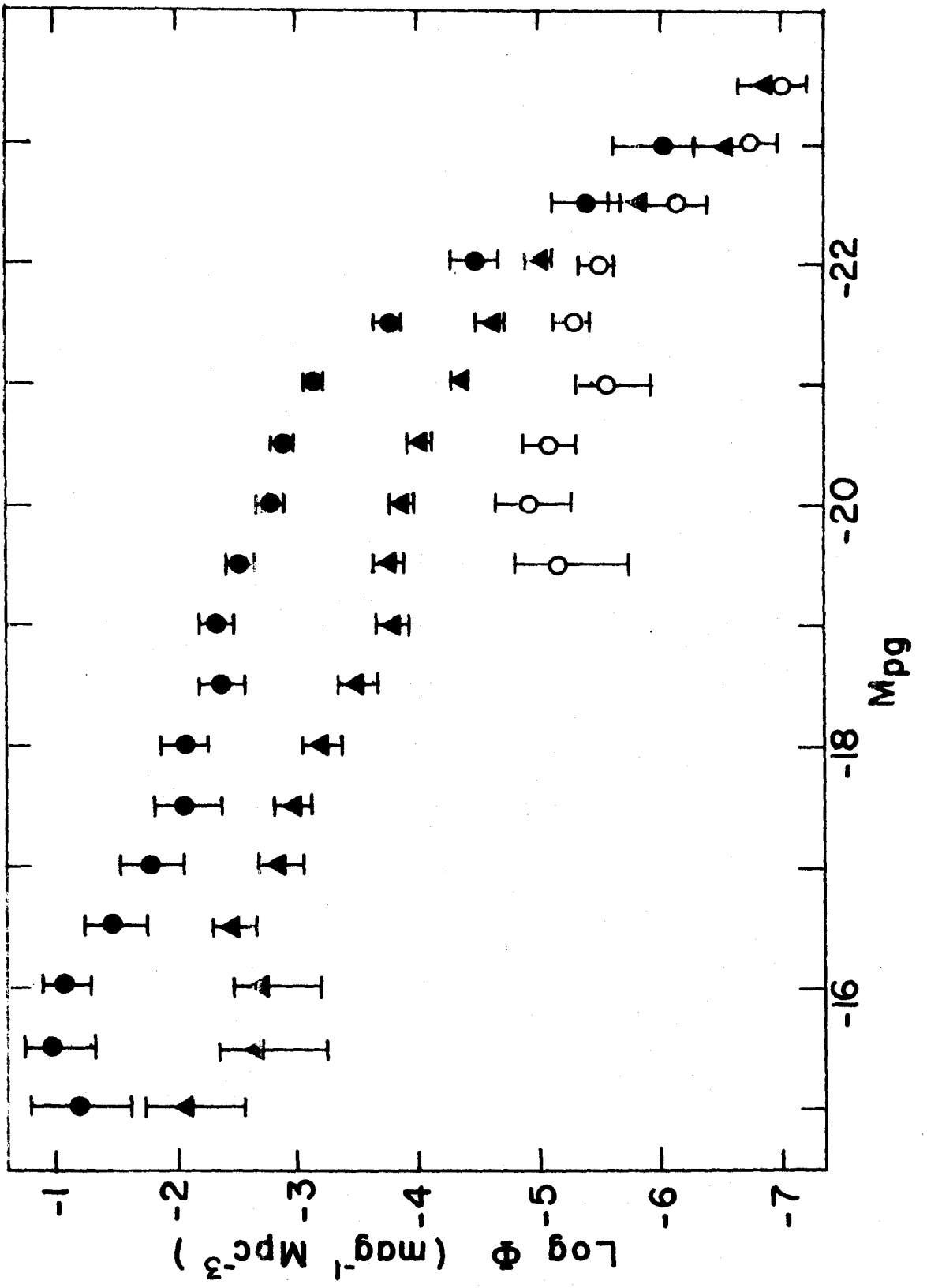
-16
-18
-20
-22
M_{pg}
-1
-2
-3
-4
-5
-6
-7
Log Φ (mag^{-1} Mpc^{-3})

TABLE 7

SPACE DENSITIES *

M_{pg} ††	Field Galaxies†		Markarian Galaxies		Markarian Seyfert Galaxies	
	log Φ	#	log Φ	#	log Φ	#
-15.0	-1.20	1	-2.06	2	...	
-15.5	-0.97	3	-2.68	1	...	
-16.0	-1.08	5	-2.72	2	...	
-16.5	-1.48	4	-2.43	7	...	
-17.0	-1.78	4	-2.89	6	...	
-17.5	-2.08	4	-2.97	10	...	
-18.0	-2.08	8	-3.22	10	...	
-18.5	-2.38	8	-3.50	11	...	
-19.0	-2.33	18	-3.80	11	...	
-19.5	-2.51	24	-3.77	24	-5.17	1
-20.0	-2.77	26	-3.84	37	-4.90	3
-20.5	-2.88	40	-4.01	52	-5.07	5
-21.0	-3.16	42	-4.34	46	-5.56	3
-21.5	-3.76	21	-4.58	52	-5.27	12
-22.0	-4.47	8	-5.03	35	-5.49	12
-22.5	-5.38	2	-5.80	12	-6.15	5
-23.0	-5.99	1	-6.61	4	-6.71	3
-23.5	...		-6.88	5	-6.97	4

* Φ is in units of galaxies mag^{-1} Mpc^{-3}

† from Christensen (1975)

†† magnitudes are on the Zwicky catalogue scale

TABLE 8

SPACE DENSITY* VERSUS COLOR

	Markarian Galaxies		Field Galaxies	
	log Φ	#	log Φ	#
U-B				
-0.75	-3.69	1	...	
-0.65	-3.69	4	...	
-0.55	-3.45	7	-3.30	1
-0.45	-2.99	11	-2.82	1
-0.35	-2.85	25	-2.34	9
-0.25	-2.62	34	-2.09	14
-0.15	-2.80	35	-1.95	20
-0.05	-2.97	27	-1.66	37
0.05	-3.25	17	-1.90	25
0.15	-3.22	7	-1.73	35
0.25	-3.52	9	-1.80	34
0.35	-3.82	6	-1.72	35
0.45	-3.99	5	-1.56	48
0.55	-4.28	1	-1.68	47
0.65	...		-2.12	18
0.75	...		-3.30	4
B-V				
0.15	-3.99	2	-3.30	0
0.25	-3.60	4	-3.30	1
0.35	-2.73	17	-2.45	6
0.45	-2.58	52	-1.83	27

TABLE 8 (continued)

SPACE DENSITY* VERSUS COLOR

	Markarian Galaxies		Field Galaxies	
	log Φ	#	log Φ	#
B-V (cont'd)				
0.55	-2.74	46	-1.78	31
0.65	-2.67	39	-1.57	49
0.75	-3.25	18	-1.68	38
0.85	-3.25	13	-1.57	48
0.95	-4.29	6	-1.37	81
1.05	...		-1.80	51
1.15	...		-3.00	4

*Φ is in units of galaxies per 0.1 magnitude per cubic megaparsec.

FIGURE 8

Log space density (galaxies per cubic mega-parsec per 0.1 magnitude interval in color) versus U-B for field galaxies (circles) and Markarian galaxies (triangles).

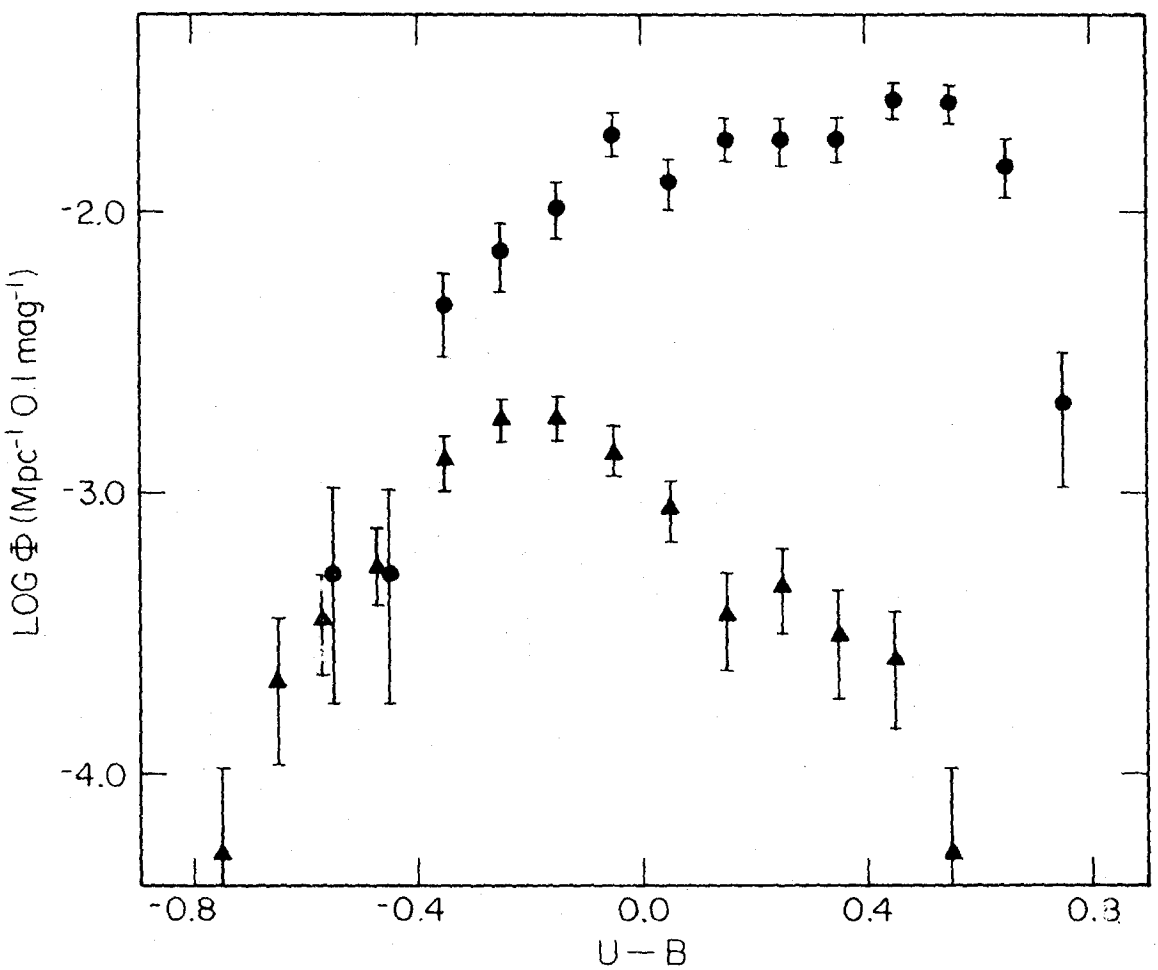
-2.0
-3.0
-4.0
LOG Φ (Mpc^{-1} 0.1 mag^{-1})
-0.8
-0.4
0.0
0.4
0.8
U — B

galaxy distribution extends bluer than the field galaxy distribution. It rises with the field galaxy distribution up to $-B = -0.25$, then drops gradually to the red while the field galaxy distribution is still rising. Markarian selects all of the very blue galaxies and a decreasing fraction of the redder ones.

(e) The Distribution of Morphological Types and Colors in Morphological Types

The evidence presented so far suggests that Markarian galaxies are just a collection of late type galaxies. The mean colors are similar to those of late type galaxies; the mass-to-light ratios are consistent with those of late type galaxies. Galaxies of types Sd to Im comprise roughly 10% of all galaxies, as do the Markarian galaxies; and the color-aperture curves for Markarian galaxies are similar to those of late type galaxies. In order to test this hypothesis, we have determined the morphological types of the 91 Markarian galaxies with $m_{pg} \leq 14.0$, and have obtained colors for 80% of these. Figure 9 compares the distribution of morphological types for the Markarian galaxy sample with the distribution of morphological types for the Schechter (1973) sample of 255 Reference Catalogue (de Vaucouleurs and de Vaucouleurs 1964) galaxies brighter than $m_{pg} = 11.75$. The cross-hatched areas in the S to Sdm bins indicate the fraction of barred spirals of each type. Mixed spirals (SAB) were counted as one-half barred and one-half normal as

FIGURE 9

The distribution of morphological types of Markarian and field galaxies. Sample size has been normalized to unity.

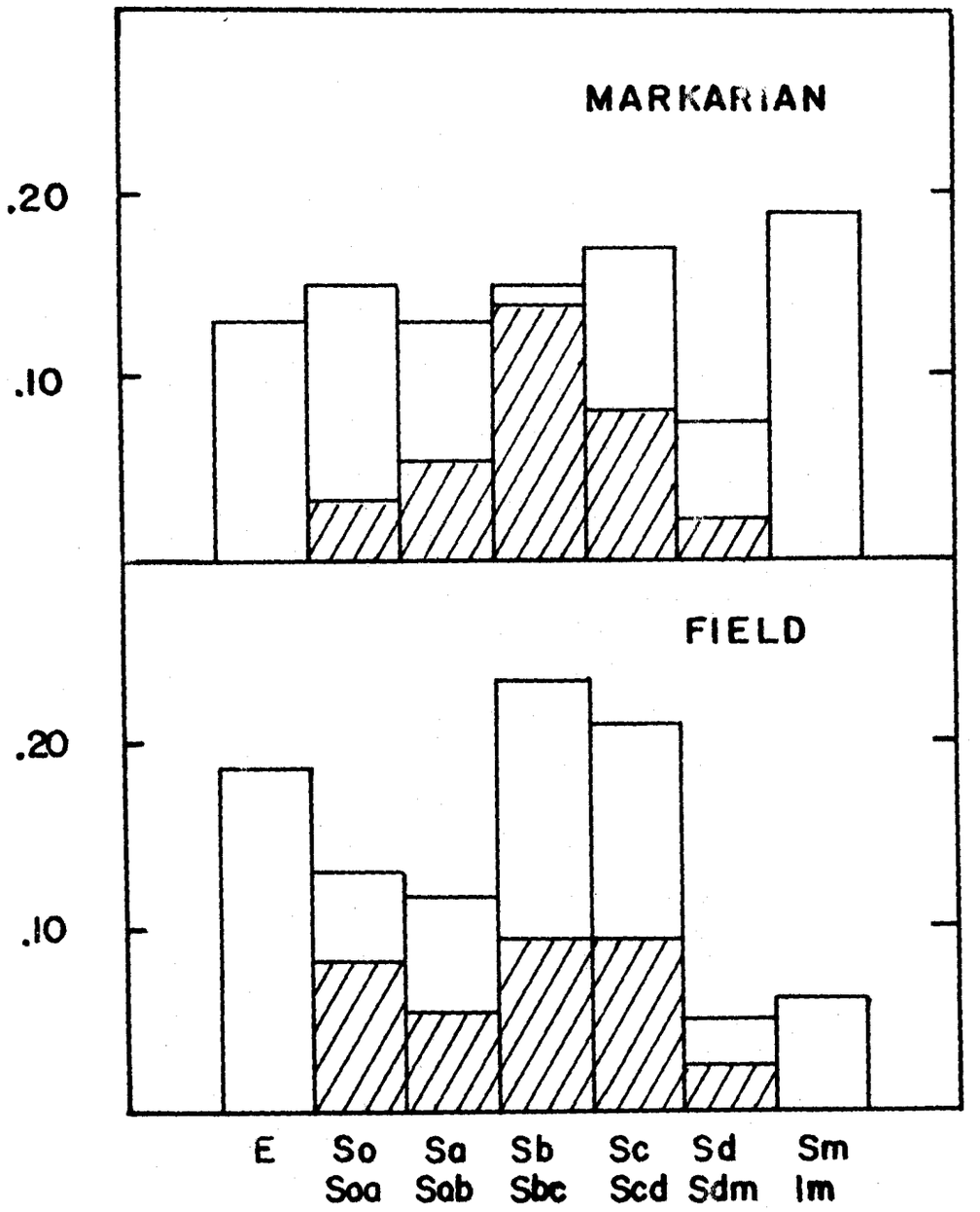
MARKARIAN
.20
.10
FIELD
.20
.10
E
So
Soa
Sa
Sab
Sb
Sbc
Sc
Scd
Sd
Sdm
Sm
Im

in Christensen (1975). The distributions are remarkably similar. There are 3 times as many Sm, Im galaxies among the Markarian galaxies as among the field galaxies, and the fractions of other types are somewhat depressed, but a substantial fraction of Markarian galaxies are early type galaxies.

The excess of barred spirals among the Sb and Sbc galaxies is probably real, but the average fraction of spirals that are barred is approximately one-half for both the Markarian and field galaxies. This result contradicts the impressions of Kalloghlian (1973) and Borngen and Kalloghlian (1975). This contradiction, however, may be a result of partially counting half of the mixed spirals as barred, as Christensen (1975) did. If they are not counted, the fraction of field spirals that are barred drops to 27%, and the Markarian spirals do show an excess of barred types.

In the morphological sample, approximately 20% of the Markarian galaxies show structural peculiarities. However, it must be remembered that 7% of all NGC galaxies are in the Arp (1966) atlas--and this is a lower limit to the percentage of peculiar galaxies because Arp's survey is not complete. Three of the Markarian galaxies (171, 271, 496) are interacting double systems, and others (e.g., 538) are parts of such systems. It is possible that dynamical interaction of galaxies could trigger star formation and thus make them bluer (Toomre and Toomre 1972), however 4% of all NGC

galaxies also appear in the Vorontsov-Velyaminov (1959) Catalogue of interacting galaxies.

Figure 10 a,b,c,d shows the distribution of colors for normal ellipticals and lenticulars, early type spirals, intermediate type spirals, and Magellanic spirals and irregulars plotted along with the colors for Markarian galaxies of those types. "Peculiar" field galaxies and the three Seyferts and two BL Lacertae type objects in the morphological Markarian sample have not been plotted. For the first three groups, the colors of the Markarian galaxies fall at the blue end but inside the distribution of colors for morphologically similar field galaxies. For the last group, the distributions overlap, but the Markarian galaxies extend $\sim$ 0.2 bluer in U-B. These effects are also seen in the mean colors of the non-Seyfert galaxies presented in Table 5.

(f) Intrinsic Diameters

Measurements of the "sizes" of galaxies depend on the limiting isophotal surface brightness used by the observer. Accurate measurements, such as those of Holmberg (1956), require calibrated, uniform photographic materials or use of area photodetectors. For a very rough comparison, however, we can use the measured sky survey diameters and the corrected Reference Catalogue diameters to derive the intrinsic diameters for our samples of galaxies. The diameter is

$$D = 20\ V_r \tan(\ D_1/2 + D_2/2\ )\ \text{kpc}, \qquad (11)$$

FIGURE 10a

The color-color distribution for elliptical, lenticular and S0 galaxies. The small circles are normal field galaxies, and the filled triangles are the Markarian galaxies.

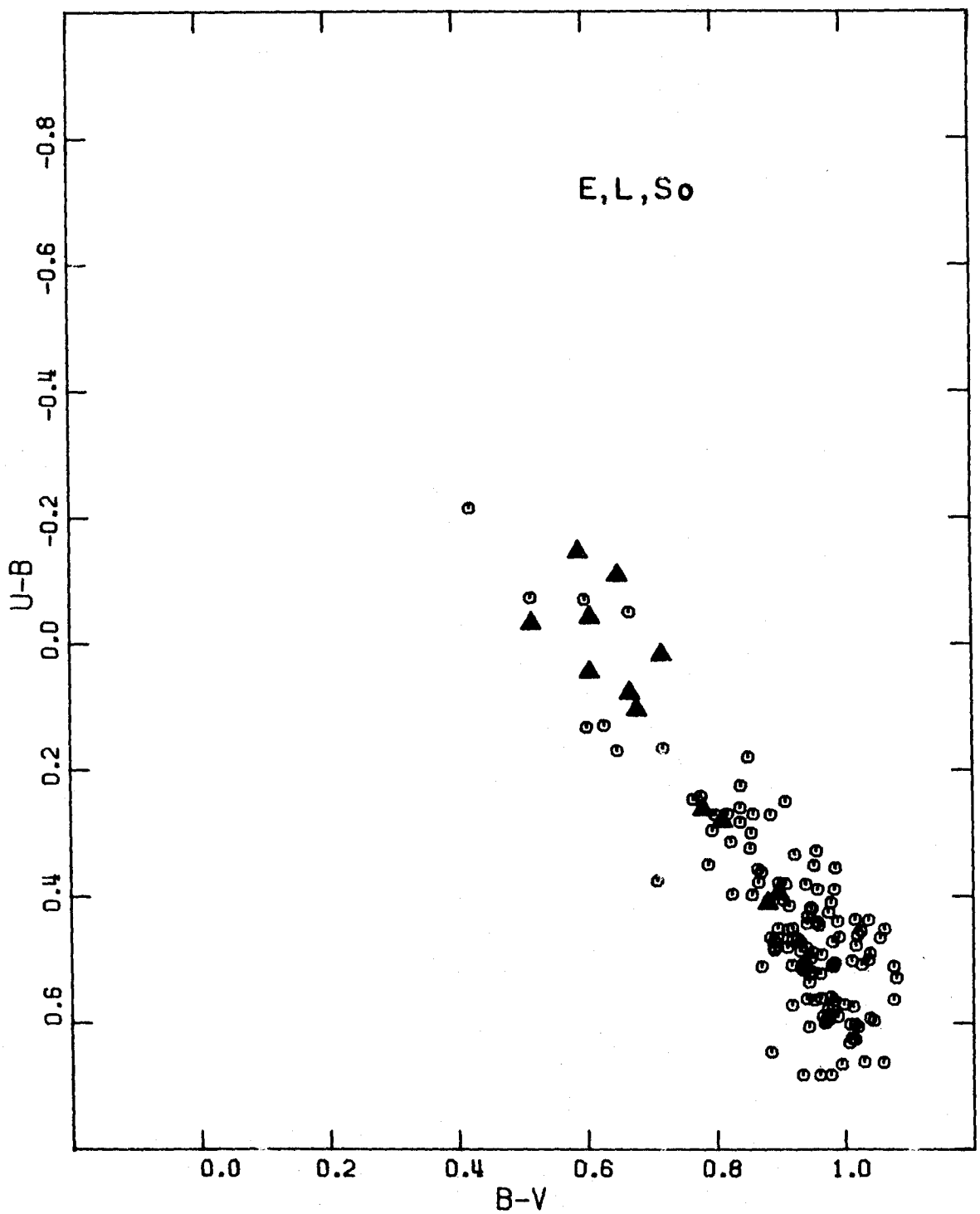
E, L, So
U-B
B-V
-0.8
-0.6
-0.4
-0.2
0.0
0.2
0.4
0.6
0.0
0.2
0.4
0.6
0.8
1.0

FIGURE 10b

Color-color distribution for early type spirals.

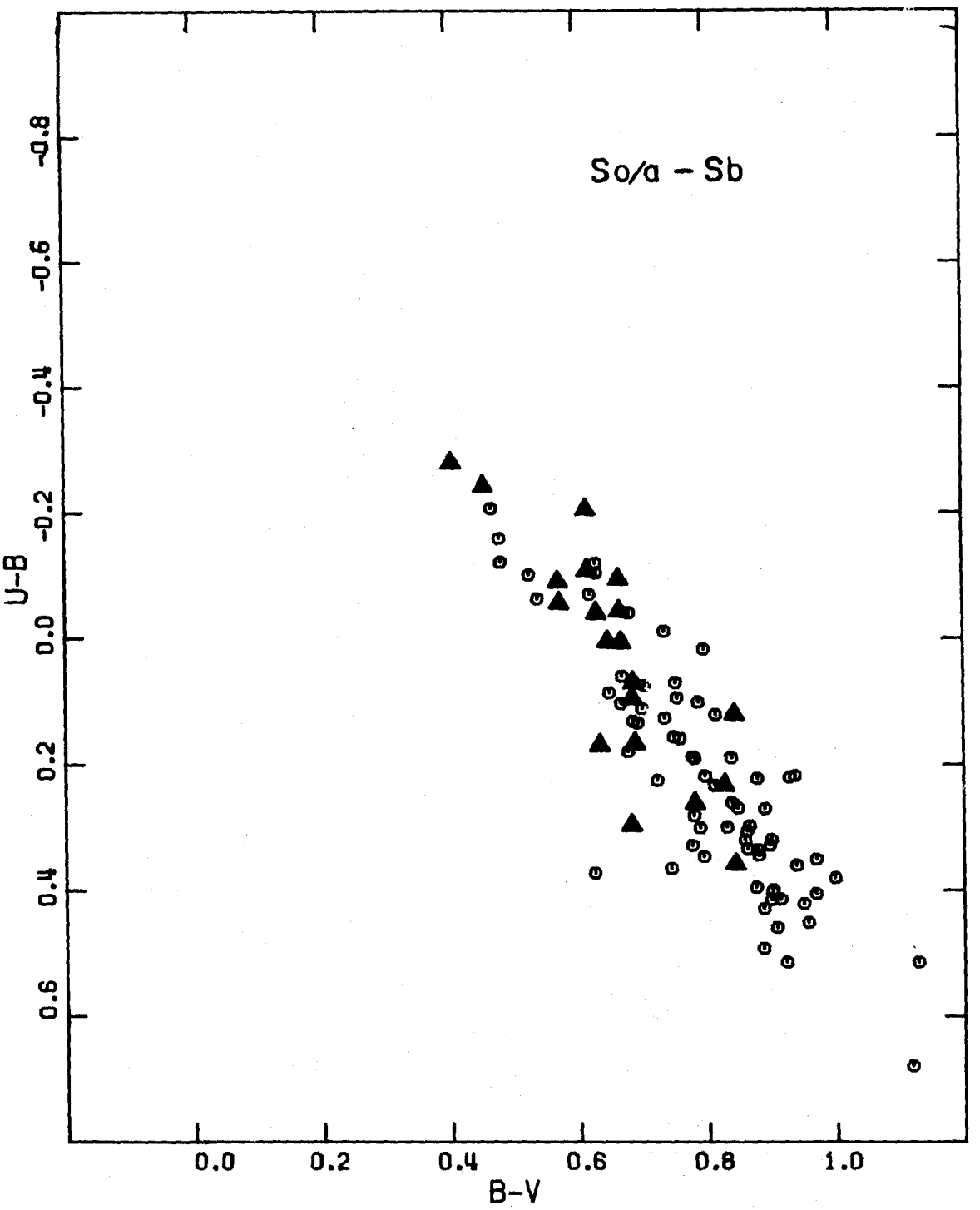
So/a - Sb
U-B
B-V
-0.8
-0.6
-0.4
-0.2
0.0
0.2
0.4
0.6
0.0
0.2
0.4
0.6
0.8
1.0

FIGURE 10c

Color-color distribution for intermediate type spirals.

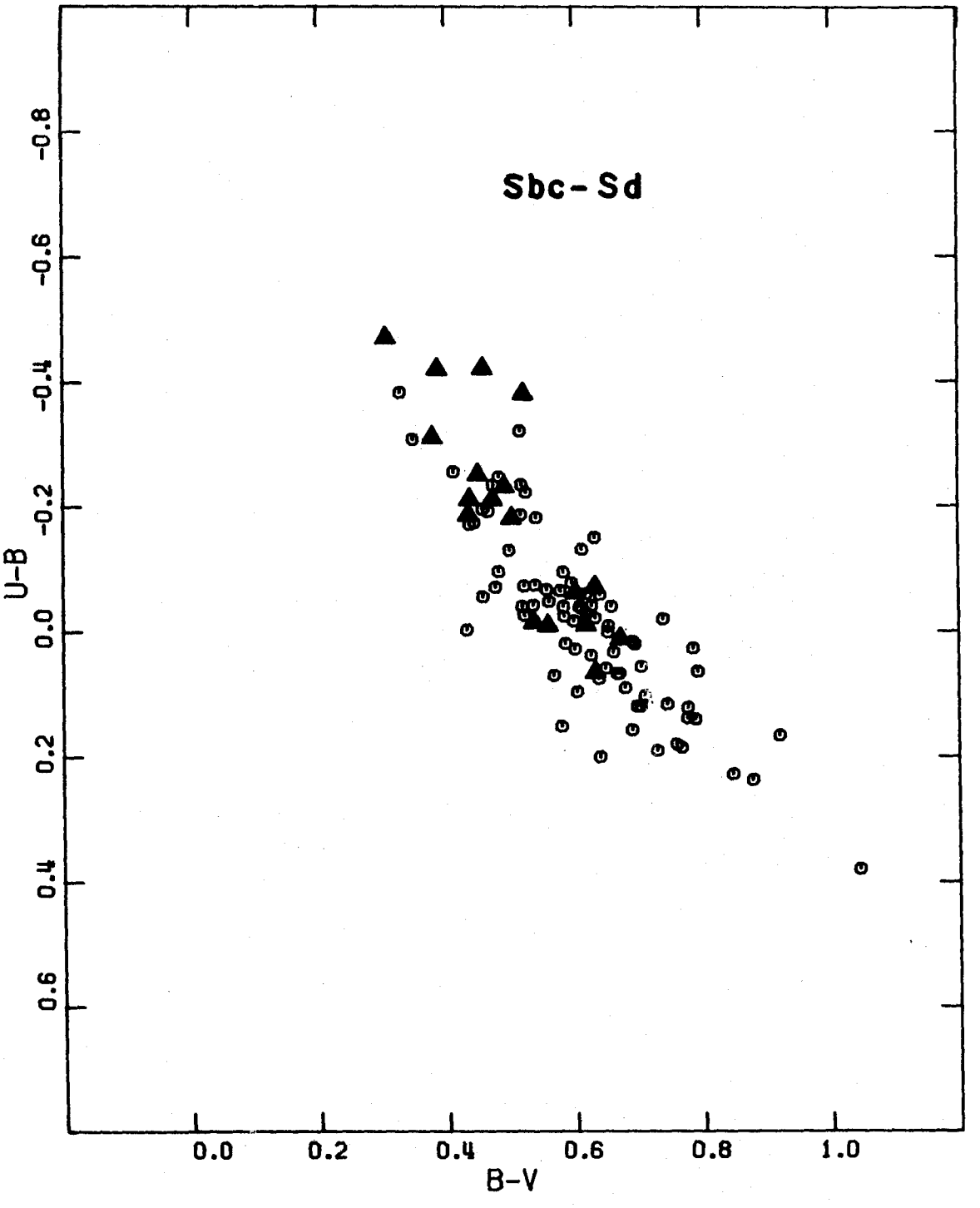
Sbc-Sd
U-B
B-V
-0.8
-0.6
-0.4
-0.2
0.0
0.2
0.4
0.6
0.0
0.2
0.4
0.6
0.8
1.0

FIGURE 10d

Color-color distribution for Magellanic spirals and irregulars.

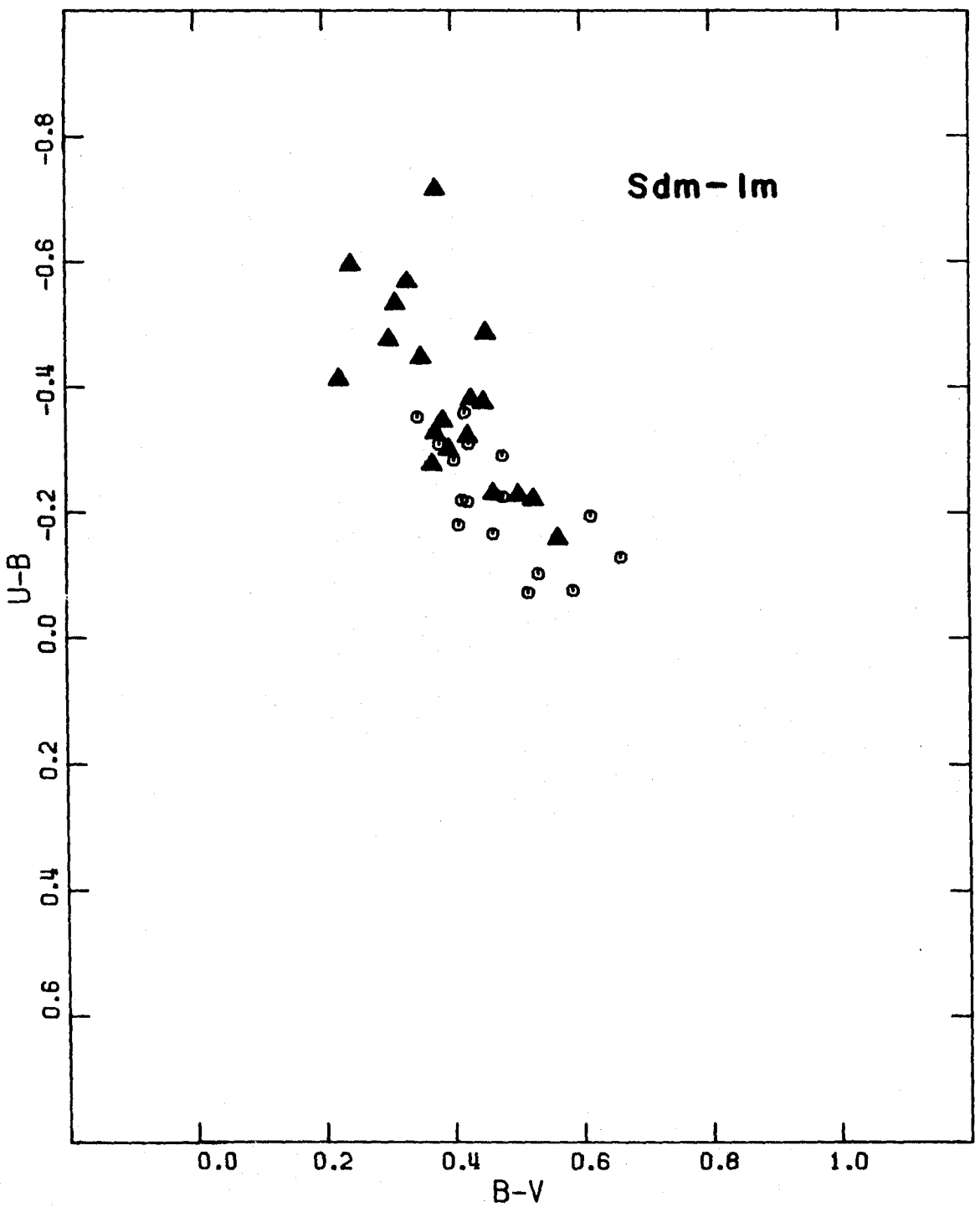
Sdm-Im
U-B
B-V
-0.8
-0.6
-0.4
-0.2
0.0
0.2
0.4
0.6
0.0
0.2
0.4
0.6
0.8
1.0

where V_r is the redshift of the galaxy in km sec^{-1} and D_1 and D_2 are its apparent major and minor axis diameters. We have not attempted to correct for inclination effects because that correction implies a priori knowledge of the intrinsic shapes of the galaxies, nor have we applied corrections for galactic or internal absorption to the diameters, as such corrections are, in general, smaller than the measuring errors in the apparent diameters. Figure 11 a,b shows the plots of log diameter versus absolute blue magnitude (Holmberg isophote) for the field galaxy sample described earlier and for the Markarian galaxies. For both samples, the "sky survey" intrinsic diameter of a galaxy with $M_B = -20$ is approximately 10 kpc. The larger scatter in the field galaxy sample is due to de Vaucouleurs' use of different limiting isophotes for different morphological types, and the use of varying types of plate material. The linear fits to this data are given by:

$$\log(D) = [\,0.97 \pm 0.01\,] - [\,0.200 \pm 0.01\,] \times (M_B + 20) \quad \text{Field} \qquad (12)$$

$$\log(D) = [\,0.95 \pm 0.01\,] - [\,0.196 \pm 0.01\,] \times (M_B + 20) \quad \text{Markarian} \qquad (13)$$

M_B is the absolute blue magnitude. In this system, the luminosity of a galaxy is almost proportional to the square of the diameter, indicating approximate constancy of mean surface brightness over the absolute magnitude interval studied--for both samples. We point out, however, that the

FIGURE 11

Log diameter (in kiloparsecs) versus absolute magnitude for (a) field galaxies, and (b) Markarian galaxies.

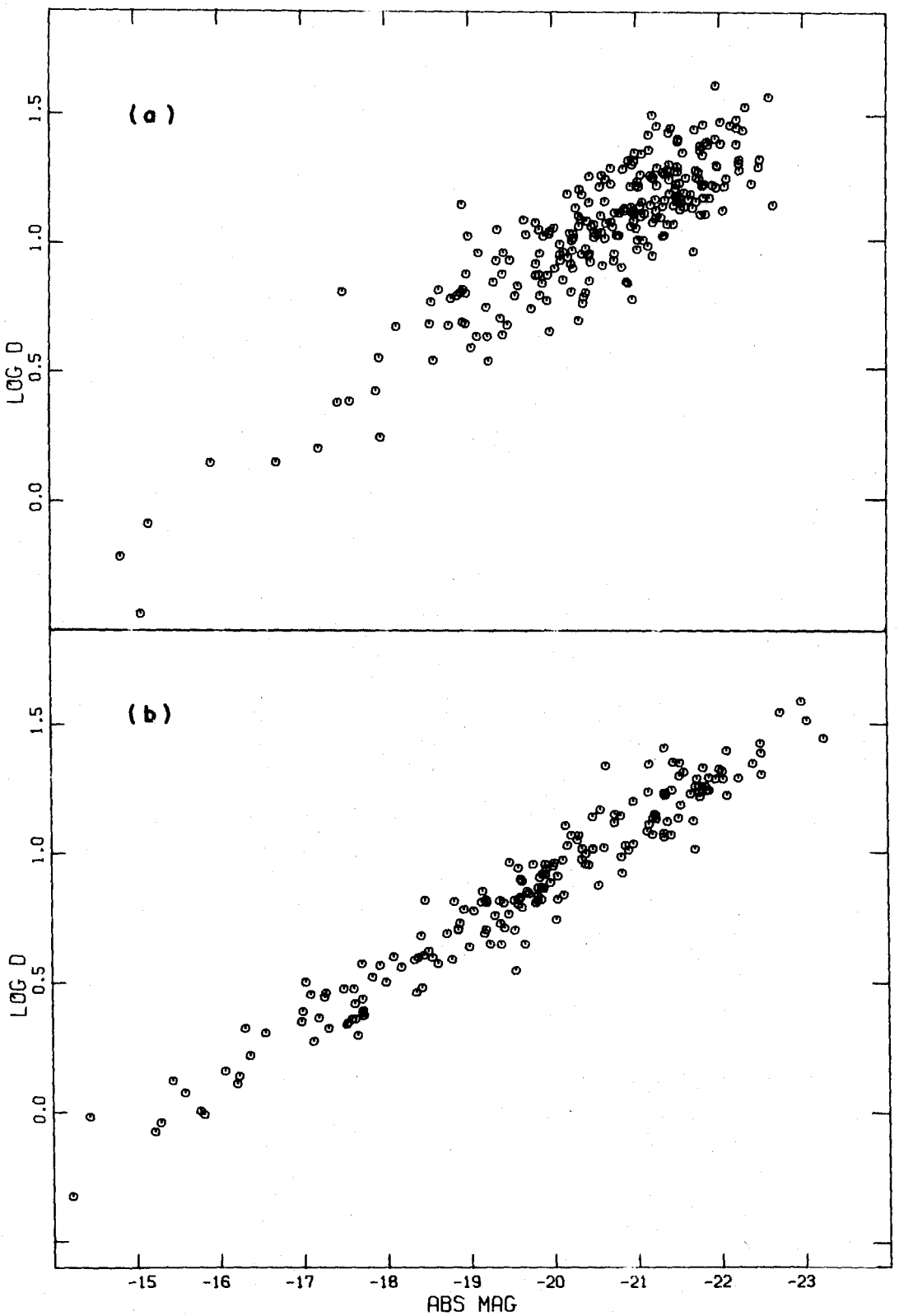
(a)
(b)
LOG D
0.0
0.5
1.0
1.5
-15
-16
-17
-18
-19
-20
-21
-22
-23
ABS MAG

data do not preclude small scale irregularities in the surface brightness distributions of the galaxies studied.

(g) Emission Line Properties

Humanson, Mayall and Sandage (1956) found that ~ 85% of spirals and irregulars and ~ 15% of ellipticals have emission lines (in particular, λ3727) in their spectra. Huchra and Sargent (1976) find that ~ 90% of the Markarian galaxies have emission line spectra. Qualitatively, the Markarian galaxy spectra cover the same range in emission line intensities as the field galaxies. Their spectra range from absorption line systems to systems like NGC 5253 with a strong, high excitation emission line spectrum that dominates the spectrum (Burbidge and Burbidge 1962).

Unfortunately, most systematic observations of galaxy spectra have been made just to obtain redshifts, thus all galaxies have not been observed at the same dispersions over the same wavelength regions with equal quality plate material. This hinders any direct comparison of spectroscopic properties. We can, however, look at the properties of some of our Markarian galaxies which have been observed over similar wavelength regions at intermediate dispersion.

We have examined the correlations, using linear correlation coefficients, between our measured emission line properties for Markarian galaxies--Hβ strength (log W(Hβ)) and excitation parameter (E ≡ [O III] λ5007/Hβ)--and other observed photometric properties. There are 103 galaxies

with photometry, redshifts, and measured emission line strengths. Table 9 gives the linear correlation coefficient R (Bevington 1969) and the parameters of the linear fits for pairs of quantities whose correlation probabilities exceed 95%. USB is the U band surface brightness, and BSB is the B band surface brightness. USB and excitation, and BSB and lob W(Hβ) were not found to be significantly correlated. Figure 12 is a plot of the two quantities with the strongest correlation--log W(Hβ) versus U-B. Most of these correlations are expected. The bluer or "hotter" objects have stronger emission lines and higher excitation. A similar effect is seen in the color-Hα correlation for spirals found by Cohen (1976). Excitation is correlated more strongly with blue surface brightness than with ultraviolet surface brightness. There is less correlation of Hβ with B-V than with U-B--possibly caused by the much smaller range in B-V colors plus the fact that the Balmer continuum emission contributes to the U-B color, whereas Hβ and the [O III] lines lie between B and V in low redshift galaxies. Both excitation and Hβ strength are correlated strongly with absolute magnitude. The intrinsically fainter systems also have stronger emission relative to their continua. This effect may be due in part to the correlation of U-B with absolute magnitude discussed below, but the emission line correlation with absolute magnitude is stronger than the color correlation with absolute magnitude. Further analy-

TABLE 9

EMISSION LINE CORRELATIONS

$Y^{\dagger}$	$X^{\dagger}$	R	$\alpha^{\dagger}$	$\beta^{\dagger}$
log W(Hβ)	U-B	-0.65	0.61±0.05	-1.39±0.16
log W(Hβ)	M_B	0.49	0.86±0.04	0.11±0.02
E	M_B	0.45	1.88±0.15	0.30±0.07
E	U-B	-0.44	1.47±0.22	-3.16±0.70
E	log W(Hβ)	0.35	1.08±0.37	1.14±0.33
USB	log W(Hβ)	-0.35	21.53±0.11	-0.40±0.11
log W(Hβ)	B-V	-0.28	1.45±0.17	-0.93±0.31
E	B-V	-0.24	3.61±0.60	-2.63±1.15
BSB	E	0.18	21.20±0.09	0.06±0.03

† Fit to the equation $Y = \alpha + \beta X$

FIGURE 12

Log of the equivalent width of Hβ in emission versus U-B.

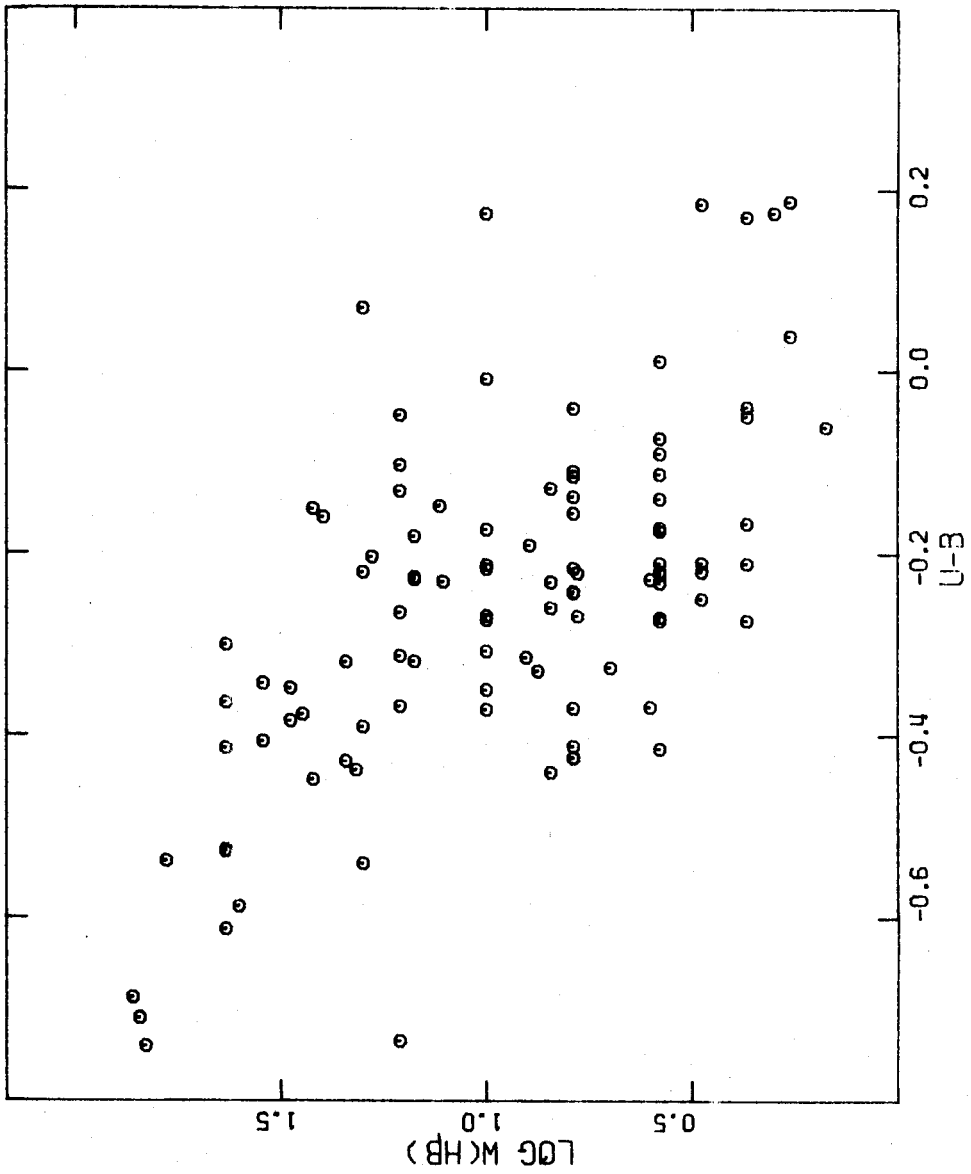
0.5
1.0
1.5
LOG W(HB)
0.2
0.0
-0.2
-0.4
-0.6
U-B

sis of observational selection effects and observations from a well defined sample are required to understand this effect.

(h) The Color-Absolute Magnitude Diagram and Possible Selection Effects

Another property of the Markarian sample is the correlation of color with absolute magnitude. This effect can be seen in Figure 13. There is a definite paucity of redder, faint Markarian galaxies. For the whole Markarian sample, the correlation coefficient of U-B with M_B is -0.38 which is significant at the 4σ level. For the complete photometric sample with $M_{pg} \geq -20.35$, the correlation coefficient is higher, -0.45, but it is also significant at the 4σ level because there are fewer galaxies in the sample. The correlation of color with absolute magnitude is not seen at such a significant level in the field galaxy sample.

In order to determine possible observational selection effects in Markarian's sample and check possible bias in our final definition of the properties of the Markarian sample, including the color-absolute magnitude effect, we examined the correlations of several observational parameters. Table 10 contains the linear correlation coefficients and slopes, β, for quantities in the photometric sample of Markarian galaxies, all Markarian galaxies, and the de Vaucouleurs field galaxy sample. Included are the color-absolute magnitude coefficients for the three samples. It is important to

FIGURE 13

The U-B / absolute magnitude distribution for Markarian galaxies.

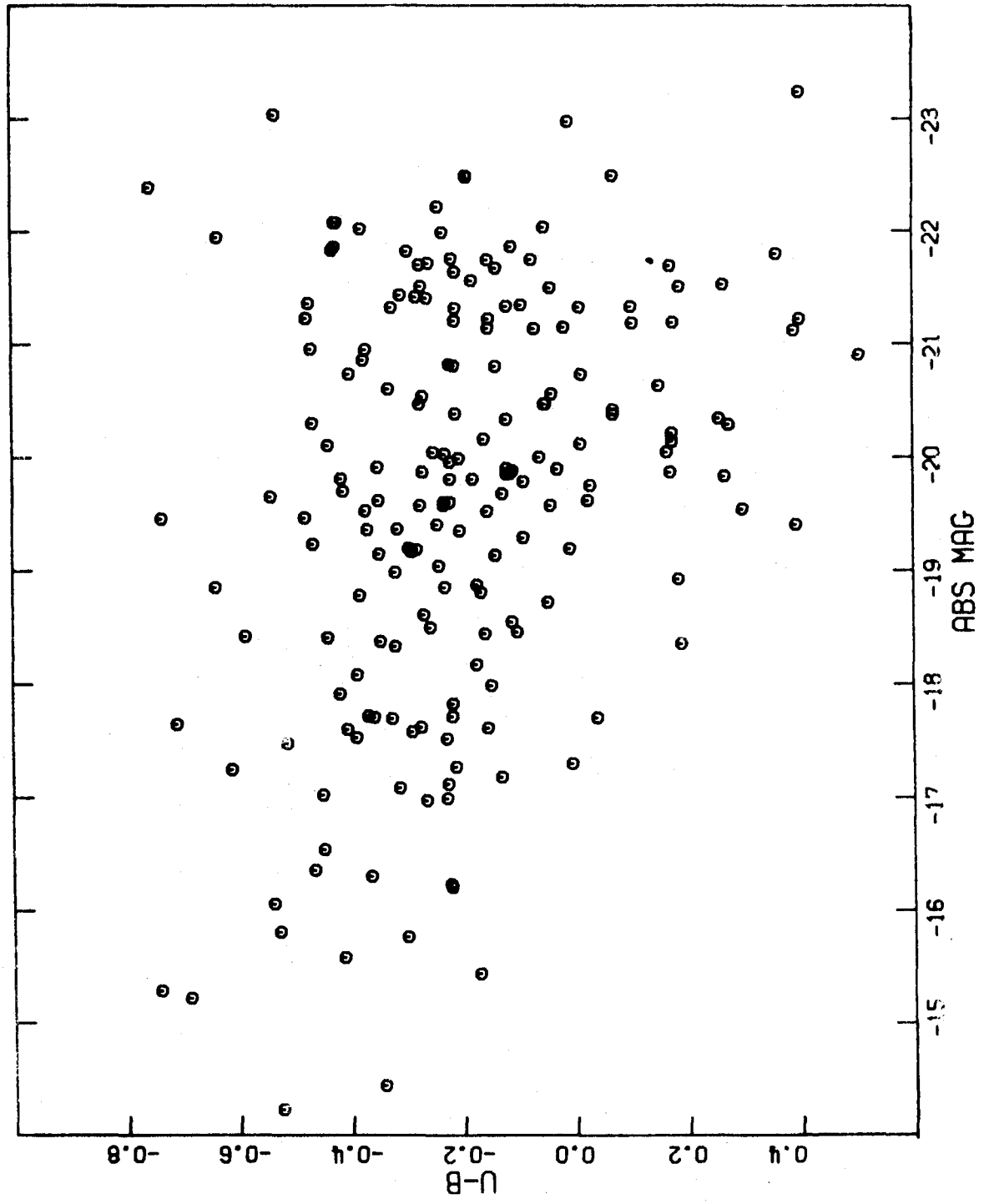
U-B
0.4
0.2
0.0
-0.2
-0.4
-0.6
-0.8
ABS MAG
-23
-22
-21
-20
-19
-18
-17
-16
-15

TABLE 10

SELECTION EFFECT COEFFICIENTS

X	Y	Photometric Sample		All Markarians		Field Galaxies	
		R	β	R	β	R	β
U-B	B	+0.03	+0.01	-0.19	-0.05	0.03	0.01
B-V	B	0.14	0.02	0.07	0.01	0.08	0.02
BSB	M_B	0.16	0.05	0.07	0.02	-0.02	-0.01
USB	M_B	-0.07	-0.03	-0.12	-0.03	-0.09	-0.05
BSB	U-B	0.13	0.25	0.09	0.16	-0.36	-0.85
U-B	M_B	-0.45	-0.08	-0.38	-0.05	-0.17	-0.04
B-V	M_B	-0.40	-0.05	-0.25	-0.02	-0.16	-0.02

remember the ranges of the parameters studied. For the Markarian samples, the B magnitude ranges from ~ 13.5 to 16.5, U-B from about -0.6 to +0.4 and M_B from about -14 to -23 in the full sample and -21 in the photometric sample. In general any photometric selection effects are small. There is a very slight tendency for Markarian to find only bluer galaxies at fainter apparent magnitudes. The large negative correlation of blue surface brightness with color (redder galaxies having higher surface brightness) in the de Vaucouleurs' field galaxy sample is caused by the morphological effect on galaxy diameter measurements--the redder elliptical galaxies are measured out to a brighter limiting isophote. The weakness of the color-apparent magnitude, and surface brightness-absolute magnitude correlations suggest that the color-absolute magnitude effect is real.

(i) Radio Data

A small number of 21cm neutral hydrogen observations of Markarian galaxies are available from the work of Bottinelli et al.(1973, 1975). These authors find that the spread of parameters such as M_{HI}/L_{pg}, the neutral hydrogen mass to photographic luminosity, is similar to that for normal galaxies. Further studies of the neutral hydrogen contents of Markarian galaxies are now under way (Lo and Fisher 1976).

In a recent 6cm radio survey, Sramek and Tovmassian (1975) detected only 5% of the Markarian objects surveyed. Half of those objects are Seyfert galaxies or objects with

no emission or absorption lines in their spectra (BL Lac type). The remaining 3% are among the most intrinsically luminous objects in the Markarian lists, and contain a large number of double, interacting systems and systems with strong structural peculiarities. These may represent the tip of the radio luminosity function for field galaxies (de Bruyn 1976; Ekers 1975). In general, the non-Seyfert, non-BL Lac type Markarian objects are not strong radio emitters.

IV. DISCUSSION

The evidence supports the viewpoint that the non-Seyfert Markarian galaxies are a subset of all field galaxies.

The Markarian sample extends further to the blue (about 0.3 magnitude in U-B) than the field galaxy sample. This can be explained, however, as the natural extension of the global space density as a function of color. The distributions of Markarian galaxy broad band colors, sizes, spectroscopic properties, neutral hydrogen content, and even colors as a function of morphological type significantly overlap the distributions of those properties for field galaxies. Collective properties such as their luminosity function and mean mass to light ratio resemble those of field galaxies. There is no evidence for strong non-thermal sources in these objects; the vast majority are not strong radio sources and their optical emission characteristics can be modeled with only stars and hot gas ionized by stars (Huchra 1976). For these reasons we conclude that the non-Seyfert, non BL Lac type Markarian galaxies - 85% of the total Markarian survey - should not be considered a new and distinct class of objects.

Because of the wide range in observed properties of these galaxies, it is difficult to assign an exact definition to 'Markarian galaxy'. There is no sharp cutoff in color or spectoscopic characteristics. A large range of

morphological types is found - from elliptical galaxies to H II regions in nearby galaxies. However, two general properties are apparent: 1. Markarian galaxies are blue for their morphological types, possibly indicating an excess of recent star formation compared to other galaxies of their type; 2. Markarian galaxies get bluer towards their centers. The Markarian sample is composed of all the bluest (U-B less than -0.3) galaxies and the bluer galaxies in a morphological class.

The data presented here extend the two color locus of galaxies to U-B = -0.75. The Markarian sample provides a base for the investigation of recent star formation in galaxies (Huchra 1976). In addition it provides more evidence for recent star formation in early type galaxies.

REFERENCES

Afanasjev, V., Karachentsev, I., and Notni, P. 1975, Astr. Nachr., 296, 233.

Arakelian, M.A., Dibai, E.A., and Esipov, V.F. 1970a, Astrofizika, 6, 39.

_____. 1972, Astrofizika, 8, 33.

Arakelian, M. A., Dibai, E. A., Esipov, V. F., and Markarian, B. E. 1970b, Astrofizika, 6, 357.

_____. 1971, Astrofizika, 7, 177.

Arakelian, M. A., Dibai, E. A., and Lyutyi, V. M. 1972, Astrofizika, 8, 473.

Arp, H. C. 1966, Ap. J. Suppl., 14, 1.

Bevington, P. 1969, Data Reduction and Error Analysis for the Physical Sciences (New York: McGraw Hill).

Borngen, F., and Kalloghlian, A. T. 1974, Astrofizica, 10, 159.

_____. 1975, Astrofizica, 11, 369.

Bottinelli, L., Duflot, R., Gouguenheim, L., and Heidmann, J. 1975, Astr. and Ap., 41, 61.

Bottinelli, L., Gouguenheim, L., and Heidmann, J. 1973, Astr. and Ap., 22, 281.

Burbidge, E. M., and Burbidge, G. R. 1962, Ap. J., 135, 694.

Bury, K. 1975, Statistical Models in Applied Science (New York: Wiley and Sons).

Casini, C., and Heidmann, J. 1975, Astr. and Ap., 39, 127.

Christensen, C. 1975, A.J., 80. 282.

Cohen, J. G. 1976, Ap. J., 203,587.

Davis, M., and Geller, M. 1975, preprint.

de Bruyn, A. G. 1976, Thesis (Sterrewacht Leiden, Netherlands).

Denisyuk, E. K. 1971a, Astr. Tsirk, 615, 4.

_____. 1971b, Astr. Tsirk, 624, 1.

_____. 1974, Astr. Tsirk, 809, 1.

Denisyuk, E. K., Babkin, I., and Sinyaeva, N. 1974, Astr. Tsirk, 837, 2.

de Vaucouleurs, G. 1959, Lowell Obs., 4, No.97, 105.

_____. 1961, Ap. J. Suppl., 5, 233.

de Vaucouleurs, G., and de Vaucouleurs, A. 1964, Reference Catalogue of Bright Galaxies (Austin: University of Texas Press).

_____. 1972, Mem. R.A.S., 77, 1.

Dibay, E. A. 1970, Astrofizika, 6, 350.

Du Puy, D. 1968, Pub. A.S.P., 80, 29.

_____. 1970, A. J., 75, 1143.

Ekers, R. D. 1975, in Structure and Evolution of Galaxies, ed. G. Setti (Dordrecht: D. Reidel), p 217.

Heidmann, J., and Kalloghlian, A. T. 1973, Astrofizika, 9, 71.

_____. 1975, Astrofizika, 11, 229.

Hiltner, W. A., and Iriarte, B. 1958, Ap. J., 128, 443.

Holmberg, E. 1958, Medd. Lund Obs. II, No. 136.

Huchra, J. 1976, in preparation.

Huchra, J., and Sargent, W. L. W. 1973, Ap. J., 186, 433.

_____. 1976, in preparation.

Humason, M., Mayall, N., and Sandage, A. 1956, A.J., 61, 97.

Kalloghlian, A. T. 1971, Astrofizika, 7, 521.

Lo, K. Y., and Fisher, R. 1976, inpreparation.

Markarian, B. E. 1967, Astrofizika, 3, 55.

_____. 1969a, Astrofizika, 5, 443.

_____. 1969b, Astrofizika, 5, 581.

_____. 1972, Astrofizika, 8, 165.

Markarian, B. E., and Lipovetsky, V. A. 1971, Astrofizika, 7, 511.

_____. 1972, Astrofizika, 8, 155.

_____. 1973, Astrofizika, 9, 487.

_____. 1974, Astrofizika, 10, 307.

Noether, G. E. 1967, Elements of Non-parametric Statistics (New York: Wiley and Sons).

Page. T. 1961, in Proceedings of the Fourth Berkeley Symposium on Mathematical Statistics and Probability, ed. J. Neyman (Berkeley, University of California).

Page, T. 1966, in Proceedings of the Sixth Berkeley Symposium on Mathematical Statistics and Probability, ed. L. M. LeCam, J. Neyman, and E. L. Scott (Berkeley: University of California).

Paturel, G. 1975a, Astr. and Ap., 40, 133.

_____. 1975b, Astr. and Ap., 45, 173.

Peebles, P. J. E., and Hauser, M. 1974, Ap. J. Suppl., 28, 19.

Sandage, A. 1961, The Hubble Atlas of Galaxies (Washington: Carnegie Institution of Washington).

_____. 1973, Ap. J., 183, 711.

_____. 1975, Ap. J., 202, 563.

Sandage, A., and Smith, L., 1963, Ap. J., 137, 1057.

Sargent, W. L. W. 1970a, Ap. J., 159, 765.

_____. 1970b, Ap. J., 160, 405.

_____. 1972, Ap. J., 173, 7.

Sargent, W. L. W., and Searle, L. 1970, Ap. J.(Letters), 162, L155.

Schechter, P. 1973, private communication.

Searle, L., and Sargent, W. L. W. 1972, Ap. J., 173, 25.

Searle, L. Sargent, W. L. W., and Bagnuolo, W. G. 1973, Ap. J., 179, 427.

Sramek, R., and Tovmassian, H. 1975, Ap. J., 196, 339.

Toomre, A., and Toomre, J. 1972, Ap. J., 178, 623.

Turner, E. L. 1975, in press.

Vorontsov-Velyaminov, B. A. 1959, Atlas and Catalogue of Interacting Galaxies (Moscow: Sternberg Institute, Moscow State University).

Vorontsov-Velyaminov, B. A., Krasnogorskaja, A., and Arhipova, V. P. 1962-1963, Morphological Catalogue of Galaxies (Moscow: Sternberg Institute, Moscow State University).

Weedman, D. 1972, Ap. J., 171, 5.

_____. 1973, Ap. J., 183, 29.

Weedman, D., and Khachikian, E. 1968, Astrofizika, 4, 587.

_____. 1969, Astrofizika, 5, 113.

Whitford, A. E. 1958, A.J., 63, 201.

Zanstra, H. 1931, Pub. Dominion Ap. Obs., 4, 209.

_____. 1961, Quarterly J.R.A.S., 2, 137.

Zwicky, F., Herzog, E., Wild, P., Karpowicz, M., and Kowal, C. 1961-1968, Catalogue of Galaxies and of Clusters of Galaxies (Pasadena: California Institute of Technology).

CHAPTER 2

STUDIES OF STAR FORMATION IN BLUE GALAXIES

I. INTRODUCTION

Recent observations of non-Seyfert galaxies in the lists of Haro, Zwicky, and Markarian have extended the color distribution of galaxies significantly bluewards. Figure 1 shows the presently known extent of galaxies in the U-B/B-V plane. Spectroscopically, the bluest objects resemble HII regions and OB associations--sites of recent star formation. Crude estimates of their space density (Huchra, 1976a) show that they constitute a significant fraction of all galaxies.

In their study of the extragalactic HII regions I Zw 18 = Markarian 116 and II Zw 40, Sargent and Searle (1970) suggest that these very blue galaxies could be very young objects. Searle et al. (1973) suggest that they might also be objects experiencing intense bursts of star formation. Evolutionary models of galaxy colors have been used to study star formation histories in galaxies (Tinsley 1968, 1972; Searle et al. 1973). The existing models of galaxy colors fit the previously known distribution of galaxy colors well, but even the flashing models of Searle et al. do not fit the observed colors of the bluest galaxies, as shown in Figure 2.

The existing models have fairly limited scope. They have been confined to a fairly narrow range in initial mass function (IMF) near the solar neighborhood value--the Salpe-

FIGURE 1

The two color distibution of galaxies. The data include measurements of field galaxies from de Vaucouleurs (1961) and de Vaucouleurs and de Vaucouleurs (1972), Markarian galaxies from Huchra (1976a), Zwicky galaxies from Sargent (1970), and Haro galaxies from Du Puy (1968,1970). The filled circles near the top of the diagram represent observations of parts of galaxies - H II regions - by Huchra (1976a, 1976b) and Sandage and Tammann (1974b).

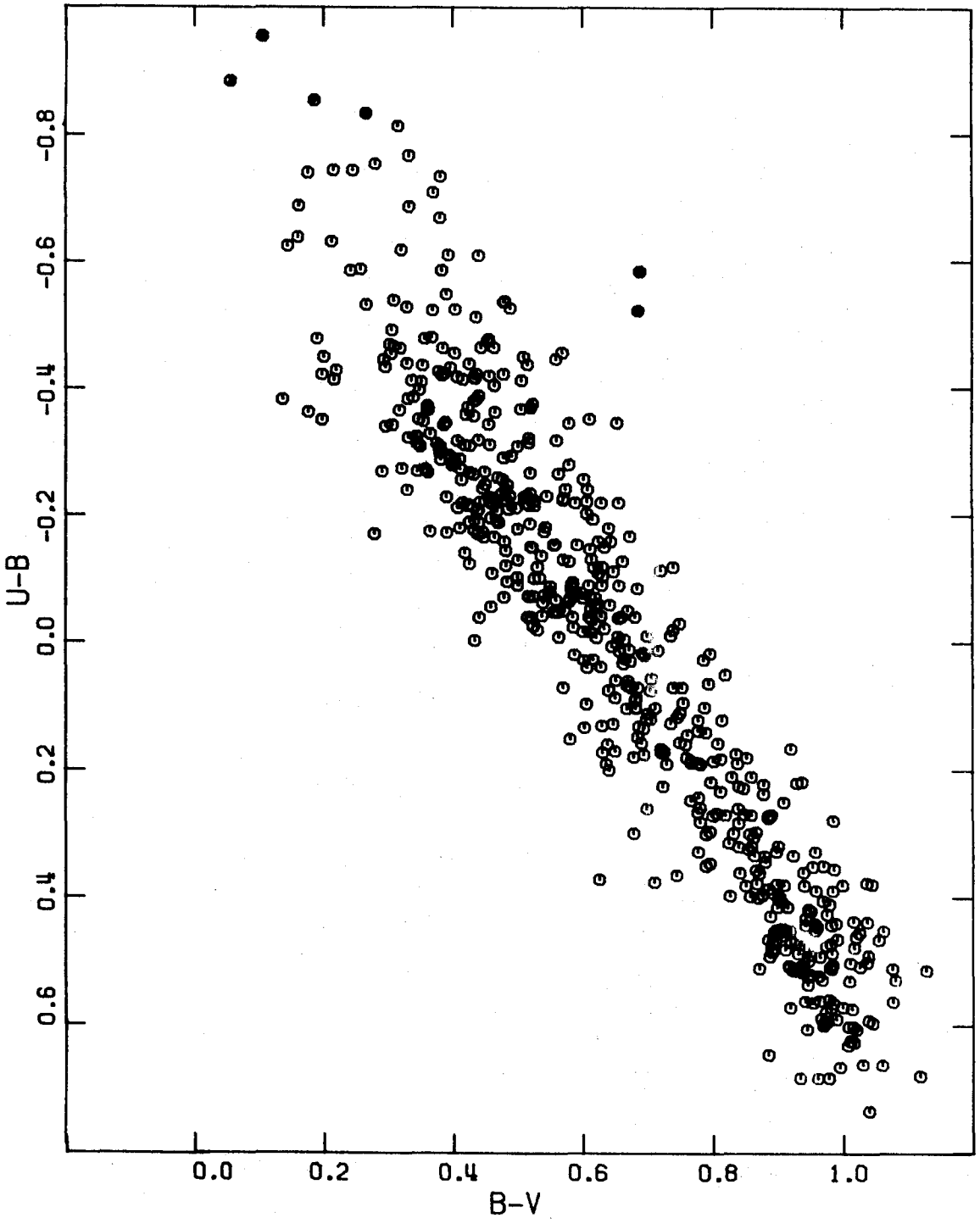
U-B
-0.8
-0.6
-0.4
-0.2
0.0
0.2
0.4
0.6
0.0
0.2
0.4
0.6
0.8
1.0
B-V

FIGURE 2

Colors for existing models of galaxies superposed on the observed envelope of galaxy colors from figure 1. The open and filled triangles are for models from Tinsley (1968,1972); open circles, squares and hexagons are from old, uniform and "flashing" galaxy models by Searle et al. (1973). Also shown is the evolutionary track for star clusters with an initial delta function star formation rate (Searle et al. 1973).

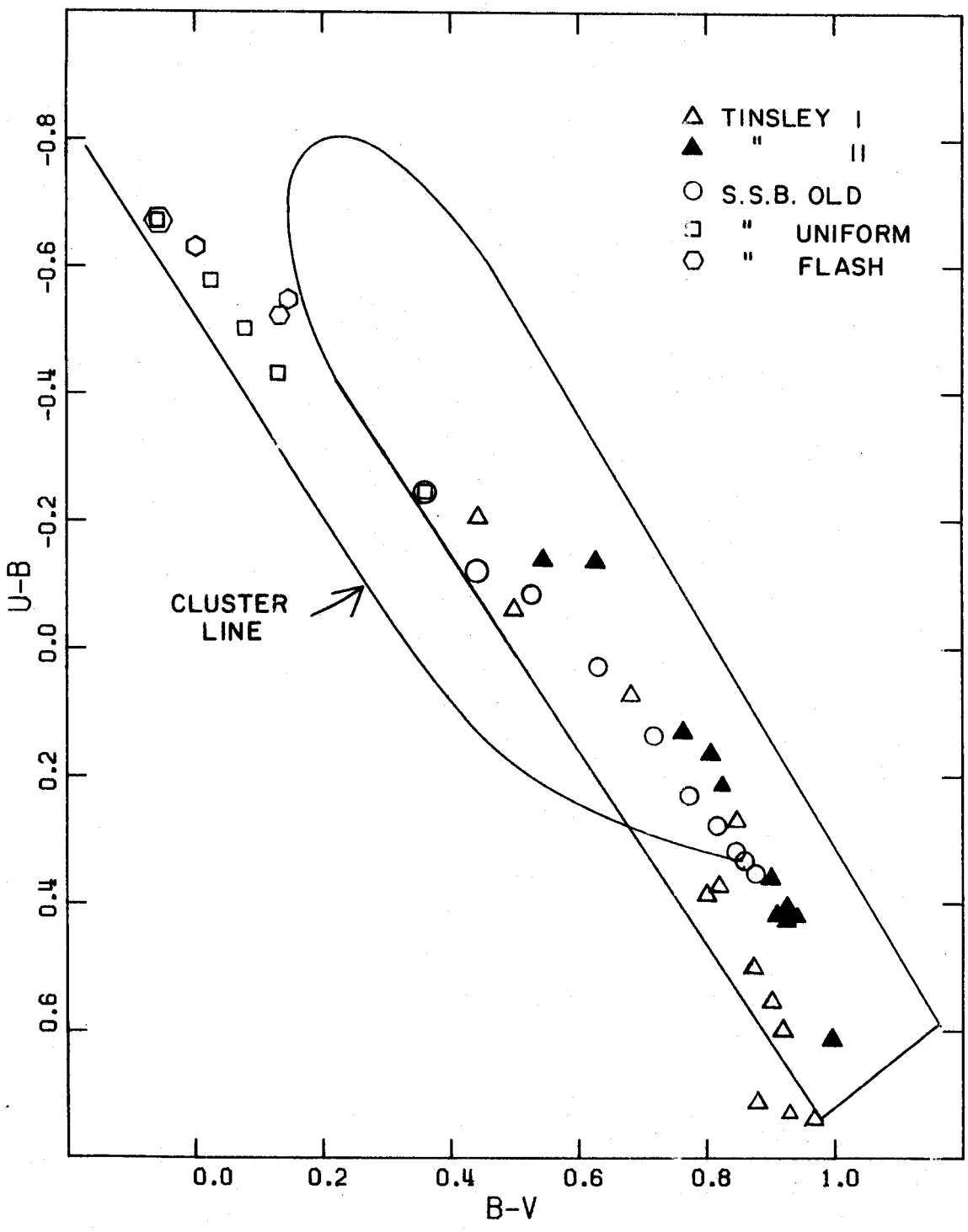
TINSLEY I
" II
S.S.B. OLD
" UNIFORM
" FLASH
CLUSTER LINE
U-B
B-V
-0.8
-0.6
-0.4
-0.2
0.0
0.2
0.4
0.6
0.0
0.2
0.4
0.6
0.8
1.0

ter function. Searle and Sargent (1972) suggest that enhanced high mass star formation or only high mass star formation might explain the blue galaxies. Searle et al. (1973) suggests a slightly flatter IMF might better explain even de Vaucouleur's colors of Magellanic irregular galaxies. In addition, the models have not included the effects of gaseous emission, which could be considerable in strong emission line systems.

In order to match the observed properties of the bluest galaxies, galaxy models have been constructed with a variety of simple evolutionary histories and luminosity functions. These models include the effects of gaseous emission, effects of red supergiant stars, and use a much finer grid of high mass stellar models than previous models have used.

The details of model construction are described in Section II, and classes of suitable models in Section III. In Section IV we compare predictions of the models with other observed properties of the blue galaxies, and discuss which models best fit these properties.

II. MODEL CONSTRUCTION

The basic model construction is similar to that used by Tinsley (1968, 1972) and Searle et al. (1973). The theoretical evolutionary tracks of stars in the log L vs log Te plane are converted into age-flux tables. The "flux" F(i) (actually an intensity) in a filter i, is defined as

$$F(i) \equiv \text{dex}\ (-M_i/2.5), \tag{1}$$

where M_i is the absolute magnitude in the filter.

The lifetime (τ) of the galaxy model under construction is divided up into a large number of time steps--usually 1000--of equal duration ($\Delta\tau$). The flux [$F_G(i,t)$] of a galaxy model at a time $T - n\Delta t \leq \tau$ in the ith bandpass is given by

$$F_G(i,t) = \sum_{j=0}^{n-1} \sum_K \left[\Psi(K,j) \int_{(n-j-1)\Delta\tau}^{(n-j)\Delta\tau} F_K(i,t')\,dt' \right] \tag{2}$$

where $F_K(i,t')$ is the flux of a star of mass type K in bandpass i as a function of its age t'. $\Psi(K,j)$ is the birthrate function which characterizes the model--the number of stars of mass type K formed in the jth time step. The flux integral is performed by piece-wise time-weighted summation over intervals in the age-flux tables.

(a) The Stellar Data

A set of stellar evolutionary models was assembled

with composition x = 0.70, Z = 0.02, and masses given in Table 1. The low mass models (m < 1.0 solar mass) were taken from a compilation by Caldwell, et al. (1974). These models were assumed not to evolve on the timescales of interest.

Models of 1.0, 1.25, 1.50, 2.25, 3.0, 5.0, and 9.0 solar masses were taken from Iben (1965b, 1966a, 1966b, 1967a, 1967b) with corrections and additions to the red giant evolution as noted by Tinsley (1972). The additional models between 1 and 9 solar masses were interpolated from the corrected Iben models.

Unlooped high mass models (models with helium ignition in the blue supergiant phase producing no loops in the log L - log Te plane) of a variety of compositions were taken from Iben (1966c), Robertson (1972), Ziolkowski (1972), Barbaro et al. (1973), Barbaro et al. (1972), and Chiosi and Summa (1970). The timescales, luminosities and temperatures of steps in each model were reduced to the standard composition using corrections derived from the models of Barbaro et al. (1973). Experimentation in the galaxy models with looped high mass stellar models (helium ignition after collapse to the red giant phase causing the star to then evolve bluewards) from Stothers (1963, 1964, 1966) and the above-listed sources did not produce significant changes in the computed galaxy properties. Intermediate mass models are again interpolated from the models in the literature.

The majority of galaxy models contained only stars of

TABLE 1

STELLAR MASSES

0.11	1.50	4.0	9	24
0.19	1.75	4.5	11	26
0.36	2.00	5.0	13	28
0.58	2.25	5.5	15	30
0.73	2.50	6.0	16	
0.88	2.75	6.5	18	35
1.00	3.00	7.0	20	40
1.25	3.50	8.0	22	60

30 solar masses or less; the IMF was integrated between 0.05 and 31 solar masses. The high mass stars (35, 40, and 60 solar masses) were included in a small number of galaxy models in order to examine the effects of increasing the upper mass limit of the IMF.

Points in the log L - log Te plane were converted into absolute magnitudes using calibrations of the bolometric corrections and colors as a function of effective temperature and luminosity class. Johnson's (1966) color calibrations were used. Hart's (1971) bolometric corrections were used for models with log Te > 4.35. For cooler models, Johnson's (1966) calibration was used.

(b) Gaseous Emission

The flux emitted in the continuum at wavelength λ by a hot gas in volume V is

$$F_\lambda = NeN_+ \gamma_\lambda(T)\ V \text{ ergs sec}^{-1}\ \text{Å}^{-1} \qquad \text{(Seaton 1960)} \quad (3)$$

where Ne and N_+ are the densities of electrons and ions. $\gamma_\lambda(Te)$ is the continuous emission coefficient as a function of temperature Te, and includes free-free emission, recombination of H^+, He^+, and He^{++}, and two-photon emission (Brown and Matthews 1970). The flux in the Hβ recombination line ($F_{H\beta}$) is given by

$$F_{H\beta} = N(H_o)\frac{\alpha^{eff}_{H\beta}}{\alpha_E(T}\ 4.09 \times 10^{-12} \text{ erg sec}^{-1} \qquad (4)$$

(Zanstra 1931, 1961). The numerical factor is the energy of one Hβ photon. $N(H_o)$ is the number of ultraviolet photons

from hot stars capable of ionizing hydrogen. $\alpha_{H\beta}^{eff}(T)$ is the effective recombination coefficient for emission in Hβ, and $\alpha_E(T)$ is the total recombination coefficient; both are functions of the gas electron temperature. For case A (a nebula optically thin in the Lyman lines), the ratio of the recombination coefficient varies by 25% from 5000°K to 20,000°K. For case B, (a nebula optically thick in the Lyman lines) the ratio is about twice that for case A, and it varies by only 4% over the same temperature range.

If it is assumed that the galaxy contains sufficient gas to be ionization bounded, the Stromgren equilibrium condition (Stromgren 1936)

$$\alpha_E(T) N_e N_+ V \tilde{=} N(H_o) \qquad (5)$$

will apply. The total number of recombinations roughly equals the total number of ionizing photons. The continuum flux then becomes

$$F_\lambda = \frac{\gamma_\lambda(T)}{\alpha_E(T)} N(H_o). \qquad (6)$$

The intensities of the hydrogen lines relative to Hβ are known from recombination theory (Pengelly 1964). As a first approximation, the intensities of other optical emission lines relative to Hβ were taken empirically from observed HII regions and planetaries.

Three sets of line ratios were assembled. The "standard" set is an average over line ratios in LMC HII regions (Peimbert and Peimbert 1974), Orion (Simpson 1973) and objects in Searle and Sargent (1972). The "high excitation"

TABLE 2

EMISSION LINE INTENSITIES†

λ (Å)	Ion	Standard	High Excitation	Extra Lines
3727	[O II]	1.11	0.76	
3869	[Ne III]	0.16	0.28	
4363	[O III]	0.13	0.09	
4471	He I	0.04	0.04	
4959	[O III]	1.13	1.68	
5007	[O III]	3.39	5.14	
5876	He II	0.14	0.28	
6548	[N II]	0.13	0.02	
6584	[N II]	0.40	0.03	
6717	[S II]	0.02	0.05	
6731	[S II]	0.05	0.12	
3133	[O III]			0.10
3312	[O III]			0.06
3341	[O III]			0.08
3346	[Ne V]			0.12
3427	[Ne V]			0.30

† Relative to H_β = 1.0

set is the average for the only extragalactic HII regions of Sargent and Searle (1970). The "extra line" set is added to the "standard" set and consists of strong ultraviolet lines in planetaries from Aller (1956).

With the above approximations, the flux in both the continuum and emission lines is a function of $N(H_o)$ and tabulated constants that are functions of temperature.

For any given T, a synthetic spectrum for the gas can be computed. Figure 3 is an example, showing the energy distribution of an 8000°K gas, with the energy given in ergs per Å per ultraviolet photon, containing the standard and extra emission lines. The colors of the gas are found by using the response functions and reduction formulae of Matthews and Sandage (1973). The absolute V magnitude of the gas per ultraviolet photon is calibrated by integrating the V response function over the energy distributions for stars of known absolute magnitude. In this way, the integrated flux in the V band for a star of 0.0th absolute magnitude is found to be 4.3×10^{31} ergs sec^{-1}. The stars used are α Lyr ($M_V = 0.5$) and ζ Oph ($M_V = -3.8$) from Oke (1971). The calibration used was that of Oke and Schild (1970), which is in close agreement with other calibrations over the wavelength range of interest (Hayes et al. 1970). It was not possible to use the previous calibrations of V magnitude in ergs sec^{-1} $Å^{-1}$ at a specified effective wavelength because the flux from the gas comes primarily from the emission

FIGURE 3

The calculated spectrum of a gas at Te = 8000°K with the S + EL line ratios. The emitted energy is calculated per ionizing ultraviolet photon.

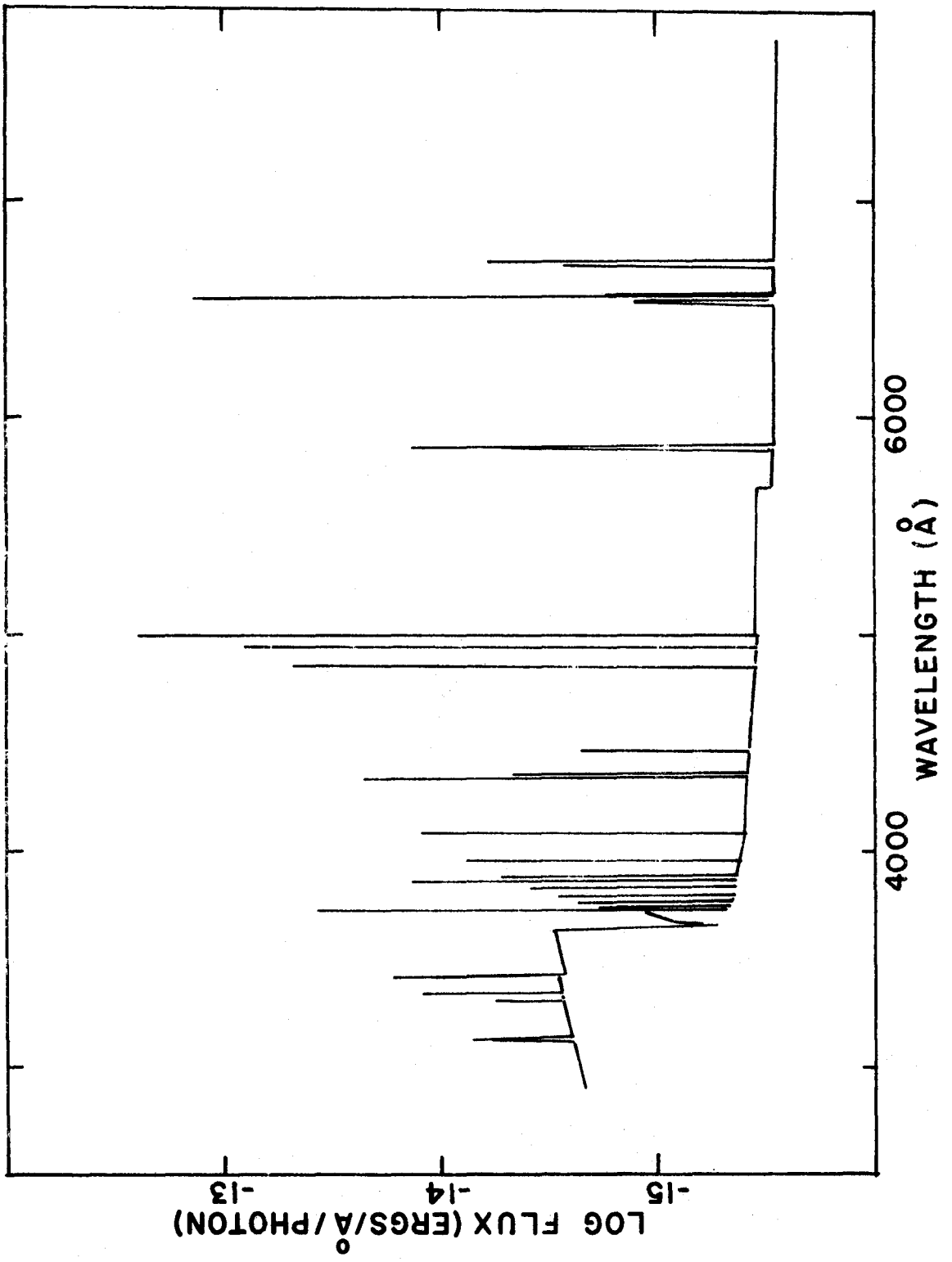
LOG FLUX (ERGS/Å/PHOTON)
-15
-14
-13
4000
6000
WAVELENGTH (Å)

lines.

Case B is assumed throughout. For calculation of the continuum, $N(He^+)/N(H^+) = 0.13$, and $N(He^{++})/N(H^+) = 0.06$, was assumed, and the $\gamma_\lambda(T)$'s of Brown and Matthews (1970) were used. The helium continuum does not contribute significantly to the optical flux, so the computed magnitude and colors are relatively insensitive to the helium ion abundances.

Several synthetic gas spectra were computed for a range in temperatures and a variety of assumptions concerning the non-Balmer emission lines. Table 3 gives the computed colors and "magnitudes" corresponding to the absolute V magnitude due to one ionizing stellar photon. S, HE, and EL indicate which sets of line intensities were used with the appropriate Balmer line intensities for each temperature. NL indicates that no emission lines, including Balmer, were added; in this case the colors and magnitude represent those of a 10,000°K lineless gas continuum. The colors and magnitudes are similar for all but the NL case. The computed colors also agree well with the gas and emission line colors of Grewing et al. (1968).

The colors of emission line systems are strongly affected by redshift (Grewing et al. (1968); Sandage 1966). The effect of shifting the spectrum of the gas in wavelength is calculated, not including the effects of redshift on total flux. Any stellar component to which the gaseous emission

TABLE 3

GAS COLORS

T (°K)	Lines	U-B	B-V	V
14000	S	-0.75	-0.02	116.24
10000	S	-0.84	-0.01	116.26
10000	N1	-1.87	0.39	117.53
10000	HE	-0.57	0.09	115.96
8000	S	-0.85	-0.02	116.31
8000	S+EL	-0.95	-0.02	116.31
8000	HE	-0.68	0.09	116.00
6000	S	-0.93	-0.02	116.34

is compared would be affected the same way. Table 4 shows the change in colors and V magnitude of the 8000°K EL gas as $z = \Delta\lambda / \lambda$ varies from 0.0 to 0.1. The U-B color is not seriously affected, but B-V gets redder as Hβ and the [OIII] lines shift into the V bandpass. This same effect causes the V flux to increase. Fortunately, the galaxies that have been observed are generally of low z, so redshift does not seriously affect the colors.

The ultraviolet photon flux $N(H_o)$ in the galaxy models was calculated by summing over the $N(H_o)$'s for the stars. The calibration of $N(H_o)$ as a function of log Te for stellar models was obtained from the stellar atmospheres calculations of Morton (1969) and Searle (1971). The absolute V magnitude of the gas in any model galaxy is

$$V = V_{gas} - 2.5 \log N(H_o) \qquad (7)$$

and the contributions to the flux in each bandpass is computed accordingly.

The equivalent width of Hβ in emission is calculated using equation (4) and interpolating the flux in the continuum per Å at 4861Å from the colors of the background stellar population. Measurement of this parameter is independent of reddening.

The basic set of galaxy models uses the 8000°K EL gas at zero redshift. We assume that the gas is ionization bounded. This assumption produces the maximum contribution from the gas. The gas flux at each model step is computed

TABLE 4

GAS COLORS AS A FUNCTION OF REDSHIFT

Z	U-B	B-V	V
0.000	-0.95	-0.02	116.31
0.005	-0.97	0.17	116.15
0.010	-0.99	0.34	115.99
0.015	-1.02	0.52	115.84
0.020	-1.04	0.67	115.71
0.025	-1.03	0.77	115.61
0.030	-1.02	0.86	115.52
0.035	-1.01	0.94	115.44
0.040	-0.99	1.02	115.37
0.045	-0.98	1.07	115.31
0.050	-0.98	1.13	115.26
0.055	-0.98	1.17	115.23
0.060	-0.98	1.21	115.19
0.065	-0.97	1.22	115.17
0.070	-0.96	1.24	115.16
0.075	-0.95	1.24	115.15
0.080	-0.95	1.25	115.15
0.085	-0.94	1.24	115.15
0.090	-0.92	1.23	115.15
0.095	-0.90	1.21	115.16
0.100	-0.88	1.19	115.18

only with the ultraviolet photon flux from stars available at that step. The recombination timescale

$$\tau_{rec} = 1.2 \times 10^{5}\ Ne^{-1}\ yrs \qquad (8)$$

for average conditions in an HII region (Ne ~ 1 -100) is much smaller than the model step size.

III. THE MODELS

Three general classes of models were constructed that can fit the observed color-color properties of the bluest galaxies: "old" galaxies, "young" galaxies, and "composite" galaxies.

(a) Old Galaxies

Old galaxies are defined as systems which started forming stars $\sim 10^{10}$ years ago, and whose rate of star formation is monotonic in time. The simple parameterization of the stellar birthrate function

$$\Psi(m,t) \propto m^{-\alpha} e^{-\beta\, t/t_o} \qquad (9)$$

of Searle et al. (1973) is used. The IMF is a power law in mass of slope α. The integrated formation rate as a function of time is independent of mass and is taken to be exponential: t_o is the age of the galaxy and β is the exponential decay rate. A system with $\beta = 0$ is still forming stars at its initial formation rate. A system with $\beta = 10$ is currently forming stars at 5×10^{-5} of its initial star formation rate. Systems with $\alpha = 2.35$ have IMFs similar to the Salpeter initial mass function (Salpeter 1955) for the solar neighborhood, those with $\alpha < 2.35$ are high mass star enriched, and those with $\alpha > 2.35$ are high mass star deficient.

A grid of models is constructed with $\alpha = 0.35$, 1.35,

1.85, 2.35, and 3.35; β = 0, 1, 3, 5, 7, 10, and 15; and $t_o = 1.5 \times 10^{10}$ years. Figure 4 shows the locus of curves of constant α and varying β , for galaxies of age 1.2×10^{10} years, superposed on the envelope of the observed galaxy color-color distribution. Points along the curves represent the models with the β's given above. Models with low β's are bluer than those of high β . The bluest models shown are those with constant rates of star formation. Models using the Salpeter IMF agree closely with the models of Tinsley (1972). and Searle et al. (1973).

The models that fit the observed colors of the blue galaxies are those with IMFs significantly flatter than the Salpeter function. Also, models with α= 1.35 require relatively constant star formation rates, i.e., $\beta < 5$. Neither decreasing the age by small fractions, nor increasing the upper mass limit of the IMF, nor using models with slightly increasing star formation rates as a function of time produced a fit of the observed colors with Salpeter IMF models. All of the above parameter changes move the models along an extension of the curves in Figure 4.

The evolution of these models in the two-color plane is close to the tracks of constant α in Figure 4. Figure 5 shows the evolution of one color (U-B) as a function of time for models of α = 1.35 and varying β. The luminosity evolution as a function of time for these models is not significantly different from the evolution seen in the models of

FIGURE 4

Colors of galaxies that are 1.2×10^{10} years old, superposed on the observed galaxy color envelope (Figure 1). The lines represent loci of models with a given α and varying β.

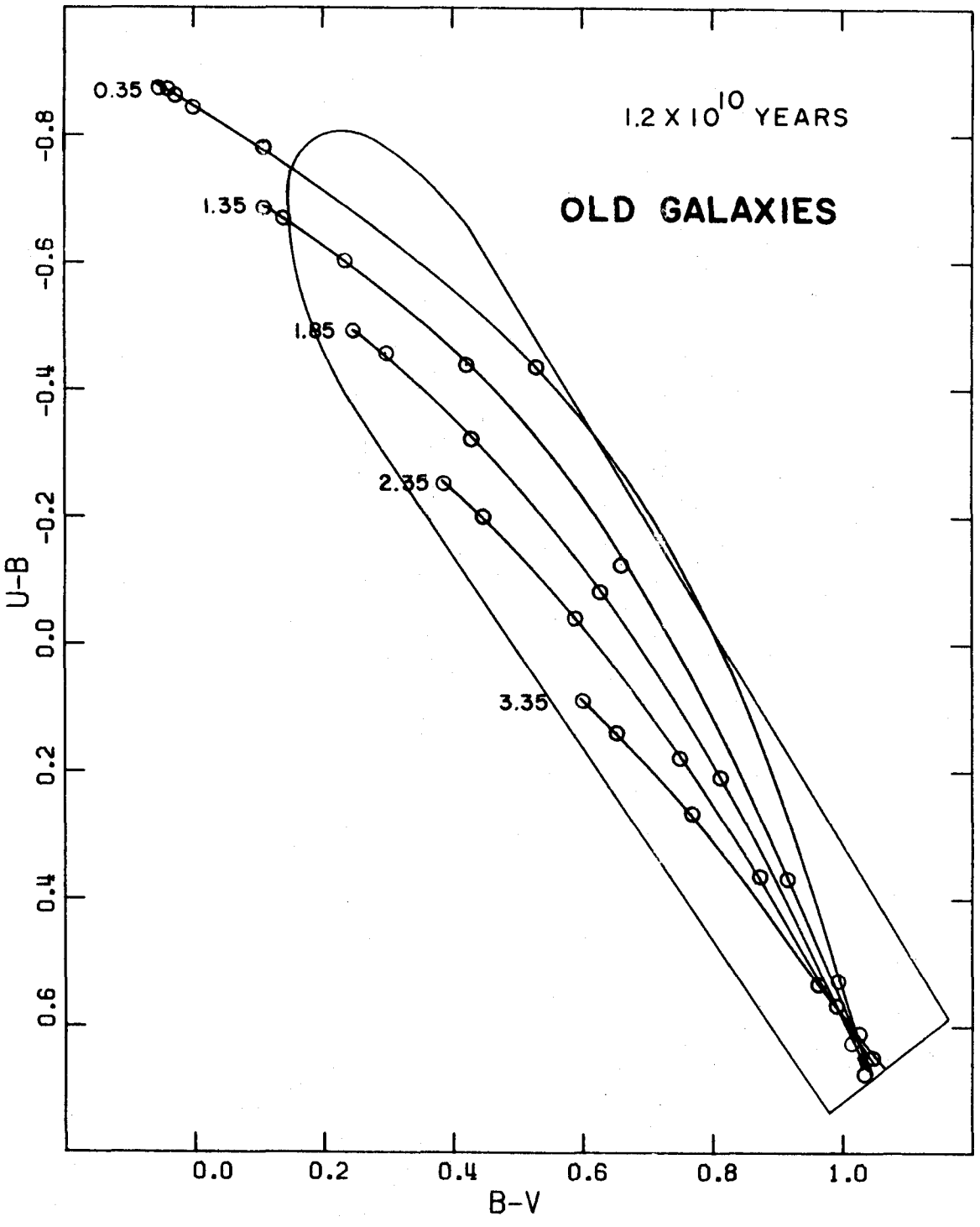
0.35
1.35
1.85
2.35
3.35
1.2 X 10^10 YEARS
OLD GALAXIES
U-B
B-V
-0.8
-0.6
-0.4
-0.2
0.0
0.2
0.4
0.6
0.0
0.2
0.4
0.6
0.8
1.0

FIGURE 5

The evolution in U-B for galaxies with $\alpha = 1.35$ and various βs.

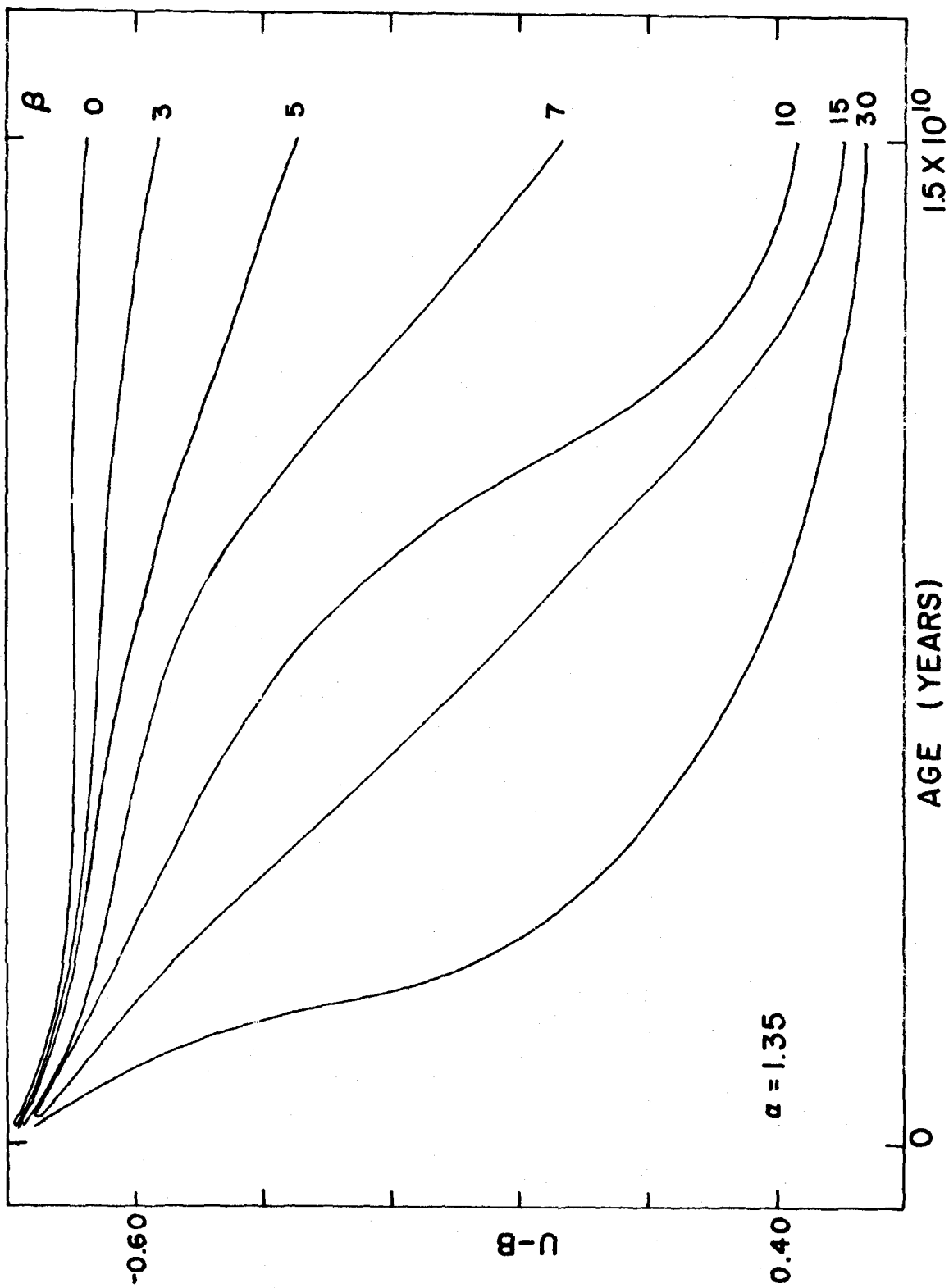
β
0
3
5
7
10
15
30
α = 1.35
U-B
-0.60
0.40
0
1.5 X 10^10
AGE (YEARS)

Tinsley (1972). Models of larger β and smaller α have the greatest total magnitude change (about 5.5 magnitudes in 1.5×10^{10} years for $\alpha = 1.35$, $\beta = 15$; about 3.5 magnitudes for $\alpha = 2.35$, $\beta = 15$; and about 0 magnitude for $\alpha = 2.35$, $\beta = 0$). It is interesting to note that elliptical galaxy colors can be matched approximately by any luminosity function studied if β is large enough so that there is no recent star formation. This is a consequence of the fact that the colors of low mass giants are relatively independent of mass.

In these models, the gas does not significantly change the galaxy colors. The gas is similar in color to the stars that are ionizing it. Also, its maximum contribution to the visible flux is 16% for the bluest model plotted. Thus our assumptions about the properties and parameters of the gas to first order do not affect the models. Decreasing α increases the gas contribution (and thus the Hβ equivalent width).

The mass-to-light ratios in the models are basically determined by the lower mass limit of the IMF. Any reasonable M/L can be produced by any model without changing its colors. Changing the upper mass limit changes the colors slightly, and changes the contribution of gaseous emission. An estimate of a reasonable upper mass limit can be made. Stothers and Simon (1968), and Larson and Starrfield (1971) argue that there is an upper mass limit of $\sim 60 M_{\odot}$ for

reasonable stellar models. The brightest stars observed in our galaxy (except for η Carinae) and other nearby galaxies (Sandage and Tammann 1974a) are consistent with an upper mass limit of 45 solar masses. For galaxy models with an IMF upper limit of 45 $M_\odot$ instead of 31 $M_\odot$, the colors of the bluest models change by less than 0.08 magnitude and the color-color track remains the same. For those models with colors inside the observed envelope the contribution of the gas is less than 15% in the V bandpass.

The effects of red supergiant evolution were also studied. Removing the red supergiant phases of evolution for high mass stars decreases U-B by less than 0.01 magnitude and B-V by less than 0.01 magnitude. Doubling the red supergiant lifetimes increases U-B less than 0.01 magnitude and B-B less than 0.04 magnitude, producing a very small shift to the right in the color-color tracks. The size of this shift is greatest for small α's and small β's. The lack of a significant change in color when the red supergiant lifetimes are doubled is also evidence that pre-main-sequence evolution does not affect the model colors; the collapse times of the stellar models to the main sequence are shorter than the red giant lifetimes.

(b) Young Galaxies

The second general class of models is the "young" ga-

laxy. These are systems that started forming stars relatively recently compared to the age of the universe, $\lesssim 10^9$ years ago.

The birthrate parameterization of the "old" galaxy models was used. For these model galaxies, though, the age t is a more important parameter than β. Figure 6 presents the colors of young galaxies with nearly constant rates of star formation ($\beta \lesssim 1$) with α = 0.35, 1.35, 1.85, 2.34 and 3.35 at ages of 2×10^8 years and 1.2×10^9 years. These are what the old galaxies of Section (a) looked like when they were one-tenth or less their age of 1.2×10^{10} years.

Increasing β causes the galaxies to get redder at a given age, with the effect being strongest for the models with large α 's. For the Salpeter function models with $\beta = \infty$, the color-color locus in time is very similar to the cluster evolution track of Searle et al. (1973) seen in Figure 2. At the youngest age calculated for this class of model, 2×10^7 years, the colors for all models with $\alpha \leq 2.35$ are approximately U-B = -0.90 and B-V = -0.10. Decreasing the age of models with the same α increases the gas contribution, as does decreasing α for models of the same age.

The model colors do not fall in our observed envelope. At a given U-B, the models are about 0.25 magnitude too blue in B-V. This cannot be remedied by changing the red

FIGURE 6

The colors of young galaxy models at 2×10^8 and 1.2×10^9 years with various IMFs and nearly constant star formation rates, superposed on the observed galaxy envelope (Figure 1). The arrows are reddening lines representing the change in color caused by one magnitude of visible extinction.

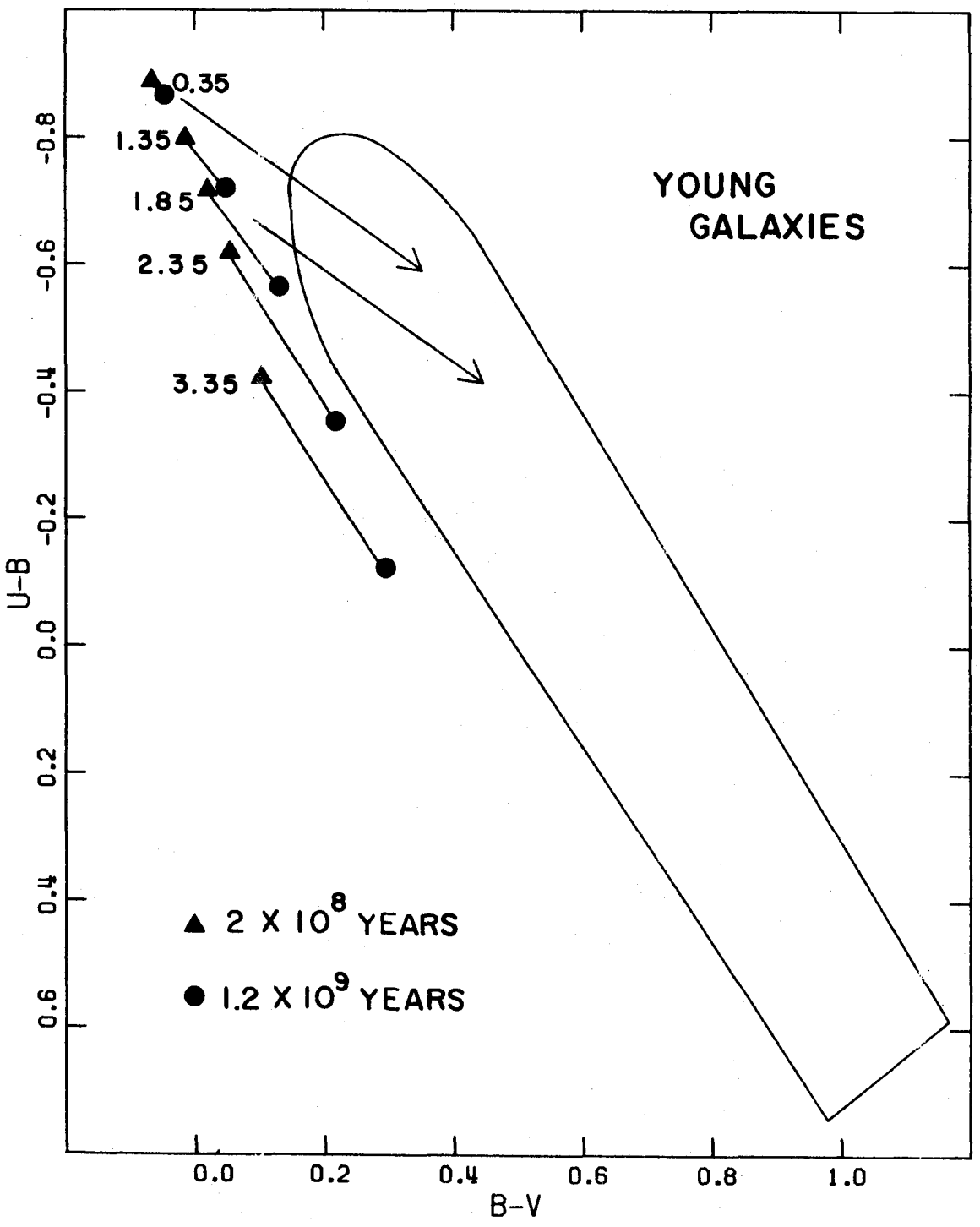
0.35
1.35
1.85
2.35
3.35
YOUNG
GALAXIES
▲ 2 X 10^8 YEARS
● 1.2 X 10^9 YEARS
U-B
B-V
-0.8
-0.6
-0.4
-0.2
0.0
0.2
0.4
0.6
0.0
0.2
0.4
0.6
0.8
1.0

supergiant evolution or the parameters of the gas. The color changes for doubling the red supergiant lifetimes are the same for these models as for the old galaxy models. The gas contributes only 20% of the V flux in the youngest, bluest model and less in all the others. Even then the colors of the gaseous emission at low redshifts are not sufficiently different from the underlying stellar component colors to produce significant changes in the models.

Reddening due to internal absorption can bring the model colors into the observed envelope. Also plotted in Figure 6 are two reddening lines whose length and direction correspond to the change in U-B and B-V due to one magnitude of visual extinction. This assumes that the Whitford law is applicable for the mean extinction of an ensemble of stars and gas. Since absorption is observed in galaxies (Holmberg 1958; Heidmann et al. 1972), and is associated with some galactic sites of star formation (e.g. Strom et al. (1975) highly reddened young galaxies might be a viable explanation of the bluest galaxies observed.

A constraint still exists on the ages of models of differing α's. To produce the systems with U-B <-0.40, models with a Salpeter IMF must on the average be younger than 10^8 years, especially if they have not been forming stars at a mearly continuous rate. Huchra (1976a) gives 1% as a crude estimate of the fraction of galaxies bluer than the above limit. Unless the formation rate of young

galaxies is higher now than it was in the past, the statistical lifetime versus Hubble time argument suggests that these systems are forming stars with IMFs flatter than the Salpeter function.

(c) Composite Galaxies

The third general class of models are the "composite" galaxies. Simple systems consist of an old galaxy, like the models in Section (a), plus a burst of recent star formation. These are basically the sum of an old galaxy and a very young galaxy. This type of model can be generalized to galaxies composed of multiple bursts of star formation at different ages--the superposition of star clusters (Searle et al. 1973).

Simple models for bursts of star formation have been computed. A power law IMF was again used. The star formation rate was taken to be a rectangle function, constant for an interval of 1, 2.5, 5, or 10 x 10^7 years and zero afterwards. These intervals are similar to observed cluster formation times (Hartmann 1970; Schlesinger 1972). Smoothing the rectangle to a Gaussian profile did not significantly affect the colors as a function of time.

The burst models have an interesting property. For bursts of duration $\leq$ 5 x 10^7 years and $\alpha \leq 2.35$, the colors and their time evolution are almost independent of duration, α , and the upper mass limit.

As in the earlier types of model the gas contribution

increases as the slope of the IMF decreases. However, at the very early stages of the burst (in a few million years) the fractional contribution of the gas reaches almost 50% in the models with $\alpha = 0.35$. The stellar continuum colors are U-B = -1.12, B-V = -0.31. After adding the gas, the model colors are U-B = -1.06, B-V = -0.16. This effect is less pronounced in the models with steeper IMFs whose stellar continua are redder than those of the $\alpha = 0.35$ model. As the burst ages before it turns off, the ratio of very massive stars to less massive stars decreases and the luminosity of the burst increases. At maximum luminosity, which occurs near the end of the burst's duration, the gas contribution drops to 20% or less. During the most luminous phases of the burst, the gas does not significantly affect its colors.

Figure 7 shows the loci in the two-color plane for simple two-component systems composed of different concentrations of bursts superposed on old galaxies. Three curves are plotted, connecting two burst models with two old galaxy models. The bursts are the bluest points on the curves; the underlying old galaxies are the reddest. Intermediate points correspond to systems with varying contributions of the burst to the V-band light. The filled symbols represent systems with equal contributions to the V band from the burst and the old galaxy components. The curvature of these loci is similar to that in Sandage's

FIGURE 7

The colors of two component composite galaxy models. The points along the curves represent different contributions of the burst to the models total V-band light, ranging from zero at the lowest points on the curves to 100% at the uppermost points. The filled square, triangle and circle represent models where the burst contributes 50% of the light.

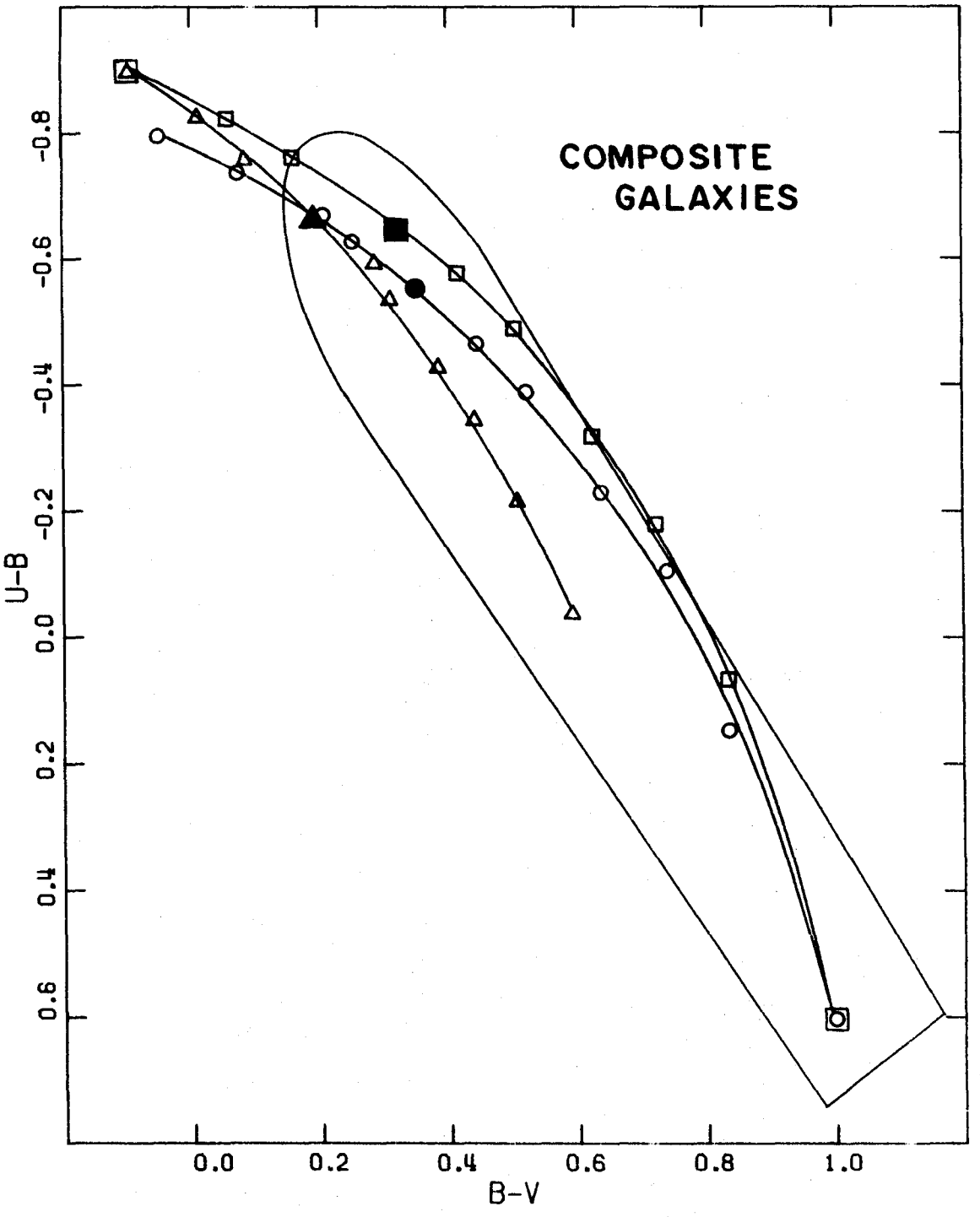
COMPOSITE
GALAXIES
U-B
B-V
-0.8
-0.6
-0.4
-0.2
0.0
0.2
0.4
0.6
0.0
0.2
0.4
0.6
0.8
1.0

(1973) composite models of N galaxies. It is caused by the greater contribution of the burst to the light in the bluer bandpasses.

In Figure 8 we see the color-color evolution of two representative composite models. The burst in both is a model with $\alpha = 1.35$ and a duration of 2.5×10^7 years. Its colors at maximum are U-B = -0.91 and B-V = -0.09, and its strength has been adjusted to be 50% of the V light at its maximum light. The underlying old galaxy models are the 1.2×10^{10} years, $\alpha = 2.35$, with $\beta = 3$ and $\beta = 10$. The evolutionary track is 10^8 years long, with tick-marks at 10^7 year intervals. The old galaxy models do not evolve on this time scale. The loci of the color-color track for composite models using burst models of other durations and IMFs and a single old galaxy model are similar. Only the timescales along the tracks change. Models with lower α's for the burst decay more rapidly in color.

The luminosity evolution of the bursts is similar to that for cluster models. 5×10^8 years after it stops forming stars, an $\alpha = 2.35$ burst has dimmed about 3 magnitudes, and an $\alpha = 1.35$ burst has dimmed more than 5 magnitudes. The composite galaxy models with equal burst and old galaxy at maximum can dim, at most, 0.75 magnitude on any time scale for which the old galaxy does not evolve.

Composite models for the blue galaxies are attractive for several reasons. In nearby irregular galaxies star

FIGURE 8

The color evolution of two composite galaxy models. The burst is the same for both, $\alpha = 1.35$ and duration 2.5×10^7 years, but differnt underlying galaxy models (circles) have been added. The tick marks along the tracks represent steps of 10^7 years, and a total time of 10^8 years is shown.

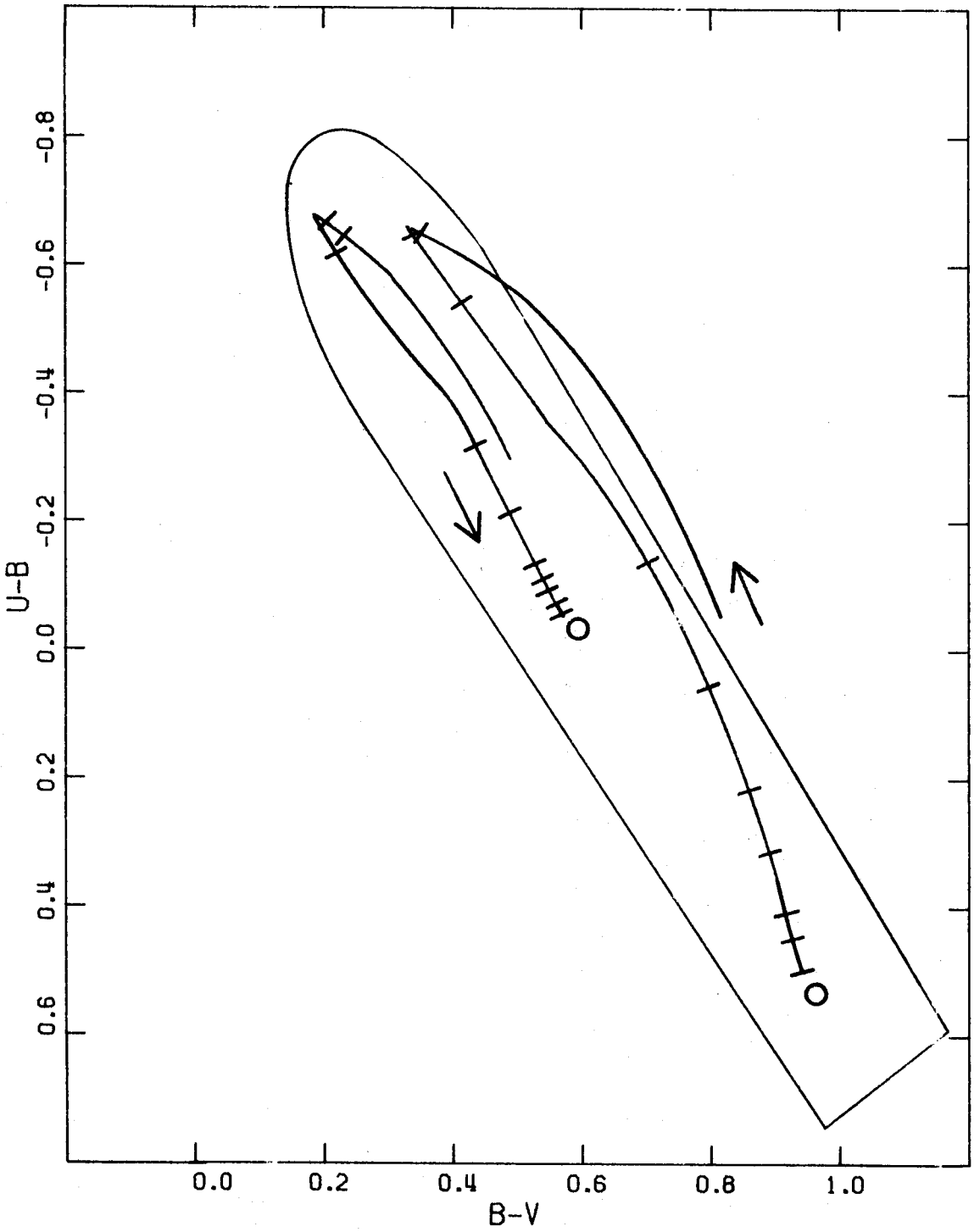
-0.8
-0.6
-0.4
-0.2
0.0
0.2
0.4
0.6
U-B
0.0
0.2
0.4
0.6
0.8
1.0
B-V
O
O

formation has occurred at different epochs in different regions of the galaxy. Markarians 59 and 71 are good examples of this in the blue galaxy sample. In addition, the color-aperture curves for the Markarian galaxies (Huchra 1976a) suggest the presence of an underlying redder component.

IV. COMPARISON WITH OTHER OBSERVATIONAL PROPERTIES

(a) Hβ Emission and Color

Huchra (1976a) has collected crude H emission equivalent width data and colors for over 100 Markarian galaxies. Data are also available for selected objects from Arp and O'Connell (1975), Searle and Sargent (1972), and Neugebauer et al. (1976).

Figure 9 shows the predictions of the models superposed on the observed log W(Hβ) in Å and U-B color data. The smooth, solid curves are the old galaxy models; the curves are again parameterized by constant α and varying β. From the bottom upwards, the curves represent α= 3.35, 2.35, 1.85, 1.35, and 0.35. The blue ends of the curves are the models with constant star formation. The dashed lines at the very blue end represent the tracks for very young galaxies (less than 10^8 years old) with exponential star formation rates. As they evolve, their tracks join the tracks of the old galaxies. The arrows show the change in U-B and log W(Hβ) for three models caused by increasing the IMF upper mass limit to $45M_\odot$ from $31M_\odot$ and using stellar models as massive as $40M_\odot$. Increasing the limit to $65M_\odot$ (with $60M_\odot$ models) doubles their length. The dotted lines are examples of the looped evolutionary tracks of composite models. Models with flatter IMF bursts have larger

FIGURE 9

Model predictions for the log of the Hβ equivalent width in emission versus U-B, superposed on the observed values (Huchra 1976a). The solid lines represent the old galaxy models with constant IMF and varying β. The dashed lines represent young galaxies with different ages and IMFs. The dotted loops represent the evolution of two composite models with the same underlying old galaxy component and bursts of α = 1.85 (lower) and 0.35 (upper) and the same duration. The arrows show the effects of increasing the upper limit of integration of the IMF from 31 to 45 solar masses.

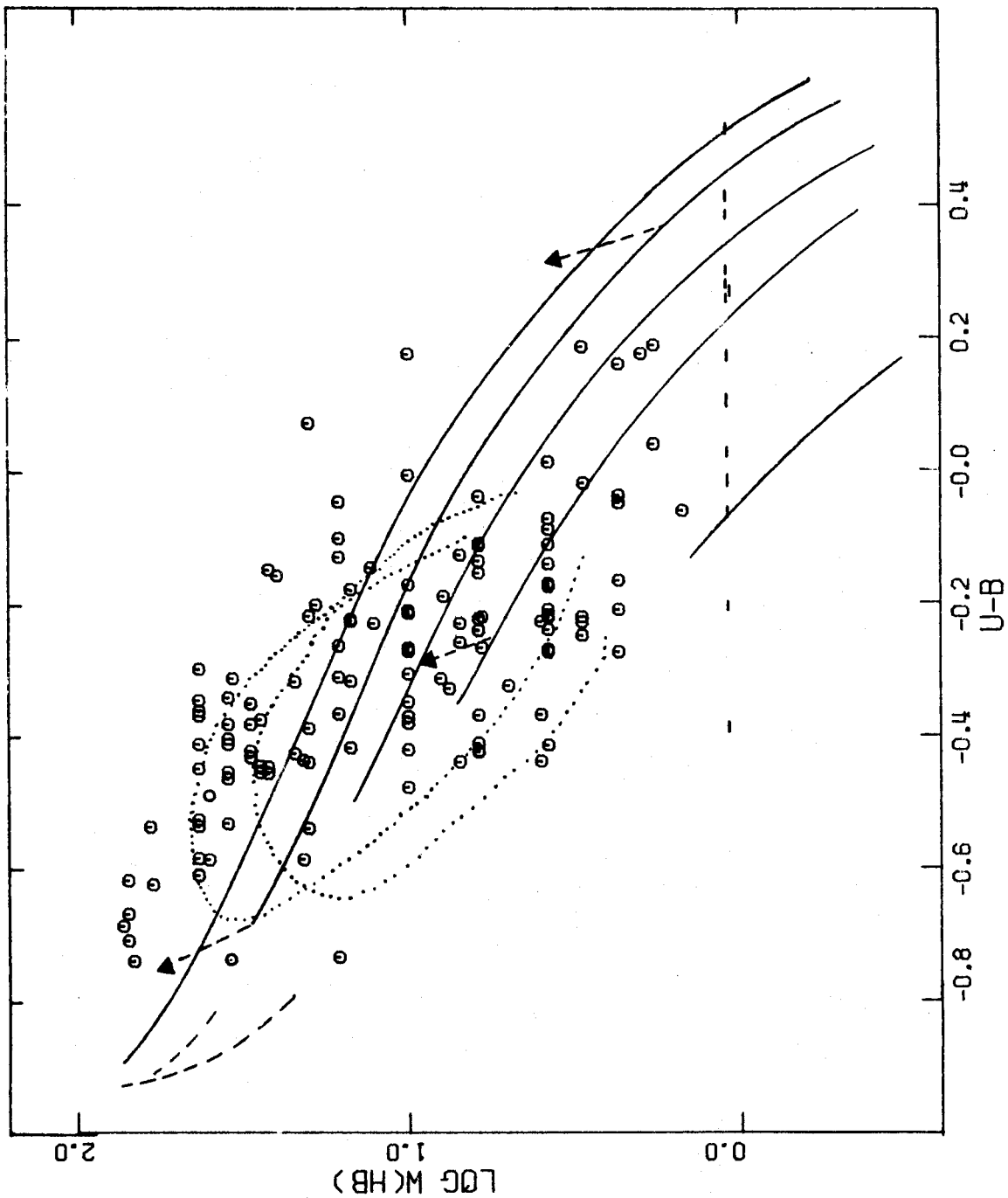
LOG W(HB)
0.0
1.0
2.0
U-B
0.4
0.2
-0.0
-0.2
-0.4
-0.6
-0.8

log W(Hβ) at any given color. Unlike the color-color evolution, the shape of these loops is critically dependent on the shape of the star formation burst (rate as a function of time), and its duration. Smoothing the shape of the burst decreases the width of the loop. In general, however, for bursts of duration $\geq 2.5 \times 10^7$ years, the composite models spend more than 80% of the duration of the burst at the tip of the loop. For a composite model with a burst of a given IMF, this tip falls on the old-young curve for that IMF. Bursts themselves evolve in an almost vertical straight line, with the slope slightly dependent on the IMF and duration for the sets of parameters we used. At their earliest stages, U-B is about -1.10, and log W(Hβ) is > 2.0. By the time these systems redden to U-B = -0.7, log W (Hβ) has dropped off the diagram. This is caused by the pile-up of optical colors for hot stars coupled with the shortness of the lifetimes of the highest mass stars. This feature of the burst evolution is the cause of the loops in the composite model evolution.

The optical data suffer from the use of different observational techniques. The equivalent widths are, in general, measured from slit spectra, while the photometry is from large apertures. Estimates of the observational effects, however, suggest that systematic effects are small. The color-aperture curves (Huchra 1976a) are not steep, and the slit spectra in general show emission throughout the

galaxies. In addition, comparisons of Hβ widths derived from the aperture data of Neugebauer et al. (1976) with slit spectra estimates show no significant differences.

Comparison of the models with the data strengthens some previous model constraints and adds new ones. Old models must have very flat IMFs. Even with the addition of 60 solar mass star models, the Salpeter models do not produce enough emission, no do they get blue enough. Young galaxies must be highly reddened. Reddening lines are horizontal in this plot. Young models are also likely to have flat IMFs. Even with constant star formation, Salpeter models have to be younger than 10^8 years to produce equivalent widths of Hβ much greater than 15Å. Composite models do not need reddening, and their looped nature helps provide an explanation of the redder systems with large Hβ widths. However, composite models also must have bursts with IMFs flatter than the Salpeter function. Models with Salpeter bursts can be made to fit the data with the upper parts of their loops by increasing the relative strength of the bursts. However, this would substantially overpopulate the left-hand side of the diagram, as the evolution of such systems becomes dominated by the burst evolution.

We also note that if the case B approximation is not true and the Lyman lines are optically thin, the calculated Hβ emission decreases. This would make it even more difficult to fit the observed Hβ emission with a Salpeter IMF.

(b) Chemical Composition

Searle and Sargent (1972) find that two of the blue galaxies, I Zw 18 = Markarian 116 and II Zw 40, have oxygen and neon abundances 1/10 and 1/3 of the values for galactic HII regions. Neugebauer et al. (1976) find that two blue galaxies, Markarians 35 and 59 have oxygen abundance 1/2 of the galactic value and one, Markarian 36 = Haro 4, has an oxygen abundance 1/4 of the galactic value.

In current galactic chemical evolutionary schemes (for example, Quirk and Tinsley 1973; Talbot and Arnett 1973) heavy element enrichment is accomplished by massive stars. The low measured oxygen abundances are thus very strong evidence against the old galaxies with flat IMFs. Significant infall of unenriched gas (Quirk and Tinsley 1973) might provide a way out of this problem, but this does not seem likely.

The metal abundance does not place any constraint on the young galaxy model IMF. In the composite models, the amount of mass in the burst is a very small fraction of the total system mass. The underlying old galaxy could easily have a time-averaged enrichment rate less than that in the solar neighborhood. Thus constraints cannot be put on the burst IMF, but only on the total system enrichment rate.

Although all the galaxy models have used stellar models with population I abundances, we do not think that this will seriously affect the blue galaxy colors. Population II

stellar models (Trimble et al. 1973; Chiosi and Nasi 1974) are hotter, slightly more luminous, and have almost no red supergiant phase. These effects will probably cause the galaxy models to become bluer in both colors. A low abundance gas will have a higher excitation and electron temperature (Searle 1971), all other things being equal. This reddens both U-B and B-V (see Table 3) for the gas, but the Hβ emission is relatively insensitive to temperature (Osterbrock 1974). The effects of composition on the stellar ultraviolet photon flux, thus the total gaseous emission contribution, require further examination.

(c) The Color-Luminosity Distribution: A Statistical Test

Sargent and Searle (1971) and later Searle et al. (1973) suggest that young galaxies might be distinguished from "flashing" systems--the composite models--by an examination of the color distribution of galaxies as a function of absolute magnitude. We can compare model predictions with the color-absolute magnitude data compiled for a sample of Markarian galaxies (Huchra 1976a).

The basic scheme goes as follows: if the bluest galaxies are young systems, then the relative numbers of galaxies of different colors should be related by the time spent at each evolutionary stage, weighted by their luminosities and the galaxy formation rate. For example, if galaxies have been forming at a constant rate, there should be 10

times as many galaxies 10^9 years old as there are galaxies 10^8 years old. For galaxy evolution, other than flat with very flat α and low β models, this predicts more red galaxies than blue ones. Composite galaxies, on the other hand, would have blue-to-red galaxy ratios dependent on the duration and relative frequencies of the bursts.

The color-absolute magnitude data for the Markarian galaxy sample is shown in Figure 10. There is a definite lack of faint red systems. Composite models could explain this easily. Figure 11 shows the color evolution of a composite model with a burst of duration 2.5×10^7 years. This model spends almost twice as much time between U-B = -0.2 and -0.6 as between U-B = -0.2 and +0.2, and is about half a magnitude brighter when it is bluer. Doubling the burst duration will double the time ratio. The bright galaxies could be multiple burst systems.

Young galaxy models that eventually evolve through these regions do indeed spend more time in the redder region but they are one to two magnitudes fainter in that region. In addition, there is a class of models such as $\alpha = 1.35$, $\beta \lesssim 6$ (see Figure 5) or $\alpha = 2.35$, $\beta \lesssim 3$, that never evolve redwards of U-B = -0.2. However, the metals abundance arguments also apply here. The blue systems cannot be systems forming stars at high rates for long periods of time.

Unfortunately, the Markarian galaxy sample is not well defined in terms of color alone. Selection effects may

FIGURE 10

The observed distribution of Markarian galaxies in color and absolute magnitude from Huchra (1976a).

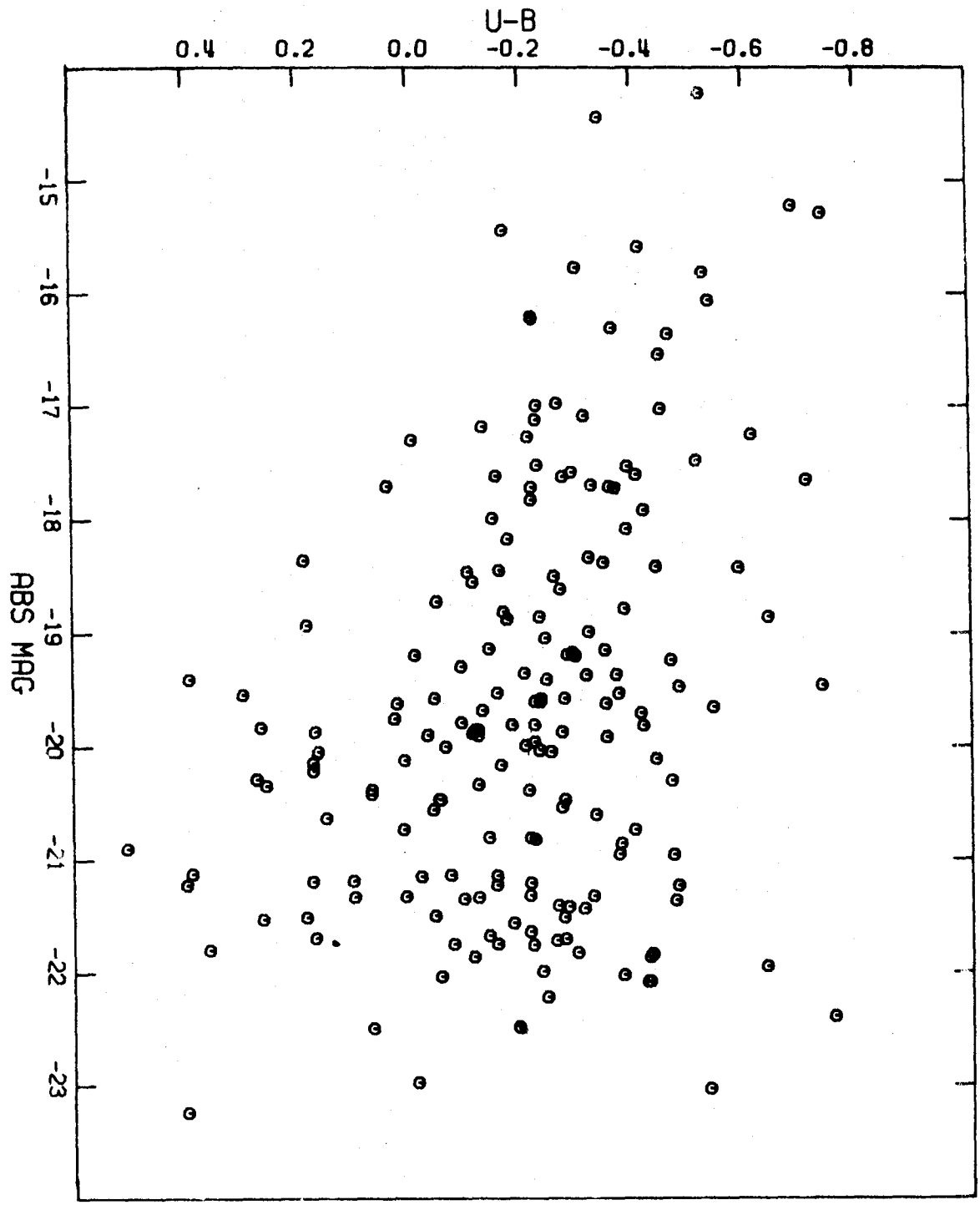
U-B
0.4
0.2
0.0
-0.2
-0.4
-0.6
-0.8
ABS MAG
-15
-16
-17
-18
-19
-20
-21
-22
-23

FIGURE 11

The evolution in U-B of a composite galaxy model with a burst of duration 2.5×10^7 years and maximum contribution to the system luminosity of 50%.

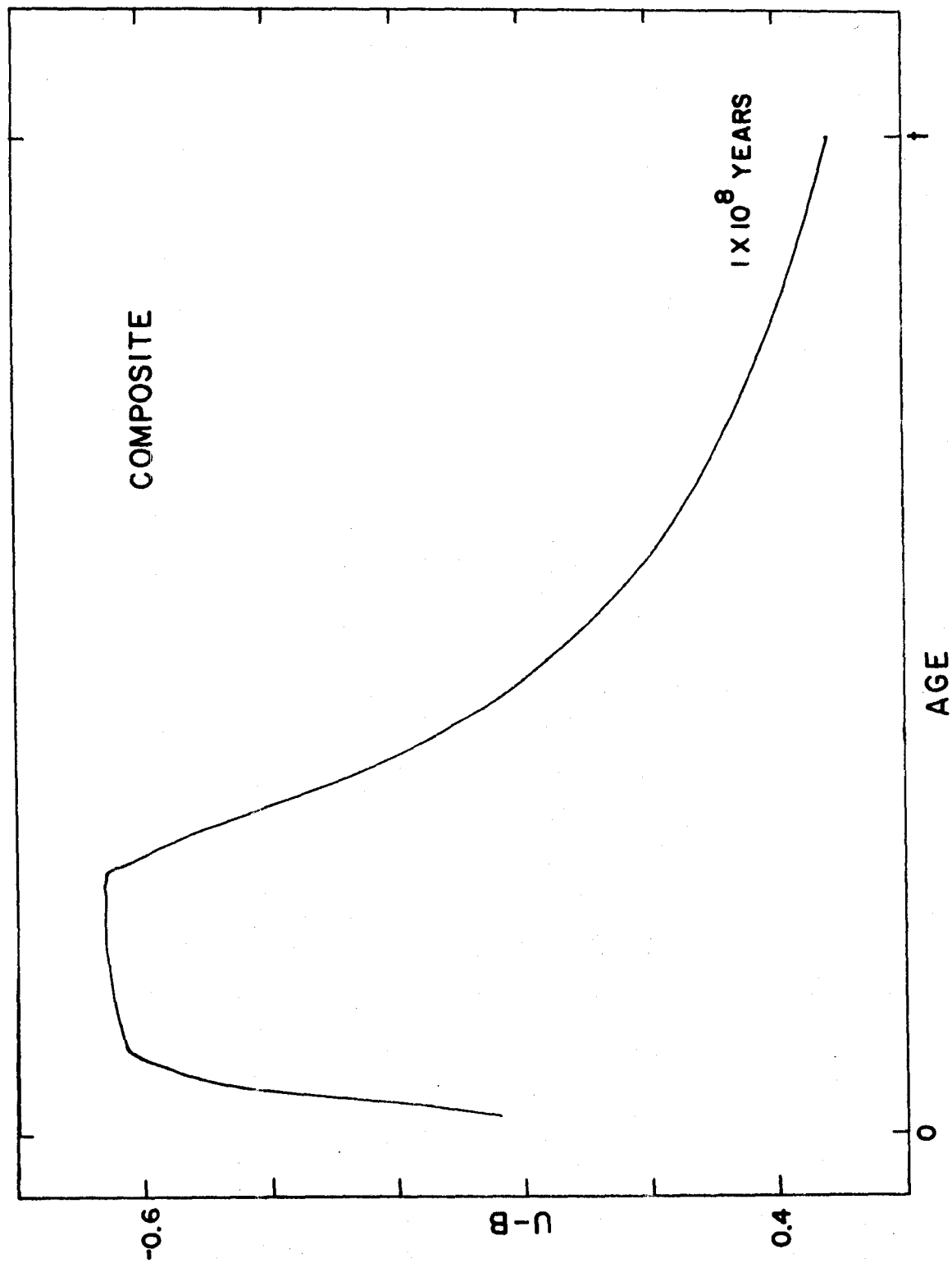
COMPOSITE
1 X 10^8 YEARS
AGE
0
t
-0.6
U-B
0.4

hinder the finding of redder galaxies (for example, Figure 8 of Huchra 1976a). Although the color-magnitude data are suggestive, they are not conclusive.

(d) Internal Absorption

In order to explain both the colors and the Hβ emission as a function of color, the young galaxy models need to be reddened by 1 to 2 magnitudes of visual absorption. Measurements of the absorption are strong tests of the young galaxy models.

A crude estimate of the absorption can be obtained from neutral hydrogen measurements. Knapp (1975) has calibrated the galactic gas-to-dust ratio, giving the absorption A_V and reddening E_{B-V} in terms of the neutral hydrogen surface density σ_H in atoms per square cm:

$$A_V = \sigma_H/(2 \pm 1 \times 10^{21}) \text{ atm cm}^{-2} \text{ mag}^{-1}, \quad (10)$$

and $$E_{B-V} = \sigma_H/(7 \pm 3 \times 10^{21}) \text{ atm cm}^{-2} \text{ mag}^{-1}. \quad (11)$$

Bottinelli et al. (1973), Bottinelli et al. (1975), Chamaraux (1970), and Gottesman and Weliachew (1972) have obtained neutral hydrogen measurements of several of the blue galaxies. Assuming that the HI is spread uniformly over the optical image of the galaxy (cylindrical distribution), with half in front of the galaxy, we derive the values of A_V and E_{G-V} shown in Table 5. The σ_H value for II Zw 40 (Gottesman and Weliachew 1972) is a peak surface density as opposed to the mean surface density. In general, the HI distribution is greater in extent than the optical galaxy image, so

we will tend to overestimate the mean surface densities. The values derived by this method depend on the similarity of the characteristics of the gas-to-dust ratio and absorption for our galaxy and the blue systems.

A somewhat better estimate of the absorption can be obtained from the Balmer decrement. For a case B gas radiative recombination spectrum, the $H\alpha/H\beta$ ratio is approximately 3 (Pengelly 1964). Reddening will cause the $H\alpha/H\beta$ ratio to increase by a factor of 1.55 per magnitude of visual extinction (Allen 1973). Using the spectrophotometric observations of $H\alpha/H\beta$ of Neugebauer et al.(1976) and Sargent and Searle (1970), we derive the absorption and reddening for systems with photometry (Huchra 1976a, 1976b). Table 6 presents the Balmer decrement data. $H\alpha/H\beta$ ratios in brackets are upper limits, with $H\alpha$ blended with the NII lines. Because II Zw 40 is very close to the galactic plane, the colors and the values for A_V and E_{B-V} are strongly affected by galactic extinction. This method suffers from a number of defects. Underlying stellar absorption lines can change the $H\alpha/H\beta$ ratio, usually increasing it above the recombination theory value, thereby causing overestimation of the absorption. In reality, the gas, stars, and dust in a model are mixed, and the Whitford law may not apply. Radiative transfer effects (deviations from pure case B) can raise or lower the $H\alpha/H\beta$ ratio (Osterbrock 1974).

Accepting the sets of estimates as they are, the inter-

TABLE 5

NEUTRAL HYDROGEN AND ABSORPTION

Galaxy	U-B	σ (10^{21} n_H/cm^2)	A_V	E_{B-V}
II Zw 40	[-0.48]	0.8	0.2	0.06
Mk 8	-0.40	1.0	0.3	0.07
Mk 325	-0.43	0.6	0.2	0.04
Mk 5	-0.35	4.5	1.4	0.32
Mk 7	-0.38	1.4	0.4	0.10
Mk 12	-0.37	0.7	0.2	0.05
Mk 33	-0.52	1.0	0.3	0.07
Mk 89	-0.35	2.9	0.6	0.21
Mk 178	-0.34	0.4	0.1	0.03
Mk 22	-0.43	<2.5	<0.6	<0.18
Mk 685	-0.41	1.3	0.3	0.12

TABLE 6

THE BALMER DECREMENT AND ABSORPTION

Galaxy	U-B	Hα/Hβ	A_V	E_{B-V}
Mk 19	-0.68	3.90	0.59	0.17
Mk 33	-0.52	[4.79]	<1.13	<0.32
Mk 36	-0.68	2.96	0.01	0.00
Mk 49	-0.39	[3.55]	<0.37	<0.11
Mk 59	-0.70	2.62	0.00	0.00
Mk 67	-0.40	[4.87]	<1.18	<0.34
Mk 35	-0.37	3.67	0.44	0.13
Mk 116	-0.73	3.38	0.27	0.08
NGC 5471	-0.85	3.08	0.06	0.02
II Zw 40	[-0.48]	7.63	[2.13]	[0.61]

nal absorption in the bluest systems appears to be too small to support the young galaxy hypothesis. Further observations of additional reddening estimators--the SII lines (Miller 1968), or other hydrogen recombination lines--combined with models of absorption in composite systems are required to lay this problem to rest.

V. CONCLUSIONS

We have examined three simple classes of model galaxies in order to study the star formation histories and initial mass functions required to produce the bluest galaxies.

Old galaxy models fit the observed colors and Hβ emission if they have sufficiently flat (high mass star enriched) initial mass functions or, for somewhat steeper IMFs, nearly constant rates of star formation. Models with these parameters predict relatively metal rich abundances, but observations do not support this.

Young galaxy models fit the observed colors and Hβ emission if they are internally reddened by 1 to 2 magnitudes of visual extinction. Flat IMFs are attractive for these models on statistical grounds. The color-absolute magnitude data suggest that the young galaxy hypothesis is not correct, but the strongest arguments against this hypothesis are the relatively low values of measured internal absorption.

Composite galaxies fit the observed colors without reddening, but require flatter than Salpeter IMFs in order to fit the Hβ emission. The looped evolution of these models in the Hβ - color plane helps explain some of the redder systems with strong emission and the bluer systems with weak emission. Bursts of a few times 10^7 years' duration

and maximum luminosity equal to the underlying stellar component can produce the observed color-luminosity distribution for faint galaxies.

With reasonable upper mass limits for the IMF, the color and Hβ emission data strongly suggest that at least some of the blue galaxies are forming stars with an IMF flatter than the Salpeter function. This conclusion is weakened if very massive stars ($M > 65M_{\odot}$) exist.

REFERENCES

Allen, C. W. 1973, Astrophysical Quantities (london: Athlone Press).

Aller, L. H. 1956, Gaseous Nebulae (London: Chapman and Hall, Ltd.).

Arp, H. C., and O'Connell, R. 1975, Ap. J., 197, 291.

Barbaro, G., Bertelli, G., Chiosi, C., and Nasi, E. 1973, Astr. and Ap., 29, 185.

Barbaro, G., Chiosi, C., and Nobili, L. 1972, Astr. and Ap., 18, 186.

Bottinelli, L., Duflot, R., Gouguenheim, L., and Heidmann, J. 1975, Astr. and Ap., 41, 61.

Bottinelli, L., Gouguenheim, L., and Heidmann, J. 1973, Astr. and Ap., 22, 281.

Brown, R., and Matthews, W.1970, Ap. J., 160, 939.

Caldwell, J., Gott, R., and Hart, M. 1974, private communication.

Chamaraux, P., Heidmann, J., and Lauque, R. 1970, Astr. and Ap., 8, 424.

Chiosi, C., and Nasi, E. 1974, Astr. and Ap., 35, 81.

Chiosi, C., and Summa, C. 1970, Ap. and Sp. Sci., 8, 478.

de Vaucouleurs, G. 1961, Ap. J. Suppl., 5, 233.

de Vaucouleurs, G., and de Vaucouleurs, A. 1972, Mem.R.A.S., 77, 1.

Du Puy, D. 1968, Pub. A.S.P., 80, 29.

_____. 1970, A.J., 75, 1143.

Gottesman, S., and Weliachew, L. 1972, Ap. Lett., 12, 63.

Grewing, G., Demoulin, M. H., and Burbidge, G., 1968, Ap. J., 154, 477.

Hart, M. 1971, private communication.

Hartmann, W. 1970, Mem. S.R. de Liege, 19, 49, (16th Liege Symposium: Pre-Main Sequence Evolution).

Hayes, D., Oke, J., and Schild, R. 1970, Ap. J., 162, 361.

Heidmann, J., Heidmann, N., and de Vaucouleurs, G. 1972, M.N.R.A.S., 76, 121, 1972.

Holmberg, E. 1958, Medd. Lund Obs., 136, 2.

Huchra, J. P. 1976a, in preparation.

_____. 1976b, unpublished results.

Iben, I. 1965a, Ap. J., 141, 993.

_____. 1965b, Ap. J., 142, 1447.

_____. 1966a, Ap. J., 143, 483.

_____. 1966b, Ap. J., 143, 505.

_____. 1966c, Ap. J., 143, 516.

_____. 1967a, Ap. J., 147, 624.

_____. 1967b, Ap. J., 147, 650.

Johnson, H. L. 1966, Ann. Rev. Astr. and Ap., 4, 193.

Knapp, G. 1975, A.J., 80, 111.

Larson, R., and Starrfield, S. 1971, Astr. and Ap., 13, 190.

Matthews, T., and Sandage, A. 1963, Ap. J., 138, 30.

Miller, J. 1968, Ap. J.(Letters), 154, L57.

Morton, D. 1969, Ap. J., 158, 629.

Neugebauer, G., Becklin, E., Oke, J., and Searle, L. 1976, Ap. J., 205, 29.

Oke, J. 1971, private communication (scanner standards).

Oke, J., and Schild, R. 1970, Ap. J., 161, 1015.

Osterbrock, D. 1974, Astrophysics of Gaseous Nebulae (San Francisco: Freeman).

Pengelly, R. M. 1964, M.N.R.A.S., 127, 145.

Peimbert, M., and Peimbert, S. T. 1974, Ap. J., 193, 327.

Quirk, W., and Tinsley, B. 1973, Ap. J., 179, 69.

Robertson, J. W. 1972, Ap. J., 177, 473.

Salpeter, E. 1955, Ap. J., 121, 161.

Sandage, A. 1966, Ap. J., 146, 13.

_____. 1973, Ap. J., 180, 687.

Sandage, A., and Tammann, G. 1974a, Ap. J., 191, 603.

_____. 1974b, Ap. J., 194, 223.

Sargent, W. L. W. 1970, Ap. J., 160, 405.

Sargent, W. L. W., and Searle, L. 1970, Ap. J.(Letters), 162, L155.

Schlesinger, B. 1972, A.J., 77, 584.

Searle, L. 1971, Ap. J., 168, 327.

Searle, L., and Sargent, W. L. W. 1972, Ap. J., 173, 25.

Searle, L., Sargent, W. L. W., and Bagnuolo, W. G. 1973, Ap. J., 179, 427.

Simpson, J. 1973, Pub. A.S.P., 85, 479.

Stothers, R. 1963, Ap. J., 138, 1074.

_____. 1964, Ap. J., 140, 514.

_____. 1966, Ap. J., 143, 91.

Stothers, R., and Simon, N. 1968, Ap. J., 152, 233.

Strom, S., Strom, K., and Grasdalen, G. 1975, Ann. Rev. Astr. and Ap., 13, 187.

Stromgren, B. 1939, Ap. J., 89, 526.

Talbot, R., and Arnett, W. 1973, Ap. J., 186, 51.

Tinsley, B. 1968, Ap. J., 151, 547.

_____. 1972, Astr. and Ap., 20, 383.

Trimble, V., Paczynski, B., and Zimmerman, B. 1973, Astr. and Ap., 25, 35.

Whitford, A. E. 1958, A.J., 63, 201.

Zanstra, H. 1931, Pub. Dominion Ap. Obs., 4, 234.

_____. 1961, Quarterly J.R.A.S., 2, 137.

Ziolkowski, J. 1972, Acta Astr., 22, 327.